Ministère de l'Enseignement Supérieur et de la Recherche Scientifique
Université Hassiba Benbouali de Chlef
Faculté des Sciences Exactes et Informatique
Département de Physique

THÈSE

Présentée pour l'obtention du diplôme de

DOCTORAT EN SCIENCES

Spécialité : Physique

Par

MOHAMMED ELHADJ KHELIFA

Thème :

INTERACTION DE SOLITONS DANS UN MILIEU NON LOCAL

Soutenue le 29/ 06/ 2021, devant le jury composé de :

Habib Rached	Professeur	Université Hassiba Benbouali Chlef	Président
Abdelâali Boudjemâa	Professeur	Université Hassiba Benbouali Chlef	Rapporteur
Ahmed Diaf	Professeur	Université djilali bounaama khemis-Miliana	Examinateur
Hocine Boukabcha	MCA	Université djilali bounaama khemis-Miliana	Examinateur
Mohamed Belabbas	MCA	Université Hassiba Benbouali chlef	Examinateur
Ahmed Bouhekka	Professeur	Centre universitaire de Tissemsilt	Examinateur

وزارة التعليم العالي والبحث العلمي
جامعة حسيبة بن بوعلي الشلف
كلية العلوم الدقيقة والاعلام الالي
قسم الفيزياء

أطروحة مقدمة لنيل شهادة دكتوراه في العلوم

التخصص :فيـــــزياء

العنوان

INTERACTION DE SOLITONS DANS UN MILIEU NON LOCAL

من إعداد

محمد الحاج خليفة

المناقشة بتاريخ 29/جوان/ 2021 من طرف اللجنة المكونة من:

راشد حبيب	أستاذ	جامعة حسيبة بن بوعلي الشلف	رئيس
بوجمعة عبد العالي	أستاذ	جامعة حسيبة بن بوعلي الشلف	مقرر
ضياف أحمد	أستاذ	جامعة ج بونعامة خميس مليانة	ممتحن
بوكابشة حسين	أستاذ محاضر-أ-	جامعة ج بونعامة خميس مليانة	ممتحن
بلعباس محمد	أستاذ محاضر-أ-	جامعة حسيبة بن بوعلي الشلف	ممتحن
بوهكة أحمد	أستاذ	المركزجامعي لتيسمسيلت	ممتحن

Ministry of Higher Education and Scientific Research
Hassiba Benbouali University of Chlef
Faculty of Exact Sciences and Informatics
Department of Physics

PhD THESIS

SOLITON INTERACTION IN NON-LOCAL MEDIA

A thesis submitted for the degree of
Doctor of physics

By
Mohammed Elhadj Khelifa

Prof. Habib Rached	Hassiba Benbouali University of Chlef	President
Prof. Abdelâali Boudjemaa	Hassiba Benbouali University of Chlef	Supervisor
Prof Ahmed Diaf	Djilali Bounaama University of Kh-M	Examiner
Dr. Mohamed Belabbas	Hassiba Benbouali University of Chlef	Examiner
Dr. Hocine Boukabcha	Djilali Bounaama University of Kh-M	Examiner
Prof. Ahmed Bouhekka	University Center of Tissemsilt	Examiner

(June 29, 2020)

Dedication

To my wife, for her endless support and patience.
To the memory of my parents, whom inspired scientific thinking in our lives
To my children's: Mohammed Al-amine, Yassine and Besma.
To my two brothers Mohammed, Abdelkader and my sister Massaouda.

Acknowledgements

My first deepest gratitude goes to my supervisor Prof. ***Abdelâali Boudjemâa*** for supporting and encouraging me during this years. His valuable advice and assistance, his efforts, motivation, endless patience and for devoting a large part of his time. Without him I would never finish this thesis. I could appreciate his exceptional personality.

Many thanks are in order to Prof. ***Usama AlKhawaja*** as well, for the very nice collaboration and fruitful discussions. I would like to thank him for the research period that I spent in his group in *Arab Emirates University, Al Ain*. In that time I met *Amaria Javad* And *Laila Al Shakkaf* whom I thank for valuable discussions.

I thank the members of the jury *Prof. H. Rached*, *Pr. A. Diaf*, Prof. A. Bouhekka, *Dr. M. Belabbas* and *Dr. H. Boukabcha* whom agreed to evaluate this work.

I would like to thank all the people in our group. Thanks to Nadia Guebli, Bakhta Cherifi, Kelthoum Ghadaoui and Karima Abbas for their helps and encouragements and for the funny moments.

My gratitude goes to all my fiends and colleagues of the physics department and the faculty of Exacte Sciences and Informatics at Hassiba Benouali University of Chlef.

I would like to than *Prof. Miloud Tahar Abbas* the director of the Laboratory of Energetics and Mechanics at Hassiba Benouali University of Chlef.

Finally, special thanks go to all my Family.

Abstract

Weakly interacting Bose-Einstein condensates with dipole-dipole interactions support intriguing macroscopic excitations in the form of bright solitons. In this thesis we present systematic studies of the static and the dynamics of one-dimensional nonlocal solitons and soliton molecules, performed by analytical (variational and exact) methods and numerical simulation of the Gross-Pitaevskii equation. The thesis has focused on three kinds of topics. The aim of the first theme is to investigate the equilibrium and scattering properties of matter wave bright three-soliton molecules with competing local and nonlocal nonlinearities.The variational and the numerical solutions of the underlying Gross-Pitaevskii equation predict that the degree of the nonlocality, the separation distance and the soliton phase may strongly affect the binding energy and the soliton width. The scattering properties of these composite nonlinear structures by Gaussian potential barrier are analyzed variationally and numerically. We show that stable transmission and reflection where the molecular structure is preserved can occur only for a specific barrier height and soliton velocity. The second subject of this thesis consists in studying the stability and the dynamical properties of interwires polar soliton molecules in a biwire setup with dipole moments aligned perpendicularly to the line of motion and in opposite directions in different wires. Importantly, the excitations spectrum of such ensembles can acquire a roton-maxon structure. We reveal that the degree of the nonlocality and the interwire separation play a key role in stabilizing the molecules. However, by modifying the interaction stength and the interwire distance, it is shown that the dynamics of such solitons complexes exhibit oscillatory behavior. Finally, the exact solution of the Gross-Pitaevskii equation has attracted much attention. In this thesis, we derive a new exact

solution to such an equation using the Darboux transformation method. Using an algebraically-decaying seed solution, we obtain a two-soliton solution with diverging peaks, which we denote as singular soliton molecule. The characteristics of these solitonic composites such as the profiles, the force and potential of interaction are deeply analyzed. Furthermore, we obtain a new solution to the nonlocal Gross-Pitaevskii equation using the same method and seed solution. The new solution in this case corresponds to an elastic collision of a soliton, a breather soliton on flat background, and a breather soliton on a background with linear ramp. We illustrate also the case of reverse-time nonlocal Gross-Pitaevskii equation.

Résumé

Les condensats de Bose-Einstein dilus en prsence des interactions dipôle-dipôle supportent des excitations macroscopiques intrigantes sous forme de solitons brillants. Dans cette thèse nous tudions analytiquement et numriquement les proprites statiques et dynamiques des solitons et de molécules de solitons non-locaux unidimensionnels l'aide de l'équation de Gross-Pitaevskii. Cette thse fait cho trois questions diffrentes actuelles: Le but du premier thme est d'étudier les proprités statiques et la diffusion de l'onde de matière brillante de trois molécules de solitons nonlocaux. Les solutions variationnelles et numériques de l'équation de Gross-Pitaevskii prdisent que le degr de la nonlocalité, la séparation entres les solitons adjacents et la phase peuvent fortement affecter l'énergie de liaison et la largeur du soliton. Les propriétés de diffusion de ces structures non linaires par une barrire de potentielle gaussiènne sont aussi analysées variationnellement et numériquement. Nous avons vu qu'une transmission et une réflection stable où la structure moléculaire est préservée ne peuvent se produire que pour des valeurs spécifiques de la hauteur de barrière et la vitesse de soliton. Ensuite nous regardons la stabilité et la dynamique des molécules de solitons polaires inter-tube dans une configuration bi-tubes avec des moments dipolaires alignés perpendiculairement à la ligne de mouvement et dans des directions opposées dans les deux différents tubes. Nous avons montr que le spectre d'excitations de tels ensembles peut acquérir une structure roton-maxon. Nous révélons que le degré de la nonlocalité et la séparation entre les tubes jouent un rôle crucial pour la stabilisation des molécules. Cependant, en modifiant la force d'interaction et la distance entre tubes, nous trouvons que la dynamique de ces deux solitons présente un comportement oscillatoire. Enfin, la solution exacte de l'équation de Gross-Pitaevskii attiré beaucoup d'attention.

Dans cette thèse, nous établissons une nouvelle solution exacte à de telle équation en utilisant la méthode de la transformation de Darboux. A l'aide d'une

fonction algébriquement dcroissante, nous obtenons une solution à deux solitons avec des pics divergents, que nous désignons par molécule de soliton singulier. Les caractéristiques de solitons telles que les profiles, la force et le potentiel d'interaction sont analysées en dtail. De plus, nous obtenons une nouvelle solution de l'équation de Gross-Pitaevskii nonlocale en utilisant la même méthode et la même solution initiale (seed zero). Nous illustrons également le cas de l'équation de Gross-Pitaevskii nonlocale possde une symtrie par renversement du temps.

ملـخص

ننشأ السوليتونات (Solitons) في الاوساط اللاخطية المشتتة وهي موجات منفردة (منعزلة) تحتفظ بشكلها اثناء انتشارها. في هذه الرسالة نقدم دراسة منهجية حول سلوك السوليتونات وجزيئات السوليتونات غير المحلية ذات بعد واحد في حالة الاستقرار واثناء تطور الزمن (الاستقرار والديناميك).

نعتمد في دراستنا على عدة طرق: تحليلية تتمثل في طريقة المتغيرات وإيجاد الحل الدقيق وكذا المحاكاة الرقمية من أجل حل معادلة(GPE) Gross Pitaevskii ذات بعد واحد. ترتكز المذكرة على ثلاث (3) محاور أساسية:

المحور الأول يتمثل في دراسة خواص حالة التوازن لجزيئات السوليتونات المشكلة من ثلاث سوليتونات مع الأخذ بعين الاعتبار درجة اللاخطية المحلية وغير المحلية . من خلال هذا المحور لاحظنا أن تفاعل الموجة المنعزلة مع حاجز كموني ينتج عنه ما يعرف بظاهرتي النفوذ والانعكاس واللتان يتحكم فيهما عاملين أساسيين سرعة السوليتون وعرض الحاجز الكموني.

المحور الثاني يتمثل في دراسة الخصائص الديناميكية لجزيئات السوليتون المتداخلة لسلكين منفصلين (biwires) والمستقطبة بثنائيي قطب متعامدين بالنسبة للسلكين ومتعاكسين في الاتجاه. حيث اتضح جليا ان المسافة بين السلكين ومعامل اللامحلية وكذا الاثارات العنصرية المتمثلة في الروتونات (Rotons) لهم دور مهم جدا في استقرار الجزيء.

من خلال المحور الثالث قمنا بإيجاد حلول جديدة لمعادلة GPE المحلية و غير المحلية باستعمال طريقة داربو (Darboux) ودالة جبرية $\frac{1}{x}$. في حالة معادلة GPE تمثل الحل في جزيء سوليتوني مكون من موجتين منعزلتين بقمتين متباينتين والذي عرف بجزيء السوليتون المنفرد. وبتطبيق نفس الطريقة ونفس الدالة بالنسبة لمعادلة GPE اللامحلية وجدنا حل عبارة عن تداخل ثلاث سوليتونات منعزلة تتمثل في سوليتون منعزل وسوليتونين من نوع (Breathers) احدهما في المستو المائل والاخر في المستو الافقي. وأخيرا قمنا بمعالجة معادلة GPE اللامحلية في اطار التناظر الزمني العكسي.

General Introduction

General introduction

A soliton is a peculiar manifestation of nonlinear wave systems arises from a competition between nonlinear and dispersive effects. It maintains its shape during the propagation at constant speed and moving without distortion. Solitons appear as particle-like self-localized coherent solutions of certain differential equations such as the well-known nonlinear Schrödinger equation (NLSE). This equation has a great relevance in the field of nonlinear optics, where it governs the propagation of the envelope of an electromagnetic pulse and plays also an essential role in the domain of BoseEinstein condensation (BEC) where it adopts the form of the GrossPitaevskii equation (GPE) [1, 2]. The soliton solutions are typically obtained by means of the inverse scattering transform owe to their stability to the integrability of the field equations.

0.1 A Brief History of Solitons

The solitary wave was first observed in August 1834 by the Scottish engineer John Scott Russell (18081882) in the Union Canal in Scotland. In 1844, Russell reproduced the phenomenon in a wave tank and named it the "Wave of Translation" [3] and demonstrated four facts namely :

i) Experimental proof of the existence of solitary waves which have the shape $A\sinh^2[p(x-vt)]$, where p depends on the nonlinearity parameter.

ii) A sufficiently large initial mass of water generates many independent solitary waves.

iii) Solitary waves cross each other without change of any kind.

iv) The velocity of the solitary wave v is an empirical and depends on the height and the acceleration of gravity implying that a large amplitude solitary wave propagates faster than of one of low-amplitude.

In 1895 Diederik Korteweg and Gustav de Vries [4] working in Amsterdam, published the deffinitive theory providing what is now known as the Korteweg-de Vries equation, including solitary wave and periodic cnoidal wave solutions.

In 1939 Frenkel and Kontorova [5] suggested a nonlinear chain to describe the structure and dynamics of a crystal lattice in the vicinity of the dislocation core (discrete Sine-Gordon

equation).

In 1954, Fermi, Pasta and Ulam [6] carried out the first and most fundamental numerical computations in the history of physics. They used the Los Alamos MANIAC computer to investigate the dynamics of energy equipartition in a slightly nonlinear crystal lattice.

In 1958, the subject of solitary waves had been reborn in plasma physics with the discovery, by Adlam and Allen [1, 7], of solitary waves in a collisionless plasma containing a magnetic field.

In 1965 Norman Zabusky of Bell Labs and Martin Kruskal of Princeton University [8] first demonstrated particle-like behavior in media subject to the Korteweg-de Vries equation [4] by numercial means using a finite difference approach.

This particle-like behavior led these authors to introduce the term soliton to replace the term solitary wave. They also discovered the interaction of solitons.

In 1967, Gardner, Greene, Kruskal and Miura developed an ingenious method "the inverse scattering transform" for finding the exact solution of the KdV equation [9].

In the same year 1967, M. Toda [10] discovered an equation that bears his name. In contrast with the Sine-Gordon system, the Toda lattice supports wave solutions, which travel freely through the lattice at constant speed.

The history of dark solitons dated back in 1971 with the pioneering paper by Tsuzuki[11], where exact soliton solutions of the GPE were obtained and their connection with Bogoliubov's phonons [12] was revealed.

In 1972, Zakharov and Shabat [13, 14] provided an exact theory of two-dimensional (2D) self-focusing and 1D self-modulation of waves in nonlinear media.

In 1973, Hasegawa [15] suggested, that the realization of a solitary wave is possible in fiber optics when a pulse-narrowing nonlinear effect balances the effect of dispersive spreading of the light pulse.

The first experimental observation of dark solitons in BEC of ^{87}Rb atoms was made in 1999 [16]. In 2002, the first experimental observation of bright solitons in BEC of ^{7}Li atoms was reported in [17, 18].

Since the mid-1970's, solitons have attracted a much attention and have become applied in diverse areas in physics such as plasmas, astrophysics, molecular biology, nonlinear

optics, spin waves, superfluidity, and BECs (see for review Ref. [19]).

0.2 Solitons in Bose-Einstein condensates

In condensed matter physics, BEC is a new state of matter that atoms reach below a certain critical temperature. This form of matter was predicted in 1924 by Satyendra Nath Bose and Albert Einstein [20, 21]. The transition to BEC occurs when the thermal de Broglie wavelength becomes comparable to the mean interparticle separation, and thus, a macroscopic fraction of the bosons occupies the lowest single-particle quantum state. The success of trapping techniques and magneto-optical evaporative cooling (see for review ([22–24]) have given rise to the realization of BEC in dilute atomic gases at temperatures of the order of fractions of microkelvins for the first time at JILA, MIT and Rice University in 1995 ([25–27]).

Atomic BECs constitute a best environment for studying nonlinear macroscopic excitations such as solitons in quantum systems. For short-range interacting BECs at low temperatures, the wavefunction of the condensate obeys the GPE with cubic local nonlinearity resulting from the interatomic interactions. The one-dimensional (1D) GPE admits stable solitonic solutions for bright (dark) solitons [13, 14] for attractive (repulsive) interactions, equivalent to the self-focusing (self-defocusing) nonlinearity in Kerr media (optical solitons). Dark solitons are characterized by a local density dip and a sharp phase gradient of the wavefunction at the position of the minimum. Robust dark solitons have been realized in Ref. [16, 28, 29] over two decades ago using the phase imprinting technique. Strictly speaking the stability of these structures holds only in 1D systems. In 2D regime they collapse into vortex-antivortex pairs, while in 3D they behave as vortex rings through the snake instability [16, 28, 29]. Bright solitons correspond to a localized peak in density. First experimental bright solitons were generated in BECs of ^{7}Li in quasi-1D regime [17, 18]. The creation of these structures was possible only by means of the Feshbach resonance and then tuning of the interactions from repulsive to attractive during the experiments. In the experiment of Strecker et *al*.[18], the formation of the bright soliton trains has been interpreted as due to quantum mechanical phase fluctuations of the bosonic field operator [30]. The most

important feature of both types of solitons is that they do not disperse due to the nonlinearity in the wave equation.

On the other hand, the experimental achievements of BEC of ^{52}Cr [31], ^{164}Dy [32], ^{168}Er [33] and recently with a degenerate Fermi gas of ^{161}Dy [34] atoms with large magnetic dipolar interaction (6 μ_B, 10μ_B and 7μ_B, respectively) has opened promising perspectives for the observation of novel quantum phases and many-body phenomena [31, 35–37]. Polar molecules which have much larger electric dipole moments than those of the atomic gases have been also produced in their ground rovibrational state [38, 39]. The most important feature of these systems is that the atoms interact via a dipole-dipole interactions (DDI) that is both long-ranged and anisotropic.

In the past decade a great deal of attention has been paid to matter-wave solitons in dipolar BECs owing to their fascinating attributes, see for review [31, 35]. The nonlocality originating from the DDI may substantially affect the physics of solitons. The competition between local and nonlocal interactions leads to the formation of bright [40, 41] and dark [42, 43] soliton molecules. The stability and the dynamics of both bright and dark solitons in quasi-1D dipolar BEC have been studied in [40–42, 44–48]. In addition, discrete and vortex solitons have been analyzed in dipolar BECs [49–53]. It has been shown also that stable and mobile dark-in-bright solitons can be formed in dipolar binary BEC [54, 55]. On the other hand, anisotropic solitons have been predicted in dipolar BECs [44, 56–60] due to the anisotropy of the DDI. Unlike the short-range interacting condensates, quasi-2D and 3D dipolar BECs can support the emergence of stable solitons [56–58, 60, 61], where the famous ”snake” instability of dark solitons is suppressed [61]. Nonlocal solitons appear also in diverse nonlinear systems such as photorefractive and liquid crystals [62–68], and ballistic atomic transport [69].

0.3 Soliton molecules

A soliton molecule is a bound state of two or more solitons. Recently, the soliton molecules have attracted a great deal of interest both theoretically and experimentally. This is mainly motivated by the application of optical solitons as data carriers in optical fibers [70–90] and

the realization of matter-wave solitons in BEC [17, 91]. Such molecules permit to encode two bits of data per clock period and beyond, enabling to increase the data carrying capacity [30, 92, 93]. Many factors affect the stability of these molecules. The number of atoms, strength of atomic interactions and the radial wave trap frequency. More intriguing is the fact that relative phase $\Delta\Phi$ and speed v of solitons have a major effect on the formation of the molecule. Therefore, the force of interaction between the two solitons depends on their relative phase and the soliton separation, play also a crucial role on the stabilization of the soliton molecule.

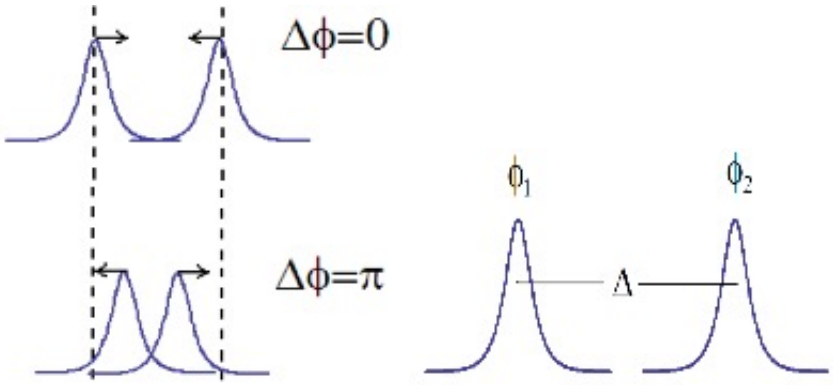

Figure 1: Characteristics of a two-solitons molecule, Δ is distance between the peaks position of the two solitons

Recently, two bright/dark nonlocal solitons molecules have attracted considerable interest in both nematic liquid crystals [94–104] and long-range dipolar BEC [43–45, 105]. Polar soliton molecules in biwire/bilayer systems were reported in [60, 61, 106]. Bound state of three interacting optical solitary waves propagating with angular momentum in bulk nematic liquid crystals was investigated in [107]. Most recently, the formation of matter wave nonlocal three soliton molecules and their normal modes have been investigated in Ref.[108].

0.4 This thesis

In the present thesis we investigate the stability, the scattering and the dynamics of nonlocal bright solitons and soliton molecules in 1D geometry. A special emphasis is paid on the properties of matter-wave solitons in dipolar BECs governed by the nonlocal GPE.

First, this manuscript deals with the propagation of 1D bright three-soliton molecules in a dipolar BEC with competing local and nonlocal nonlinearities by numerically and variationally solving the underlying the nonlocal GPE. A natural question here is, what degree of the local and nonlocal nonlinearities is necessary in order to observe a stable molecule ? Our analysis reveals that the soliton phase and the intersoliton sepration may strongly affect the the binding energy and the soltion width. A second outstanding question, however, is whether the molecular structure is preserved before and after the scattering of these composite nonlinear structures by Gaussian potential barrier. It is shown that a stable reflection is preserved only for a specific height and width of the barrier.

Another interesting configuration that can support nonlocal solitons is that of a biwire (tubes) system of a quasi-1D trap [60, 61, 106]. In this thesis we consider 1D dipolar BECs loaded in a biwire system where the dipole moments are assumed to be aligned perpendicularly to the tubes by an external field and in opposite directions in different wires. An understanding of these nonlocal solitons involves two questions:
i) how do the orientation of the dipoles in different wires affect the binding mechanism and the stability of these peculiar polar soliton molecules?
ii) what are the impacts of the degree of nonlocality and the interwire separation on the time evolution of the width and center-of-mass of such ensembles?

The last part of our work is devoted to construct, by means of the Darboux transformation method, exact new solutions to the NLSE. We first present the general approach and use an algebraically-decaying seed solution to obtain a local two-soliton solutions with diverging peaks, known as a singular bright soliton molecule. The equilibrium properties of these solitons are deeply examined. We then follow the same procedure to generate a new solution for the nonlocal NLSE. The obtained solution corresponds to the scattering of stationary soliton and two breathers on a finite background at half of space and inclined background at

the other half. The case of reverse-time nonlocal NLSE is also highlighted.

0.5 Outline

This thesis is organized as follows.

Chapter 1 is devoted to the relevant theoretical background to the topics addressed in this thesis. This will involve discussion of the local and nonlocal GPE, and the key physical properties of the condensate relevant for solitons. We briefly recall some of the different analytical methods available for constructing solitonic solutions that we use in the following chapters such as the variational method and Darboux transformation method.

Chapter 2 focuses on the equilibrium and scattering properties of 1D nonlocal bright three-soliton molecules in a dipolar BEC with competing local and nonlocal nonlinearities. We consider a suitable nonlocal response function and employ the variational approach to derive useful analytical expression for the energy of the three solitons. Our analysis reveals that the degree of nonlocality and the relative phase of solitons may strongly influence the binding energy and the soliton width. We then study the propagation and interaction of the three solitons using numerical simulations of the full nonlocal GPE. On the other hand, we investigate the scattering of these three-soliton molecules by Gaussian barrier and show that these molecular ensembles exhibit markedly different behavior due to the interaction with the potential barrier. To the best of our knowledge, this fascinating new result has never been existed before in the literature. Some of the results of this chapter are available in:
Equilibrium and scattering properties of a nonlocal bright three-soliton molecule, Mohammed Elhadj Khelifa and Abdelaali Boudjemaa, Phys. Scr. **96** *025212 (2021).*

Chapter 3 deals with the stability and the dynamics of 1D interwires polar soliton molecules in a biwire setup with dipole moments aligned perpendicularly to the line of motion and in opposite directions in different wires. Numercial results based on a nonlocal GPE point out the existence of a bound state leading to the formation of a molecule. We show that the degree of the nonlocality and the interwire separation play a chief role in equilibrium and the time evolution of the molecules. The most relevant results of this chapter are published in:

Interwires polar soliton molecules in a biwire system, Mohammed Elhadj Khelifa, Abdelaali Boudjemaa and U. Al-Khawaja, Phys. Scr. **94***, 085402 (2019).*

Chapter 4 is dedicated to derive an exact solution to the local and nonlocal NLSE employing the Darboux transformation method. This method is one of the strongest methods to find the exact solutions to the NLSE. Using an algebraically-decaying seed solution, we obtain a two-soliton solution with diverging peaks, which we denote as singular soliton molecule. We find that the new solution has a finite binding energy. We calculate the force and potential of interaction between the two solitons, which turn out to be of molecular-type. The new solution describes the profile and dynamics of a two-soliton molecule. We then extend our study to the nonlocal NLSE using the same method and seed solution. The new solution in this case corresponds to an elastic collision of a soliton, a breather soliton on flat background, and a breather soliton on a background with linear ramp. Finally, we consider an NLSE which is nonlocal in time rather than space. The results presented in this chapter have been the object of the following paper:
Singular Soliton Molecules of Local and Nonlocal Nonlinear Schrödinger Equations, Mohammed Elhadj Khelifa, Laila Al Sakkaf, U. Al-Khawaja, and Abdelâali Boudjemâa, Phys. Rev. E **101***, 042221 (2020).*

Last part concludes the thesis. We first summarize the content of each chapter and then discuss prospects for future works.

Contents

List of Figures

Chapter 1

Gross-Pitaevskii Equation

Contents

1.1 Introduction

In this chapter we briefly review the basics of BEC with short-ranged contact interactions as well as its mean-field description and collective excitations. Presentation of soliton theory is given with solutions to the 1D GPE. We then move on to present the relevant two-body interactions in a dipolar BEC and discuss its stability.

1.2 Gross-Pitaevskii Equation

Let us consider a system of a dilute trapped Bose gas. The many-body problem can be described within the framework of second quantization, where the second-quantized Hamiltonian for the Bose field operator is expressed as,

$$\hat{H} = \int d\mathbf{r}\,\hat{\Psi}^{\dagger}(\mathbf{r}) h^{sp} \hat{\Psi}(\mathbf{r}) + \frac{1}{2}\int d\mathbf{r} \int d\mathbf{r}' \hat{\Psi}^{\dagger}(\mathbf{r})\hat{\Psi}^{\dagger}(\mathbf{r}')V(\mathbf{r}-\mathbf{r}')\hat{\Psi}(\mathbf{r}')\hat{\Psi}(\mathbf{r}), \tag{1.1}$$

where $\hat{\Psi}^{\dagger}$ and $\hat{\Psi}$ denote, respectively the usual creation and annihilation field operators, satisfying the usual canonical commutation rules $[\hat{\Psi}(\mathbf{r}), \hat{\Psi}^{\dagger}(\mathbf{r}')] = \delta(\mathbf{r}-\mathbf{r}')$, $[\hat{\Psi}(\mathbf{r}), \hat{\Psi}^{(}\mathbf{r}')] = [\hat{\Psi}^{\dagger}(\mathbf{r}), \hat{\Psi}^{\dagger}(\mathbf{r}')] = 0$, and $h^{sp} = -(\hbar^2/2m)\Delta + U(\mathbf{r})$ is the single particle Hamiltonian, with $U(\mathbf{r})$ being the external trap. Here $V(\mathbf{r}-\mathbf{r}')$ is the two-body interaction potential. For dilute gases at very low temperature, the common procedure is to approximate the true interatomic interaction by a "contact" potential which is short-range and isotropic

$$V(\mathbf{r}-\mathbf{r}') = g_{3D}\delta(\mathbf{r}-\mathbf{r}'), \tag{1.2}$$

where $g_{3D} = 4\pi\hbar^2 a/m$ is the coupling constant and a is the s-wave scattering length. This potential means that the interatomic forces are important only when the atoms are close to each other.

Substitution into the Hamiltonian (1.1) then gives

$$\hat{H} = \int d\mathbf{r}\,\hat{\Psi}^{\dagger}(\mathbf{r}) h^{sp} \hat{\Psi}(\mathbf{r}) + \frac{g_{3D}}{2}\int d\mathbf{r}\hat{\Psi}^{\dagger}(\mathbf{r})\hat{\Psi}^{\dagger}(\mathbf{r})\hat{\Psi}(\mathbf{r})\hat{\Psi}(\mathbf{r}). \tag{1.3}$$

Hamiltonian (1.3) allows for finding the time evolution of the field operators. Using the Heisenberg equation and the commutation rules, we obtain the equation of motion:

$$i\hbar\frac{\partial}{\partial t}\hat{\Psi}(\mathbf{r},t) = \left[\hat{\Psi}(\mathbf{r},t),\hat{H}\right] = \left(\frac{-\hbar^2}{2m}\Delta + U(\mathbf{r}) + g_{3D}\hat{\Psi}^{\dagger}(\mathbf{r})\hat{\Psi}(\mathbf{r})\right)\hat{\Psi}(\mathbf{r}). \tag{1.4}$$

Let us now devide the Bose-field operator into two parts: the condensate contribution ψ (c-number), which corresponds to the macroscopic occupation of a single quantum state and noncondensed part $\hat{\tilde{\Psi}}$ which corresponds to thermally-excited atoms, quantum fluctuations.

$$\hat{\Psi}(\mathbf{r},t) = \psi(\mathbf{r},t) + \hat{\tilde{\Psi}}(\mathbf{r},t). \tag{1.5}$$

At $T = 0$, almost of the particles are in the condensate state and owe to the weakly-interacting nature of the condensate. Therefore, the noncondensate operator can be neglected ($\hat{\tilde{\Psi}} = 0$), we consider only the classical field $\hat{\tilde{\Psi}} = \psi$ in the Hamiltonian (1.3). Note that the assumption of zero temperature is generally satisfied in reality for temperatures much less than the transition temperature for condensation. The exact Heisenberg equation of motion (1.4) reduces then to the so-called local GPE [1, 2]

$$i\hbar\frac{\partial\psi(\mathbf{r},t)}{\partial t} = \left(\frac{-\hbar^2}{2m}\Delta + U(\mathbf{r}) + g_{3D}|\psi(\mathbf{r},t)|^2\right)\psi(\mathbf{r},t). \tag{1.6}$$

The function ψ is a classical field having the meaning of an order parameter and is often called the "wave function of the condensate". Equation (1.6) is nothing else than the nonlinear Schrödinger equation, corresponding to the zero temperature hydrodynamic description of Bose gases, first introduced to study vortex lines in an imperfect Bose gas. Its validity is based on the condition that the *s*-wave scattering length be much smaller than the average distance between atoms and for large number of atoms in the condensate $N \gg 1$. An analytical solution of equation (1.6) is in general not possible and the use of numerical tools becomes necessary. However, there is a useful approximation such as the Thomas-Fermi approximation or a variational method in the stationary case, which provide some analytical insights.

The stationnary solutions can be found via the transformation:

$$\psi(\mathbf{r},t) = \psi(\mathbf{r})\exp(-i\mu t/\hbar), \tag{1.7}$$

where μ is the chemical potential. Substituting (1.7) into (1.6) yields the time-independent GPE:

$$\left(\frac{-\hbar^2}{2m}\Delta + U(\mathbf{r}) + g_{3D}|\psi(\mathbf{r})|^2 - \mu\right)\psi(\mathbf{r}) = 0. \tag{1.8}$$

Here the wave function is normalized to the total number of particles, i.e. $\int |\psi|^2 d^d r = N$. The GP equation gives a good description of the condensate dynamics, including the oscillations of collective modes, the time evolution of solitons and vortices, and interference effects associated with the phase of the condensate's order parameter (see for books [109, 110]).

1.3 Excitations in Bose condensates

The study of the excitation of an inhomogeneous system (small amplitude oscillations) can be done by linearizing the GPE (1.6) around a static solution (weak perturbations). To do so, we consider the wavefunction of the form:

$$\psi(\mathbf{r},t) = [\psi_0(\mathbf{r}) + \delta\psi(\mathbf{r},t)]\, e^{-i\mu t/\hbar}, \tag{1.9}$$

where $\delta\psi/\psi_0 \ll 1$.
The left-hand side of equation (1.6) becomes $i\hbar\frac{\partial\psi(\mathbf{r},t)}{\partial t} = e^{-i\mu t/\hbar}\left[\mu\psi_0 + \mu\delta\psi + i\hbar\frac{\partial\delta\psi}{\partial t}\right]$.
The zeroth order gives the stationary GPE

$$\mu\psi_0 = h^{sp}\psi_0(\mathbf{r}) + g_{3D}|\psi_0|^2\psi_0. \tag{1.10}$$

The first order terms yield

$$i\hbar\frac{\partial\delta\psi}{\partial t} = \left[h^{sp} + 2g_{3D}|\psi_0|^2 - \mu\right]\delta\psi + g_{3D}\psi_0^2\delta\psi^*. \tag{1.11}$$

Now we solve equation (1.11) with the ansatz

$$\delta\psi(\mathbf{r},t) = u_k(\mathbf{r})e^{-i\varepsilon_k t/\hbar} + v_k(\mathbf{r})e^{i\varepsilon_k t/\hbar}, \tag{1.12}$$

which leads we to a set of coupled equations in terms of the Bogoliubov quasi-particle amplitudes $u_k(\mathbf{r})$ and $v_k(\mathbf{r})$. They can be written in the form of a matrix equation

$$\begin{pmatrix} \hat{\mathscr{L}} & \mathscr{M} \\ \mathscr{M}^* & \hat{\mathscr{L}} \end{pmatrix} \begin{pmatrix} u_k(\mathbf{r}) \\ v_k(\mathbf{r}) \end{pmatrix} = \varepsilon_k \begin{pmatrix} u_k(\mathbf{r}) \\ -v_k(\mathbf{r}) \end{pmatrix}, \tag{1.13}$$

where $\hat{\mathscr{L}} = h^{sp} - \mu + 2g_{3D}|\Phi_0|^2$ and $\mathscr{M} = g_{3D}\Phi_0^2$.
Equation (1.13) are called the Bogoliubov-de-Gennes equations (BdG) for elementary excitations of a dilute Bose gas. They give the eigenfunctions and eigenfrequencies of the excitations.

For a homogeneous system ($U(\mathbf{r}) = 0$) with background density n and chemical potential $\mu = ng_{3D}$. Due to the translational invariance the solutions may be chosen of the form $u_k(\mathbf{r}) = u_k e^{i\mathbf{k}.\mathbf{r}}$ and $v_k(\mathbf{r}) = v_k e^{i\mathbf{k}.\mathbf{r}}$, which reduces the set (1.13) to

$$\begin{pmatrix} E_k + ng_{3D} - \varepsilon_k & ng_{3D} \\ ng_{3D} & E_k + ng_{3D} + \varepsilon_k \end{pmatrix} \begin{pmatrix} u_k \\ v_k \end{pmatrix} = 0, \tag{1.14}$$

where $E_k = \hbar^2 k^2/2m$ is the energy of free particle and $u_k, v_k = (\sqrt{\varepsilon_k/E_k} \pm \sqrt{E_k/\varepsilon_k})/2$.
Solutions to this matrix equation gives the famous Bogoliubov [12] spectrum of a dilute Bose gas

$$\varepsilon_k = \sqrt{E_k^2 + 2E_k n g_{3D}}. \tag{1.15}$$

For small momenta $k \to 0$, the dispersion law (1.15) is linear in k and well approximated by the phonon-like linear dispersion form

$$\varepsilon_k = \hbar c_s k, \tag{1.16}$$

where $c_s = \sqrt{ng_{3D}/m}$ is the sound velocity.

In the limit of large momenta, the Bogoliubov dispersion law (1.15) reduces to the free-particle form $\varepsilon_k = E_k$.

The balance between the linear (the interaction energy, $g_{3D}n$) and the quadratic (kinetic energy) spectrum occurs at the length scale $\xi = \hbar/\sqrt{mng_{3D}}$. This distance defines the healing length of the fluid, which characterises the length scale over which the fluid density can respond to perturbation. For length scales longer than ξ atoms move collectively and for shorter length scales these behave as free particles.

1.4 Quasi-one-dimensional GPE equation

By employing highly-anisotropic trap geometries it is possible to engineer the effective dimensionality of the condensate. Consider a cylindrically-symmetric trap geometry $U(r) = m\omega_\rho^2(\rho^2 + \lambda^2 z^2)/2$, where $\rho^2 = x^2 + y^2$, ω_ρ and ω_z are the radial and the longitudinal trap frequencies, respectively, and $\lambda = \omega_z/\omega_\rho$ is anisotropy parameter which defines three types of condensates:

i) $\lambda = 1$, the BEC is spherical.

ii) $\lambda > 1$, the condensate takes the form of disk- or pancake-shaped (quasi-2D).

iii) $\lambda < 1$, the BEC adopts the highly-elongated "cigar"-shape (quasi-1D).

The quasi-1D limit occurs using the adiabatic approximation which considers that in a cigar-shaped trap with tight radial binding the dynamics takes place along the axial direction and in the transverse direction the condensate wavefunction remains in the ground state [111–113]. It is then instructive to separate the wavefunction into the product of a time-dependent axial component and a time-independent transverse component,

$$\psi(\rho,z,t) = \psi(\rho)\psi(z,t) = \sqrt{m\omega_\rho/\pi\hbar}e^{-m\omega_\rho\rho^2/2\hbar}\psi(z,t). \tag{1.17}$$

Substituting these approximations into equation (1.6), we arrive at an effective 1D GPE,

$$i\hbar\frac{\partial\psi(z,t)}{\partial t} = -\frac{\hbar^2}{2m}\frac{\partial\psi}{\partial z^2} + \left[U(z) + g|\psi(z,t)|^2\right]\psi(z,t), \tag{1.18}$$

where $g = g_{3D}/4\pi l_0^2$ is 1D coupling constant, and $l_0 = \sqrt{\hbar/m\omega_\rho}$ is the transverse harmonic oscillator length, and the usual harmonic potential $U(z) = m\omega_z^2 z^2/2$. In the absence of the external potential, the 1D GPE (1.18) is identical in form to the integrable NLSE and hence, will admit the soliton solutions derived in the 1970's [13, 14].

Equation (1.18) can be further reduced to dimensionless form by introducing variables: $x \to z/l_0$, $t \to t\omega$, $\psi \to \sqrt{2a}\psi$, and $g \to g_c$

$$i\frac{\partial\psi(x,t)}{\partial t} = -\frac{1}{2}\frac{\partial\psi}{\partial x^2} + \left[U(x) + g_c|\psi(x,t)|^2\right]\psi(x,t), \tag{1.19}$$

Although the presence of a weak axial trap $U(x)$ breaks the integrability of the governing equation, many properties of localized states remain close to those of the classical solitons, as demonstrated in the recent experiment [114].

1.5 Dark and bright solitons

A- Dark solitons

A-1 Static dark solitons

Let us consider a stationary 1D GPE for $g_c > 0$ (repulsive interactions) in the absence of the external potential ($U(x) = 0$) and assume that the condensate wavefunction ψ is real:

$$\left(\frac{1}{2}\frac{d\psi}{dx^2} + g_c\psi^2 - \mu\right)\psi = 0. \tag{1.20}$$

The chemical potential can be approximated to the uniform Bose gas, $\mu = g_c|\psi_0(x,t)|^2 = g_c n$ with ψ_0 is the bulk wave function, and n is the density of the bulk. Multiplying equation (1.20) by $d\psi/dx$ and integrating over dx, we have:

$$\frac{1}{2}\int_{x_0}^{x} dx\frac{d\psi}{dx}\frac{d^2\psi}{dx^2} = g_c\int_{\psi_0}^{\psi}\left(\psi^3 - \psi_0^2\,\psi\right)d\psi. \tag{1.21}$$

This gives

$$\frac{1}{g_c}\left(\frac{d\psi}{dx}\right)^2 = \frac{1}{4}\left(\psi^2 - \psi_0^2\right)^2. \tag{1.22}$$

Integrating (1.22), we immediately obtain

$$\psi = \psi_0 \tanh(x/2\sqrt{\xi}), \tag{1.23}$$

where $\xi = 1/\sqrt{g_c n}$ is the healing length. According to the solution (1.23), the soliton wavefunction approaches its bulk value ψ_0 for $x \sim \xi$. The profiles from (1.23) are displayed in Figure.1.1.

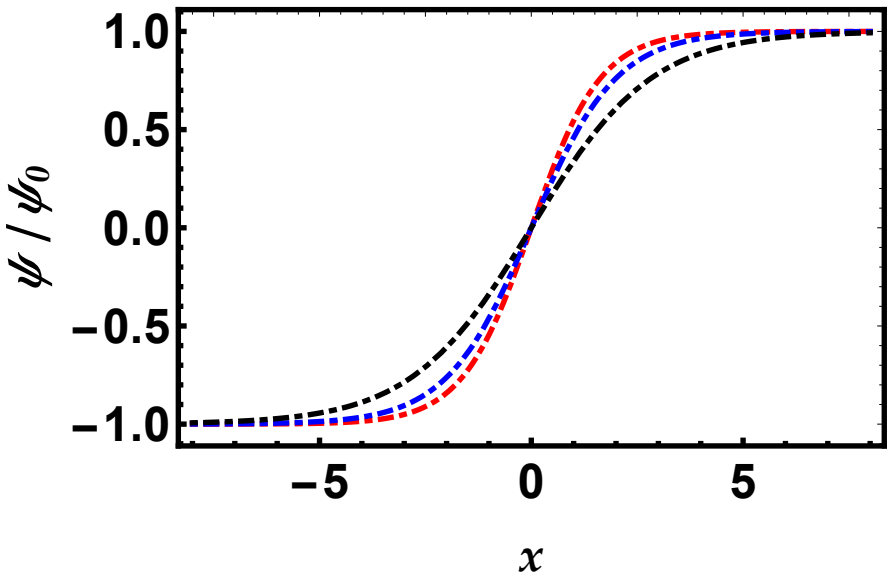

Figure 1.1: Soliton profile for different values of ξ. Black line : $\xi = 0.5$, blue line : $\xi = 1$, and the red line : $\xi = 1.5$.

A-2 Moving dark solitons

We now analyze moving dark solitons which obay the time-dependent GPE (1.19). Writting the wave function as:

$$\psi(x,t) = \psi(x) e^{(-i\mu t)} \tag{1.24}$$

In free space, the 1D GPE (1.18) takes the form:

$$i\frac{d\psi(x,t)}{dt} + \left[\frac{1}{2}\frac{d^2}{dx^2} - g_c|\psi(x,t)|^2 - \mu\right]\psi(x,t) = 0, \tag{1.25}$$

We then suppose that the function ψ depends only on the variable $x-vt$, where v is the soliton velocity. So, it is useful to represent the ψ as:

$$\psi(x,t) = \sqrt{n} f[(x-vt)/\xi]. \tag{1.26}$$

For $|z| = |x-vt|/\xi \to \infty$, one has $f \to 1$ and $df/dz \to 0$. Thus, equation (1.25) simplifies to

$$i\frac{v}{c_s}\frac{df}{dt} = \frac{1}{2}\frac{d^2f}{dz^2} + (1-|f|^2)f, \tag{1.27}$$

where $c_s = 1/\sqrt{\mu}$ is the sound velocity. Writting $f = f_1 + if_2$, where f_1 and f_2 are real. Then, we find after some algebra

$$\psi(x,t) = \sqrt{n}\left\{ i\frac{v}{c_s} + \sqrt{1-\frac{v^2}{c_s^2}}\tanh\left[\frac{x-vt}{\xi}\sqrt{1-\frac{v^2}{c_s^2}}\right]\right\}. \tag{1.28}$$

Hence, the density reads

$$n(x,t) = n\left\{ \frac{v^2}{c_s^2} + \left(1-\frac{v^2}{c_s^2}\right)\tanh^2\left[\frac{x-vt}{\xi}\sqrt{1-\frac{v^2}{c_s^2}}\right]\right\}. \tag{1.29}$$

The density has a minimum $n_{min} = nv^2/c_s^2$ in the center of the soliton. For $v = 0$, the minimum is zero and this solution corresponds to a static dark sotion. Whereas for $v \neq 0$, the minimum does not reach zero, and thus, solitons are called gray. For $v = c_s$, the grey soliton is transformed into a uniform BEC with $|\psi| = \sqrt{n}$. For increasing velocity, the density dip get smaller, and soliton width $\xi/\sqrt{1-v^2/c_s^2}$ broadens as is seen in figure 1.2.

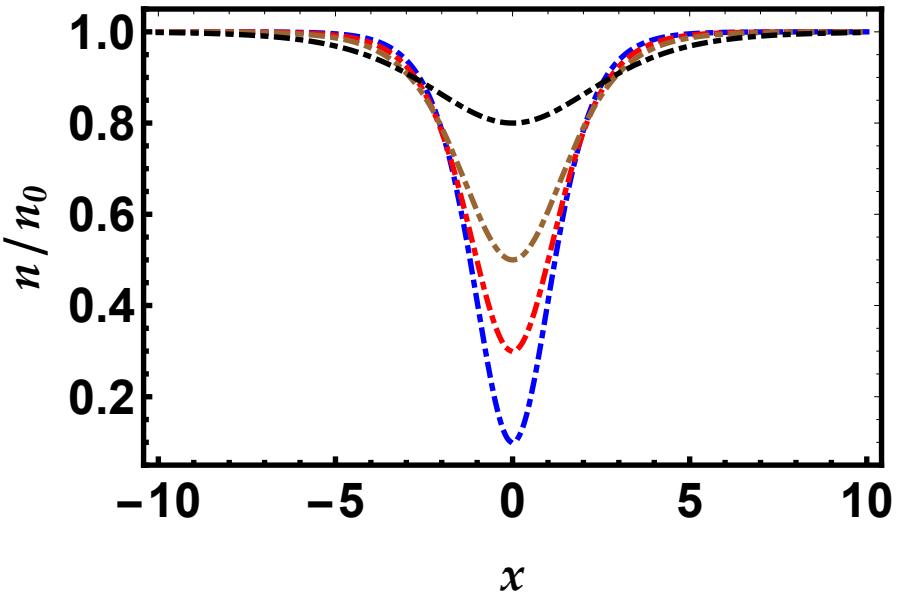

Figure 1.2: Density profile of drak soliton for different values of parameter $\alpha = v^2/c_s^2$, Blue color: $\alpha = 0.1$, red color: $\alpha = 0.3$, brown color: $\alpha = 0.5$ and $\alpha = 0.8$ for the black color $g_c = 1$.

A-3 Soliton energy

The energy of dark solitons is defined as

$$E_s = \int_{-\infty}^{\infty} dx \left[\frac{1}{2} \left| \frac{d\psi}{dx} \right|^2 + g|\psi(x,t)|^4 - \frac{Ng_c}{2} |\psi(x,t)|^2 \right], \tag{1.30}$$

Using the identity $\int_{-\infty}^{\infty} dy \, \mathrm{sech}^4 y = 4/3$, we get

$$E_s = \frac{Mc_s^2}{3} \left(1 - \frac{v^2}{c_s^2} \right)^{3/2}, \tag{1.31}$$

where $M = 4n\xi$ is the soliton mass. Equation (1.31) shows that the dark soliton energy decreases with rising its velocity.

B- Bright solitons

B-1 Static bright solitons

We turn now to discuss bright solitons which can be obtained from the 1D GPE for attractive interactions $g < 0$ and the chemical potential thus become negative ($\mu < 0$). Assuming that the condensate wave function is real:

$$\left(-\frac{1}{2}\frac{d}{dx^2} - g_c\psi - \mu\right)\psi = 0. \tag{1.32}$$

Following the same procedure outline for dark solitons. Multiplying equation (1.20) by $\frac{d\psi}{dx}$ and integrating over dx, we get:

$$\left(\frac{d\psi}{dx}\right)^2 = -\left(g_c\psi^2 + 2\mu\psi^2 - C\right), \tag{1.33}$$

where C is the integration constant. Assumig that at certain point say $x = 0$, $d\psi/dx = 0$, equation (1.33) yields

$$\left(\frac{d\psi}{dx}\right)^2 = -\left[g_c\psi^2 + 2\mu\psi^2 - g_c\psi^2(0) - 2\mu\psi^2(0)\right], \tag{1.34}$$

Using the boundary conditions $\psi(\infty) = 0$ and integrating this equation, we arrive at the solution

$$\psi = \sqrt{n_0}\,\mathrm{sech}\left(\frac{x}{\xi}\right), \tag{1.35}$$

where $\xi = 1/\sqrt{gn(0)}$ is the heanling length characterizes the soliton width with $n(0)$ being the central density. The profiles of such solitons are shown in figure 1.3.

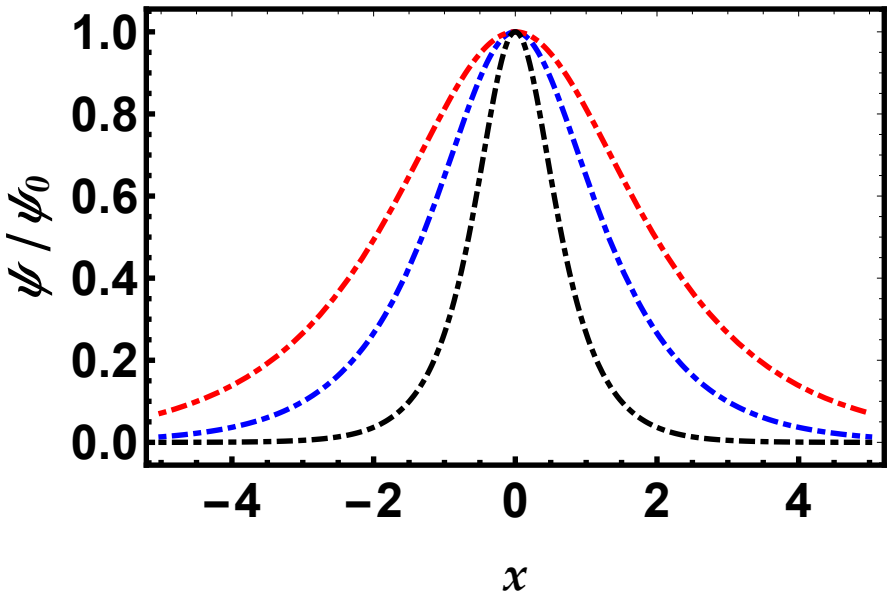

Figure 1.3: Density profile for the bright soliton for different values of ξ. Black line : $\xi = 0.5$, blue line: $\xi = 1$ and for the Red line: $\xi = 1.5$.

B-1 Moving bright solitons

Analytical moving bright solitons can be found in more detail through the inverse scattering transform [13, 14], by means of the Galilean invariance of the wave function to the GPE, or by solving the Bogoliubov-de-Gennes equations. Let us employ the Galilean invariance, thus

$$\psi(x,t) \rightarrow \psi(x-vt,t)\exp\left[i(vx-v^2t/2)\right] \tag{1.36}$$

In the frame of the hydrodynamic approach, where the fluid moves with velocity v, the wavefunction turns out to be given as: $\psi(x,t) = \sqrt{n_0}\exp(i\theta)$, where the phase

$$\theta(x,t) = vx - (\mu + v^2/2)t. \tag{1.37}$$

The superfluid velocity is given by $v = \partial\theta(x,t)/\partial x$. Inserting these transformations into the time-dependent GEP, we obtain

$$\psi = \sqrt{n_0}\,\mathrm{sech}\left(\frac{x-vt}{\xi}\right)\exp\{-i[-vx+(\mu+v^2/2)t]\}. \tag{1.38}$$

We see that the velocity of bright soliton can exceed the sound velocity in contrast to the dark soliton.

1.6 Dipole-dipole interactions

In this section we illustrate the relevant two-body interactions in a dipolar BEC. The dipolar interactions can be found in a broad class of systems as they can be realized via electric or magnetic forces and are extensively studied in the context of highly magnetic atoms [31–33], polar molecules [115–123], and Rydberg gases [124–129]. More detailed can be found in the review articles [31, 35–37]. The DDI potential between two particles with dipole moments oriented along the unit vectors e_1 and e_2 reads

$$V_{dd} = \frac{C_{dd}}{4\pi}\frac{(\mathbf{e_2}.\mathbf{e_2})r^2 - 3(\mathbf{e_1}.\mathbf{r})(\mathbf{e_2}.\mathbf{r})}{r^5}, \tag{1.39}$$

where C_{dd} is the dipolar interaction strength which takes the form $C_{dd} = \mu_0\,\mu^2$ where μ_0 is the vacuum permeability and μ the magnetic dipole moment. For electric dipoles, $C_{dd} = \frac{d^2}{\varepsilon_0}$, where d is the electric dipole moment and ε_0 the vacuum permitivity. When the dipoles are polarized by an external electric or magnetic field in the same direction, where $\mathbf{e_1}.\mathbf{e_2} = \mathbf{1}$ and $\mathbf{e_1}.\mathbf{r} = \mathbf{e_2}.\mathbf{r} = \mathbf{r}\cos\theta$, the expression for the dipolar potential (1.39) turns out to be given:

$$V_{dd}(\mathbf{r}) = \frac{C_{dd}}{4\pi}\frac{(1-3\cos^2\theta)}{r^3}, \tag{1.40}$$

where θ is the angle between the position of the particles and the polarization.

The DDI is anisotropic as it repulsive if they are side by side (see figure 1.4.a), and attractive between two dipoles placed in a head-to tail configuration (see figure 1.4.b), and vanishing at the magic ($\theta = \arccos(1/3) = 54,7$) angle. The configuration depicted in figure 1.4.c represents the polarization case while the fourth configuration show s non-polarized case (see figure 1.4.d). Additionally, the DDI in contrast to short-range contact interaction (1.2), is long-ranged as it decays with a power law of $\frac{1}{r^3}$ and anisotropic since the strength and sign of the interaction depend on the angle θ between the polarization direction and the relative position of the particles. We refer the reader to the review articles [31, 35–37] for

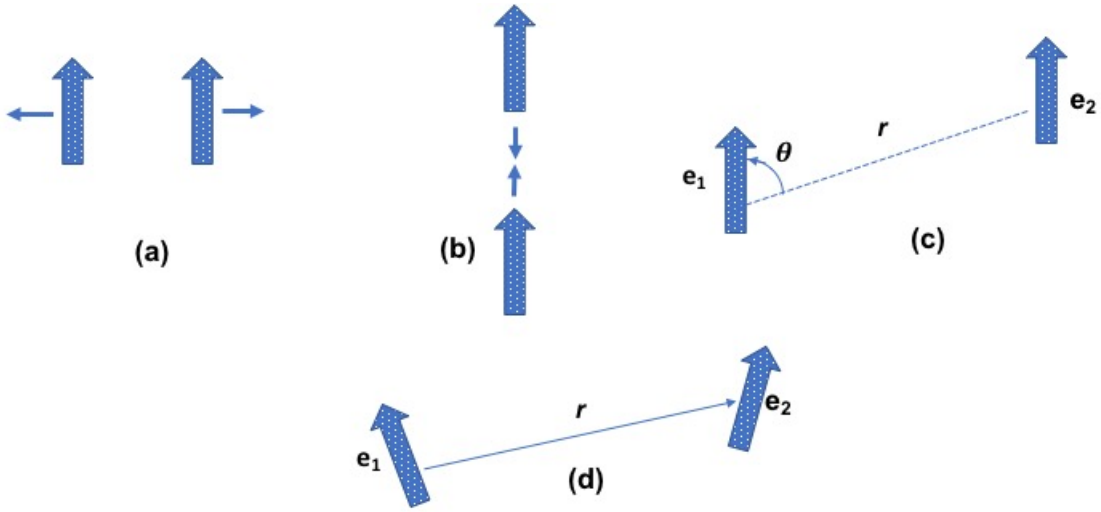

Figure 1.4: Two polarized dipoles interacting with each other via the DDI separated by the distance r. The interaction strength depends on the angle θ, leading to an attractive interaction for dipoles in a head-to tail configuration ($\theta = 0$), whereas dipoles sitting besides each other repel ($\theta = \pi/2$) [31].

more details and references therein.

1.6.1 Fourier Transfrom

The Fourier transformed dipole-dipole potential is used in many calculations involving the dipolar interaction. It is defined as:

$$V_{dd}(\mathbf{k}) = \int V_{dd}(\mathbf{r}) e^{-i\mathbf{k}.\mathbf{r}} d^d r. \tag{1.41}$$

In 3D, Fourier integral (1.41) can be evaluated by expanding the exponential factor $e^{-i\mathbf{k}.\mathbf{r}}$ in terms of spherical harmonics and using the identity $-4\sqrt{\pi/5}Y_2^0(\theta,\varphi) = 1 - 3\cos^2\theta$, where $Y_2^0(\theta,\varphi)$ is the spherical harmonic, we find [31, 35]

$$V_{dd}(\mathbf{k}) = \frac{C_{dd}}{3}(3\cos^2\theta_k - 1), \tag{1.42}$$

where θ_k is the angle between the vector $\mathbf{k}$ and the polarization direction. Unlike the DDI in position space the Fourier transform $V_{dd}(\mathbf{k})$ does not diverge or posses any singular points.

1.7 Nonlocal Gross-Pitaevskii equation

If the interaction (1.40) in addition to the contact interaction (1.2) is taken into account, the well known GPE (1.6) gets the form

$$i\hbar\frac{\partial\psi(\mathbf{r},t)}{\partial t}=\left[\frac{-\hbar^2}{2m}\Delta+U(\mathbf{r})+g_{3D}|\psi(\mathbf{r},t)|^2+\int d\mathbf{r}'V_{dd}(\mathbf{r}-\mathbf{r}')|\psi(\mathbf{r}',t)|^2\right]\psi(\mathbf{r},t). \quad (1.43)$$

The GPE for a dipolar BEC becomes an integro-differential equation for the condensate wave function. In the absence of the nonlocal integral term, equation (1.43) simplifies to the local GPE (1.6). The nonlocality of DDI implies that the wavefunction in r depends on the wavefunction in r' through a kernel $V_{dd}(\mathbf{r}-\mathbf{r}')$.

In quasi-1D geometry, the dimensionless nonlocal GPE can be obtained by just adding the new variable $g_d \to C_{dd}/\sqrt{l^3\hbar\omega}$ to the local GPE (1.43):

$$i\frac{\partial\psi(x,t)}{\partial t}=-\frac{1}{2}\frac{\partial\psi}{\partial x^2}+\left[U(x)+g|\psi(x,t)|^2+g_d\int dx'V_{dd}(x-x')|\psi(x',t)|^2\right]\psi(x,t), \quad (1.44)$$

For $V_{dd}=0$, and $U(x)=0$, equation (1.44) reduces to the well-known 1D NLSE. With the nonlocal GPE (1.44) we will study in next chapters the interaction of solitons and soliton molecules in a dipolar BEC for various configurations.

1.7.1 Phonon Instability

Let us try to understand the stability of 3D homogeneous dipolar BEC. After inserting the transformation (1.12) into the nonlocal GPE (1.43), we obtain the generalized nonlocal BdG equations

$$\begin{aligned}\varepsilon_k u_k(\mathbf{r}) &= \hat{\mathscr{L}}u_k(\mathbf{r})+\hat{\mathscr{M}}v_k(\mathbf{r})+\int d\mathbf{r}'V_{dd}(\mathbf{r}-\mathbf{r}')n(\mathbf{r},\mathbf{r}')u_k(\mathbf{r}') \quad (1.45)\\ &\quad+\int d\mathbf{r}'\Phi_0(\mathbf{r}')V_{dd}(\mathbf{r}-\mathbf{r}')\Phi_0(\mathbf{r})v_k(\mathbf{r}'),\\ -\varepsilon_k v_k(\mathbf{r}) &= \hat{\mathscr{L}}v_k(\mathbf{r})+\hat{\mathscr{M}}u_k(\mathbf{r})+\int d\mathbf{r}'V_{dd}(\mathbf{r}-\mathbf{r}')n(\mathbf{r},\mathbf{r}')v_k(\mathbf{r}') \quad (1.46)\\ &\quad+\int d\mathbf{r}'\Phi_0(\mathbf{r}')V_{dd}(\mathbf{r}-\mathbf{r}')\Phi_0(\mathbf{r})u_k(\mathbf{r}'),\end{aligned}$$

where $\hat{\mathscr{L}} = h^{sp} + 2gn(\mathbf{r}) + \int d\mathbf{r}' V_{dd}(\mathbf{r}-\mathbf{r}')n(\mathbf{r}') - \mu$, $\hat{\mathscr{M}} = g\Phi_0^2(\mathbf{r})$, $n(\mathbf{r},\mathbf{r}') = \Phi_0^*(\mathbf{r}')\Phi_0(\mathbf{r})$. The solution of equations (1.45) and (1.46) gives the eigenfunctions $u_k(\mathbf{r}), v_k(\mathbf{r})$ of the excitations which obey the normalization condition: $\int d\mathbf{r}[u_k^*(\mathbf{r})u_{k'}(\mathbf{r}) - v_k^*(\mathbf{r})v_{k'}(\mathbf{r})] = \delta_{kk'}$ and the corresponding Bogoliubov eigenfrequencies ε_k

$$\varepsilon_k = \sqrt{E_k^2 + 2E_k g_{3D} n[1 + \varepsilon_{dd}(3\cos^2\theta_k - 1)]}, \tag{1.47}$$

where $\varepsilon_{dd} = C_{dd}/3g_{3D}$ is the dimensionless relative strength which describes the interplay between the DDI and short-range interactions. Note that for $\varepsilon_{dd} > 1$ the DDIs are donimant. Unlike the case of contact interactions, the dispersion relation of a dipolar BEC (1.47) has an anomalous momentum dependence due to the momentum dependence of the DDI. In the low momenta limit $k \to 0$, the Bogoliubov spectrum reduces:

$$\varepsilon_k = \hbar c_s k\sqrt{1 + \varepsilon_{dd}(3\cos^2\theta_k - 1)}, \tag{1.48}$$

where $c_s = \sqrt{gn/m}$ is the sound velocity for a nondipolar BEC. It is evident that for $\theta_k = \pi/2$, $\varepsilon_k = \hbar c_s k\sqrt{1-\varepsilon_{dd}}$ indicating that for $\varepsilon_{dd} > 1$, some excitation modes are purely imaginary. Therefore, the homogeneous 3D dipolar BEC is dynamically unstable against long-wave length excitations. We call this instability "phonon instability" [31]. We shall see in chapter 3 that this phonon instability plays a crucial role in the formation of bright polar soliton molecules in a biwire system.

Chapter 2

Chapter 2

Equilibrium and scattering properties of a nonlocal bright three-soliton molecule in dipolar Bose-Einstein condensates with competing nonlinearities

Contents

2.1 Introduction

Recently, solitons in nonlocal media have attracted considerable interest both theoretically and experimentally (see for review [130, 131]) owing to their potential applications to signal processing and communications.

The aim of this chapter is to study the equilibrium and scattering properties of 1D nonlocal bright three-soliton molecules in dipolar BEC with competing local and nonlocal nonlinearities. In dipolar condensates, competing nonlinearities appear naturally with the simultaneous presence of contact (local) and dipolar (nonlocal) interaction potentials that can be controlled with help of Feshbach resonance. We consider a suitable nonlocal response function and employ the variational approach to derive useful analytical expression for the energy of the three solitons. We show in particular that such an energy is finite and has a local minimum depending on the medium parameters. An increasing energy corresponds to attraction between the two solitons, while a decreasing potential corresponds to repulsion. Our analysis reveals also that the degree of nonlocality and the relative phase of solitons may drastically influence the binding energy and the soliton width. We then study the propagation and interaction of the three solitons using numerical simulations of the full nonlocal (GPE). We proceed to look at how the variation of the separation between adjacent solitons and the relative phase can perturb the molecule.

On the other hand, we investigate the scattering of the three-soliton molecules by Gaussian barrier. The interaction of matter-wave solitons with a potential barrier is crucial for soliton matter-wave interferometry [132]. Recently, the scattering of dipolar and nondipolar two-soliton molecules by Gaussian potential barriers and wells has been studied in Ref.[133, 134]. We reveal the role of solitons velocity, barrier height and its width in the soliton width and in the intersoliton separation. We also show that such molecular ensembles can be reflected/transmitted through the barrier depending on the barrier height and soliton velocity. The calculation is performed using a variational scheme and the findings are checked by numerically solving the underlying nonlocal GPE.

2.2 Nonlocal Gross-Pitaevskii equation

We recall that to construct soliton states, we consider the 1D nonlocal GPE (1.44)

$$i\frac{\partial\psi}{\partial t} = -\frac{1}{2}\frac{\partial^2\psi}{\partial x^2} + U(x)\psi - g_c|\psi|^2\psi \\ - g_d\psi\int R(|x-x'|)|\psi(x',t)|^2dx', \tag{2.1}$$

where $\psi(x,t)$ accounts for the mean-field wavefunction, g_c and g_d represent, respectively the strengths of the local contact and the dipole-dipole nonlocal interactions, and $U(x)$ is an external potential. The response function $R(x)$ explains the nonlocal nonlinearity. In the local response limit, $R(x) = \delta(x)$, equation (2.1) simplifies to the standard NLSE. For analytical tractability, we will employ a Gaussian nonlocal response function

$$R(x) = \frac{1}{\sqrt{2\pi}\sigma}\exp\left(-\frac{x^2}{2\sigma^2}\right), \tag{2.2}$$

The function (2.2) is sufficient for understanding the considered problem and it may capture the main properties of soliton molecules in dipolar BEC [108, 135]. Very recently, it has been checked that all the results obtained from Gaussian kernel (2.2) for three soliton molecules [108, 135] can be qualitatively preserved when the calculations are performed with physically more realistic dipole-dipole nonlocal interaction kernel function [40, 136]. Note that other types of localized response functions have been used to study of the effect of nonlocality, such as Lorentzian, Gaussian, periodic, and rectangular functions [137]. In the weakly nonlocal limit i.e. $\sigma \ll 1$, equation (2.1) can be solved exactly for both dark and bright solitons [137].

2.3 Equilibrium solutions

Let us first consider stationary three-soliton molecules without defect potential ($U(x) = 0$). Our analysis is based on variational and numerical methods.

2.3.1 Variational method

The variational approach is proved to be efficient for the analysis of non-integrable systems. To describe the interactions of a nonlocal three-soliton molecule, we need to develop the variational method for three-soliton molecules. To this end, we utilize the generalized variational ansatz, which was successful in capturing the main features of soliton molecules in dispersion-managed optical fibers [138],

$$\psi = A\sum_{j=1}^{3}\exp\left[-\frac{(x-\eta_j)^2}{q^2}+i\varphi_j\right], \tag{2.3}$$

where A ensures the normalization condition, the variational parameters $q(t)$, $\eta(t)$, and $\varphi(t)$ stand, respectively for width, peak position, and phase of the soliton.
The Gaussian trial function (2.3) enables us to analyze both in-phase and out-of-phase beams in contrast to the trial function used in Refs.[43, 108], which has the center peak out-of-phase with the two outlying peaks.

The energy functional corresponding to equation (2.1) reads

$$E=\int_{-\infty}^{\infty}\left\{\frac{1}{2}\left|\frac{\partial\psi}{\partial x}\right|^2+U(x)|\psi|^2-\frac{g_c}{2}|\psi|^4-\frac{g_d}{2}\left[\int R(|x-\xi|)|\psi(\xi,t)|^2d\xi\right]|\psi|^2\right\}dx. \tag{2.4}$$

Equation (2.4) gives us important insights into the binding mechanism. The binding energy is the difference between the energy (2.4) and energy of well-separated three individual solitons.

For the sake of analytical tractability we will assume from now on $\eta_j=[-(N-1)/2+(j-1)]\Delta$, where Δ is the relative separation between adjacent solitons.

The normalization $N=\int_{-\infty}^{\infty}dx|\psi|^2$ to the number of solitons $N=3$ in the molecule, gives:

$$N=\sqrt{2\pi}A^2q\left[\frac{3}{2}+e^{\frac{-\Delta^2}{2q^2}}\left(\cos\phi_1+\cos\phi_2\right)+e^{\frac{-2\Delta^2}{q^2}}\cos(\phi_1+\phi_2)\right], \tag{2.5}$$

where $\phi_j=\varphi_{j+1}-\varphi_j$ is the relative phase and the index $j=1,2$. The norm N is proportional to the number of atoms in the condensate.

Using the energy formula presented by (2.4) with an integration over x, the energy of the three solitons becomes

$$\begin{aligned}\frac{E}{N} &= \frac{\frac{3}{2}-\frac{3}{2}\left(1-\frac{\Delta^2}{q^2}\right)\cos(\phi_1+\phi_2)e^{\frac{-2\Delta^2}{q^2}}+\left(1-\frac{\Delta^2}{q^2}\right)\mathscr{F}_1}{q^2\mathscr{F}_1} - \frac{Ng_c}{2\sqrt{\pi}q\mathscr{F}_1^2}\Bigg\{8e^{\frac{-\Delta^2}{q^2}}\cos(\phi_2-\phi_1)\\ &+4e^{\frac{-3\Delta^2}{4q^2}}\left[\cos\phi_1+\cos\phi_2+\cos(\phi_1-2\phi_2)+\cos(2\phi_1-\phi_2)\right]+8e^{\frac{5\Delta^2}{4q^2}}\left(\cos\phi_1+\cos\phi_2\right)\\ &+2e^{\frac{3\Delta^2}{q^2}}\left[\cos(2\phi_1)+\cos(2\phi_2)+4\right]+3e^{\frac{2\Delta^2}{q^2}}+2\left[\cos(2(\phi_2-\phi_1))+2\right]\\ &+4e^{\frac{\Delta^2}{q^2}}\left[2\cos(\phi_2-\phi_1)+\cos(\phi_1+\phi_2)\right]\Bigg\}\\ &-\frac{Ng_d}{2q\sqrt{\pi}\mathscr{F}_1^2\sqrt{\frac{2\sigma^2}{q^2}+1}}\Bigg\{\left[\cos\phi_1+\cos\phi_2+\cos(\phi_1+\phi_2)+\frac{3}{2}\right]\\ &\left(\cos\phi_1+\cos\phi_2\right)e^{\frac{\Delta^2\left(5q^2+12\sigma^2\right)}{4q^2\left(q^2+2\sigma^2\right)}}+2\cos(\phi_1+\phi_2)+e^{\frac{2\Delta^2}{q^2}}+2e^{\frac{\Delta^2\left(q^2+4\sigma^2\right)}{q^2\left(q^2+2\sigma^2\right)}}\Bigg\},\end{aligned} \tag{2.6}$$

where

$$\mathscr{F}_1=\frac{3}{2}+e^{\frac{-2\Delta^2}{q^2}}\cos(\phi_1+\phi_2)+e^{\frac{-\Delta^2}{2q^2}}(\cos\phi_1+\cos\phi_2).$$

In the case of out-of-phase solitons (relative phase $\phi_j=\pi$), the energy takes the form:

$$\begin{aligned}\frac{E}{N} &= \frac{3e^{\frac{\Delta^2}{2q^2}}+2\left(1-\frac{\Delta^2}{q^2}\right)-e^{\frac{3\Delta^2}{8q^2}}\left(4-\frac{\Delta^2}{q^2}\right)}{2q^2\left(-4e^{\frac{3\Delta^2}{8q^2}}+3e^{\frac{\Delta^2}{2q^2}}+2\right)}\\ &-\frac{g_cN\left(8e^{\frac{\Delta^2}{4q^2}}-24e^{\frac{5\Delta^2}{16q^2}}+12e^{\frac{\Delta^2}{2q^2}}+12e^{\frac{3\Delta^2}{4q^2}}-16e^{\frac{13\Delta^2}{16q^2}}+3e^{\frac{\Delta^2}{q^2}}+6\right)}{2\sqrt{\pi}q\left(-4e^{\frac{3\Delta^2}{8q^2}}+3e^{\frac{\Delta^2}{2q^2}}+2\right)^2}\\ &-\frac{9g_dNe^{\frac{\Delta^2}{2q^2}}\sqrt{2-\frac{q^2}{q^2+2\sigma^2}}\left(-4e^{\frac{\Delta^2\left(5q^2+12\sigma^2\right)}{16q^2\left(q^2+2\sigma^2\right)}}+e^{\frac{\Delta^2}{2q^2}}+2e^{\frac{\Delta^2\left(q^2+4\sigma^2\right)}{4\left(q^4+2q^2\sigma^2\right)}}+2\right)}{2\sqrt{\pi}q\sigma\left(-4e^{\frac{3\Delta^2}{8q^2}}+3e^{\frac{\Delta^2}{2q^2}}+2\right)^2\sqrt{\frac{4}{q^2}+\frac{1}{\sigma^2}}}.\end{aligned} \tag{2.7}$$

Equilibrium solution requires that the energy must have a minimum with respect to the

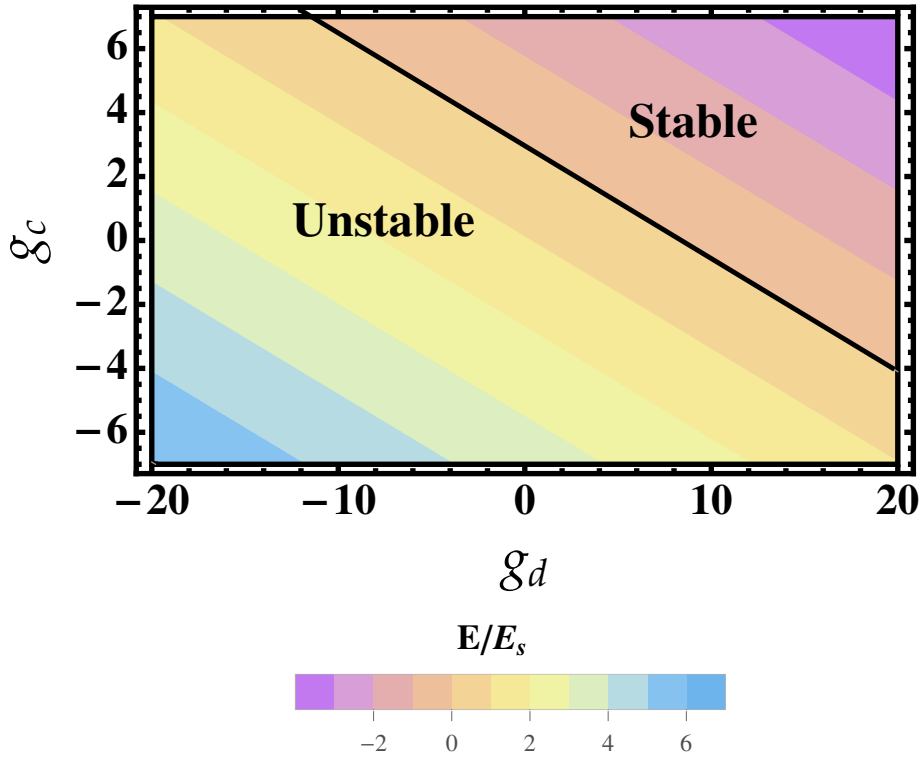

Figure 2.1: (Color online) Phase diagram of the bound state solutions as a function of g_d and g_c obtained from the variational method. The colors represent the energy of the solutions. The thick black line corresponds to $E/E_s = 0$. Here E_s is the energy of a single soliton. Parameters are: $N = 3$, $\Delta = 1.5$, $g_c = 2$, $g_d = -10$, $\sigma = 2$, $\phi = \pi$.

intersoliton separation characterized by a binding energy $E_b < 0$ [61, 106].

Figure 2.1 illustrates the nontrivial solutions (i.e. bound states) of the energy E in terms of the local and nonlocal nonlocalities strengths (g_c, g_d) as a "phase diagram". The boundary line ($E = 0$) is marked with a thick black line, below which these solutions are the stable molecule. The maximum value of E at which the bound state becomes unstable, depends on the degree of nonlocality. The results presented here belong to a family of models featuring the formation of a stable bound state tri-solitons, namely: $|g_c| < |g_d|$ (e.g. $g_d \simeq 15, g_c \simeq -2$), and $|g_c| > |g_d|$ (e.g. $g_d \simeq -1, g_c \simeq 6$).

In Figure 2.2 we illustrate some examples of the energy E from equation (2.7) for two values of the relative phase.

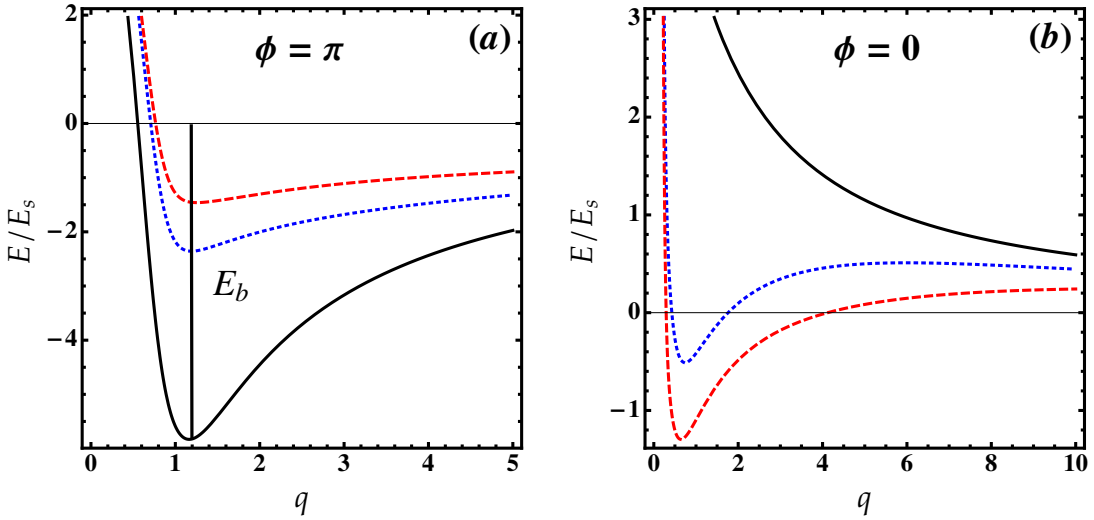

Figure 2.2: (Color online) Energy of solitons from equation (2.7) as a function of the width q for different values of the nonlocality degree σ and the relative phase ϕ. Solid lines: $\sigma = 2$. Blue dashed lines: $\sigma = 5$. Red dotted lines: $\sigma = 10$. Parameters are: $N = 3$, $\Delta = 1.5$, $g_c = 6$, $g_d = -1$.

Figure 2.2.(a) shows that the energy of out-of-phase interacting solitons has a local minimum at $q \simeq 1.1$ results in the three solitons supports three-soliton bound states corresponding to the force between the solitons is zero. Remarkably, the local minimum becomes narrower as σ increases signaling that the solitons are compressed, and thus, the action of the nonlocality is less effective. Whereas it becomes shallow for large σ, a fact that reduces localization and rises nonlocality.

In the case of in-phase ($\phi = 0$) solitons, the situation is quite different. We see from figure 2.2.(b) that a stable bound state occurs only for large degree of nonlocality ($\sigma = 5, 10$) where the energy has a local minimum at $q \simeq 0.75$. For a weakly nonlocal medium ($\sigma = 2$), the energy is positive. One can infer then, if the medium of in-phase solitons becomes more local, the three peaks of the solution become unstable. This can be interpreted as being due to the interplay of local repulsive and attractive nonlocal nonlinearities.

2.3.2 Numerical results

In order to test the accuracy of the developed variational method and to explore the the propagation of the stationary solution of bright three-soliton molecule, we numerically solve the nonlocal GPE (2.1) with the Gaussian nonlocal response function. Our numerical solution was performed by the split-step fast Fourier transform method which was proved to be quite powerful numerical tool in solving similar problems. We have used 2048 Fourier modes and the time step was $\delta t = 0.001$ [138]. The variational predicted wavefunction given by equation (2.3) is introduced into equation (2.1) as an initial condition.

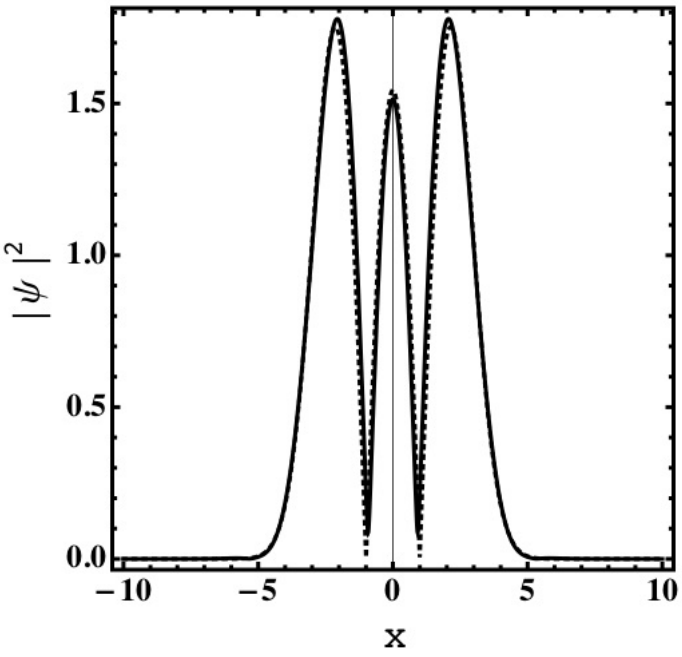

Figure 2.3: Density profiles of out-of-phase soliton molecule. Solid lines: numerical simulations. Dotted lines: variational analysis. Parameters are: $N = 3$, $q = 1.1$, $\sigma = 2$, $g_c = 6$, $g_d = -1$.

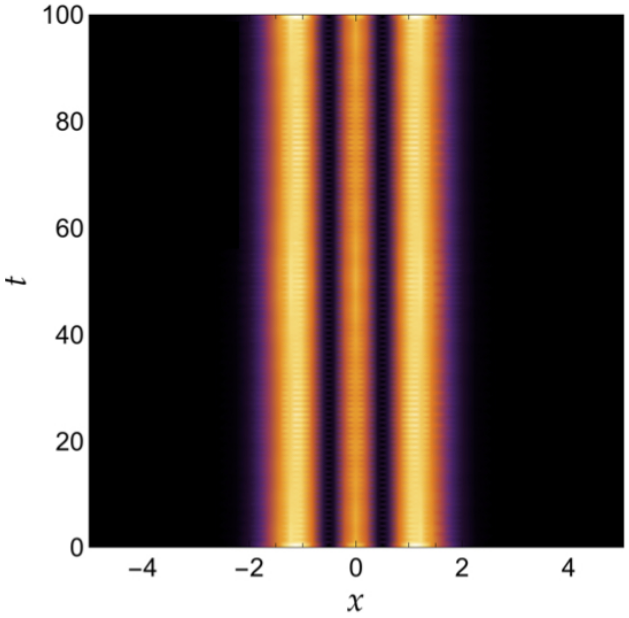

Figure 2.4: Dynamics of a three-soliton molecule placed at their equilibrium positions $\Delta = 1.5$. Parameters are: $N = 3$, $q = 1.1$, $\sigma = 2$, $g_c = 6$, $g_d = -1$.

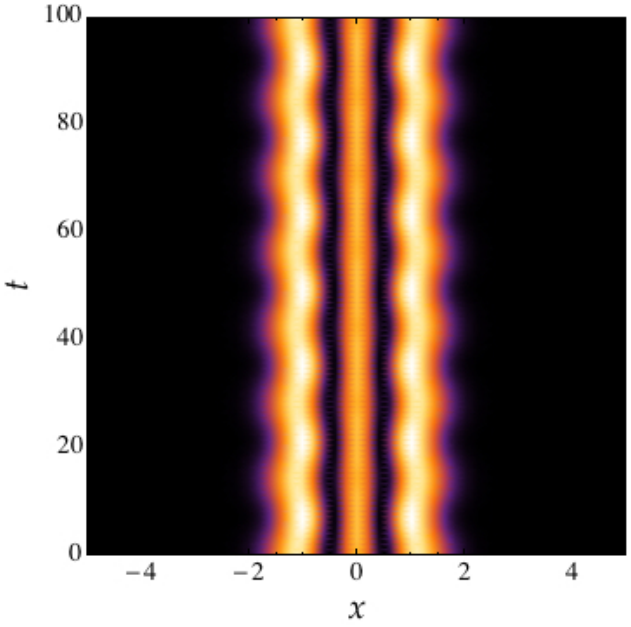

Figure 2.5: (Dynamics of a three-soliton molecule perturbed by changing the intersoliton separation (15% larger than the equilibrium separation). Parameters are: $N = 3$, $q = 1.1$, $\sigma = 2$, $g_c = 6$, $g_d = -1$.

In figure 2.3, we compare the out-of-phase three-soliton molecule profile obtained by

the variational scheme with our simulation results and good agreement is found between the two approaches. The central soliton has a smaller amplitude indicating that solitons interfere destructively which is natural for out-of-phase solitons.

Let us turn to investigate the dynamics of the above stationary solution by varying the separation between adjacent solitons. Figure 2.4 shows that when solitons are placed at their equilibrium positions, a highly stable propagation of the three-soliton molecule (where intersoliton separation is maintained) is formed.

According to figure 2.5 when the separation between the constituent solitons is suddenly increased by 15% from the equilibrium separation, the lateral solitons experience periodic oscillations in the trajectory during propagation, while the central soliton remains robust.

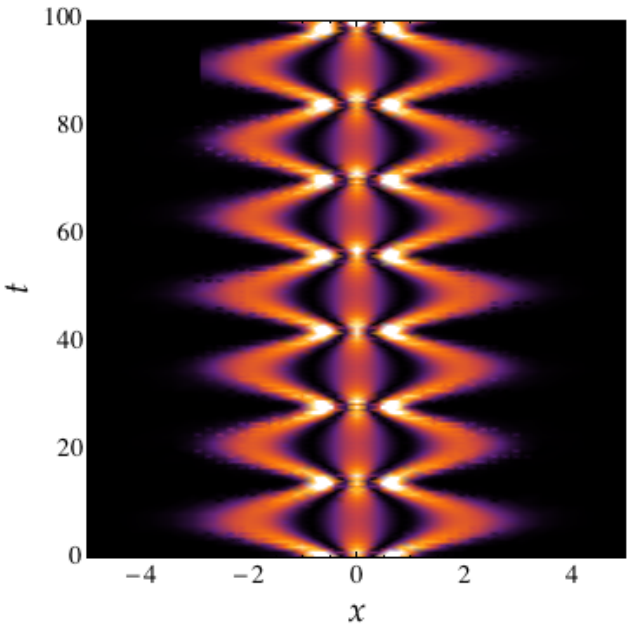

Figure 2.6: Dynamics of a three-soliton molecule for $\phi = 0.8\pi$ as value of the relative phase. Parameters are the same as in figure 2.3.

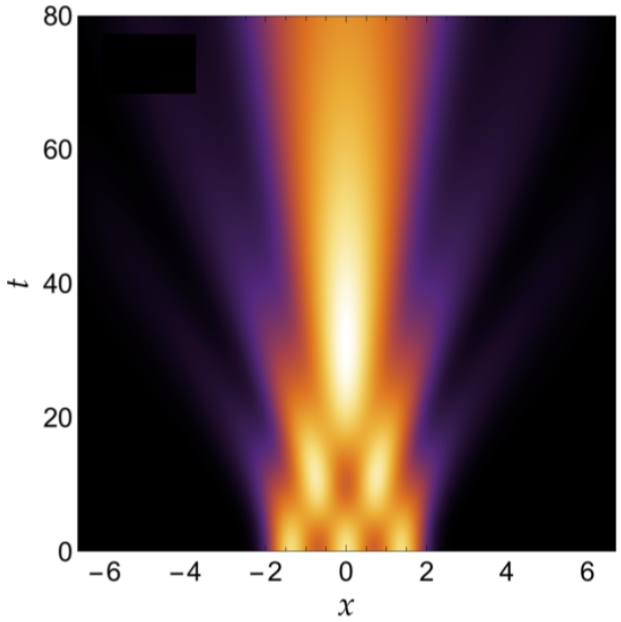

Figure 2.7: Dynamics of a three-soliton molecule for two $\phi = 0$ as value of the relative phase. Parameters are the same as in figure.2.3.

We now briefly examine the effect of changing the initial phase difference in the molecule dynamics and in the soliton width.

Figures 2.6 and 2.7 show that the initial relative phase plays a crucial role in the dynamics of a three-soliton molecule. For instance, if the relative phase is slightly reduced, the attractive force causes strong oscillations of the solitons's trajectories inside the molecule and hence they collide and repel each other periodically as is seen in figure 2.6.

Figure 2.7 depicts that the three in-phase solitons always merge into a single soliton owing to the attraction interaction induced by the nonlocality and hence, the three solitons bound state will eventually disintegrate. They are stable only at a shorter times ($t < 5$).

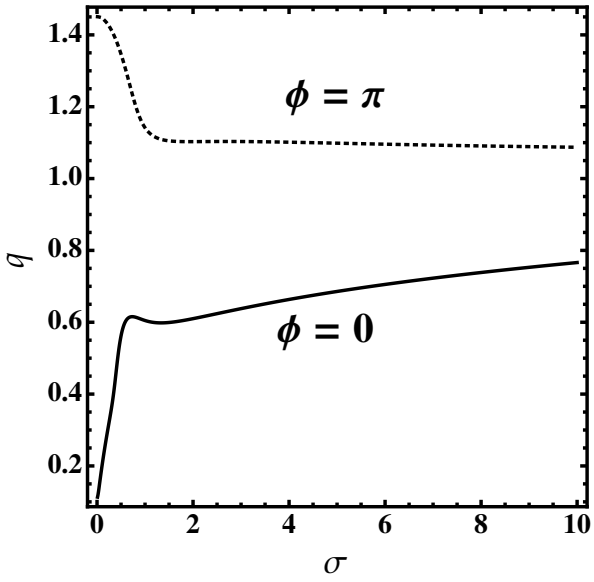

Figure 2.8: Soliton width as a function of the degree of nonlocality. Parameters are: $N = 3$, $\Delta = 1.5$, $g_c = 6$, and $g_d = -1$.

Figure 2.8 shows that when $\sigma \lesssim 1$ the soliton width sharply decreases (increases) with the degree of nonlocality for out-of-phase (in-phase) soliton molecule. For $\sigma > 1$, the soliton width decreases (increases) slowly with the degree of nonlocality. Numerically, the width is determined from the NLSE (2.1), according to the relation: $\sqrt{\int_{-\infty}^{+\infty} dx x^2 |\psi(x,t)|^2}$.

2.4 Scattering of a three-soliton molecule by Gaussian potential barriers

In this section we investigate the scattering of a three-soliton molecule by Gaussian potential barrier using variational approximation and numerical simulations. Let us consider a moving three-soliton molecule with velocity v collides with a potential barrier:

$$U(x) = U_0 e^{-x^2/2a^2}, \tag{2.8}$$

where $U_0 > 0$ is potential barrier height and a stands for its width.

Variationally, the dynamics of three solitons can be examined using the ansatz for three

solitons

$$\psi = A\sum_{j=1}^{3}\exp\left[-\frac{(x-\eta_j)^2}{q^2}+iv_j(x-\eta_j)+i\varphi_j\right], \tag{2.9}$$

Again the expression of the energy functional is too lengthy (see equation (2.10). Within the trial function (2.9), the energy functional (2.4) of three solitons in the presence of a potential barrier turns out to be given as:

$$\begin{aligned}
\frac{E}{N} &= \frac{1}{q^2\mathscr{F}_2}\left\{3\left(v^2q^2+1\right)e^{\frac{2\Delta^2}{q^2}} - 8v\Delta\sin\vartheta + 2\left(-\frac{4\Delta^2+v^2q^2}{q^2}+1\right)\cos\vartheta + 4e^{\frac{3\Delta^2}{2q^2}}\cos\left(\frac{\phi_1-\phi_2}{2}\right)\right.\\
&\times\left[\left(\frac{-\Delta^2+v^2q^2}{q^2}+1\right)\cos\left(\frac{\vartheta}{2}\right)-2v\Delta\sin\left(\frac{\vartheta}{2}\right)\right]\\
&\left.+\frac{\sqrt{2}aU_0\left[2e^{\frac{\Delta^2\left(12a^2+q^2\right)}{8a^2q^2+q^4}}\left(\cos\left(v\Delta+\phi_1\right)+2\cos\left(v\Delta+\phi_2\right)\right)+2e^{\frac{16a^2\Delta^2}{8a^2q^2+q^4}}+2\cos\vartheta+e^{\frac{2\Delta^2}{q^2}}\right]}{\sqrt{q^2+8a^2}}\right\}\\
&-\frac{Ng_c}{\sqrt{\pi}q\mathscr{F}_2^2}\left\{4e^{\frac{\Delta^2}{q^2}}\cos\vartheta+4e^{\frac{5\Delta^2}{4q^2}}\cos\left(\frac{\phi_2-\phi_1}{2}\right)\left[\cos\left(\frac{\vartheta}{2}\right)+\cos\left(\frac{3\vartheta}{2}\right)\right]\right.\\
&+8e^{\frac{13\Delta^2}{4q^2}}\cos\vartheta\cos\left(\frac{\phi_2-\phi_1}{2}\right)+2e^{\frac{3\Delta^2}{q^2}}\left[\cos(2\vartheta)\cos\left(\phi_2-\phi_1\right)+2\right]+\frac{3}{2}e^{\frac{4\Delta^2}{q^2}}+\cos\left(2\vartheta\right)\\
&\left.+2+2e^{\frac{2\Delta^2}{q^2}}\left[\cos\vartheta+\cos\left(\phi_2-\phi_1\right)\right]\right\}-\frac{Ng_d}{\sqrt{\pi}q\mathscr{F}_2^2\sqrt{\frac{2\sigma^2}{q^2}+1}}\left\{2e^{\frac{2\Delta^2}{q^2}}\left[2\cos\phi_1+2\cos(\phi_1+\phi_2)\right.\right.\\
&\left.\left.+2\cos\phi_2+3\right]e^{\frac{\Delta^2\left(5q^2+12\sigma^2\right)}{4q^2\left(q^2+2\sigma^2\right)}}\cos\vartheta\cos\left(\frac{\phi_2-\phi_1}{2}\right)+e^{\frac{2\Delta^2}{q^2}}+2e^{\frac{\Delta^2\left(q^2+4\sigma^2\right)}{q^4+2q^2\sigma^2}}+2\cos\vartheta\right\},
\end{aligned} \tag{2.10}$$

where $\vartheta = 2v\Delta+\phi_1+\phi_2$, and

$$\mathscr{F}_2 = 2\cos\vartheta+4e^{\frac{3\Delta^2}{2q^2}}\cos\vartheta\cos\left(\frac{\phi_2-\phi_1}{2}\right)+3e^{\frac{2\Delta^2}{q^2}}.$$

It is worth stressing that the external potential energy is vanishing in the limit $a\to 0$ and it is a constant for $a\to\infty$.

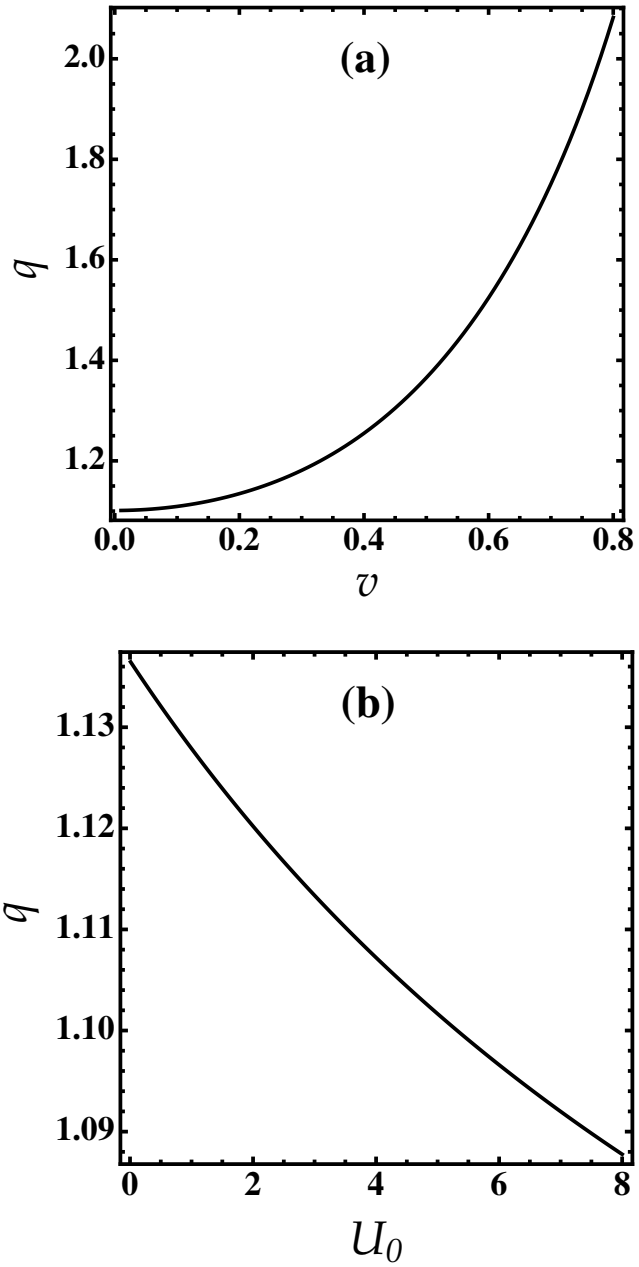

Figure 2.9: Width of out-of-phase solitons as a function of (a) soliton velocity and (b) the barrier height. Parameters are: $N = 3$, $\sigma = 2$, $g_c = 6$, $g_d = -1$, and $a = 0.5$.

We now delve into the relationship between the soliton width and its velocity, and the barrier height. In what follows we consider only the case of out-of-phase solitons. Figure 2.9 (a) shows that for fixed barrier height, the soliton width increases monotonically with the soliton velocity, causing the constituent solitons to transmit the barrier (see below). The

variation of the width as a function of the barrier height is displayed in figure 2.9 (b). We see that q is lowering with U_0 which means that the incoming solitons can be reflected. For larger barrier height, the reflected fragment becomes unstable and the molecule will eventually disintegrate (see also figure 2.12).

Figures 2.10, 2.11, 2.12 and 2.13 displays the main scattering properties of a three-soliton molecule by Gaussian barrier, different scattering regimes are obtained. We see that the molecule is reflected when the potential soliton velocity is low, $v = 0.3$ as is depicted in figure 2.10. The reason for this effect is that the kinetic energy of the molecule is much smaller than the potential energy.

Whereas, for large soliton velocity, $v = 0.4$, the molecule can transmit through the potential barrier (see figure 2.11). The same scenario holds true for two-soliton molecules [133].

Moreover, we see from figures 2.12 and 2.13 that as the height of the potential increases (i.e. strong potential barrier), the transmitted/reflected molecule exhibits a strong perturbation leading to unstable transmission/reflection results in a destruction of the molecule during its time evolution. Therefore, the molecule cannot preserve its integrity after the reflection from the potential.

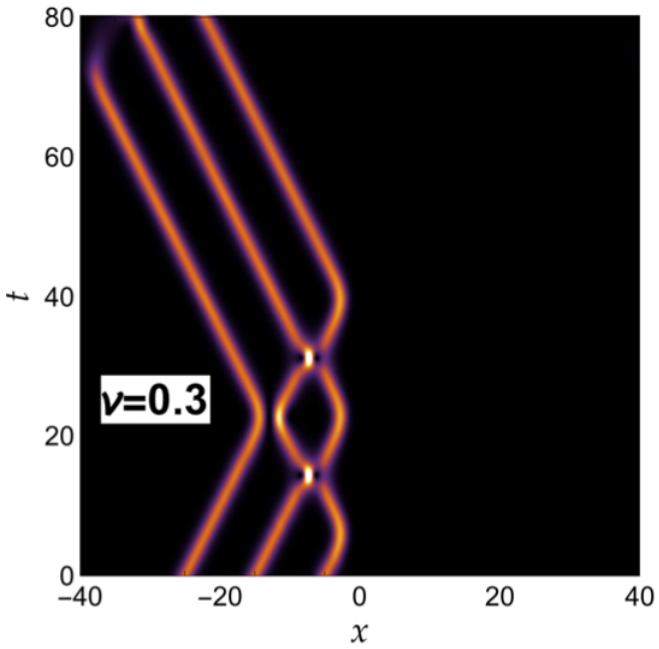

Figure 2.10: Scattering of a three-soliton molecule by a potential barrier for different values of v and $U_0 = 1$. Parameters are the same as in figure 2.9.

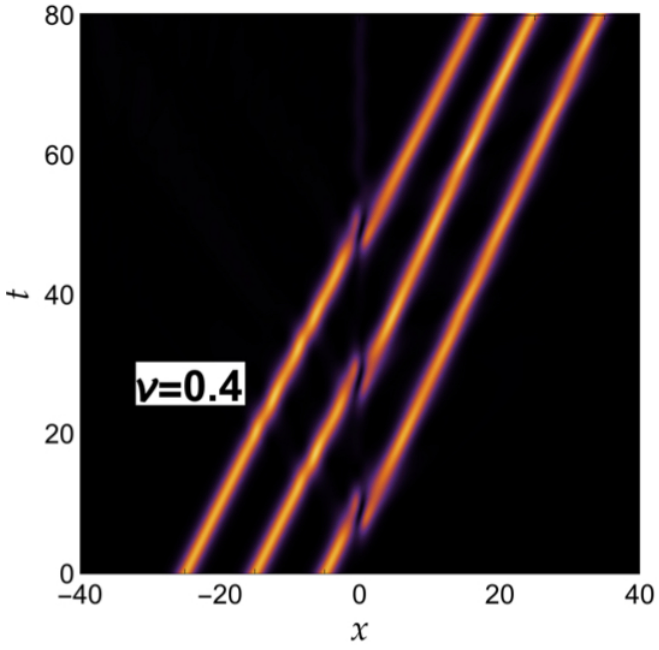

Figure 2.11: Scattering of a three-soliton molecule by a potential barrier for different values of v and $U_0 = 1$. Parameters are the same as in figure 2.9.

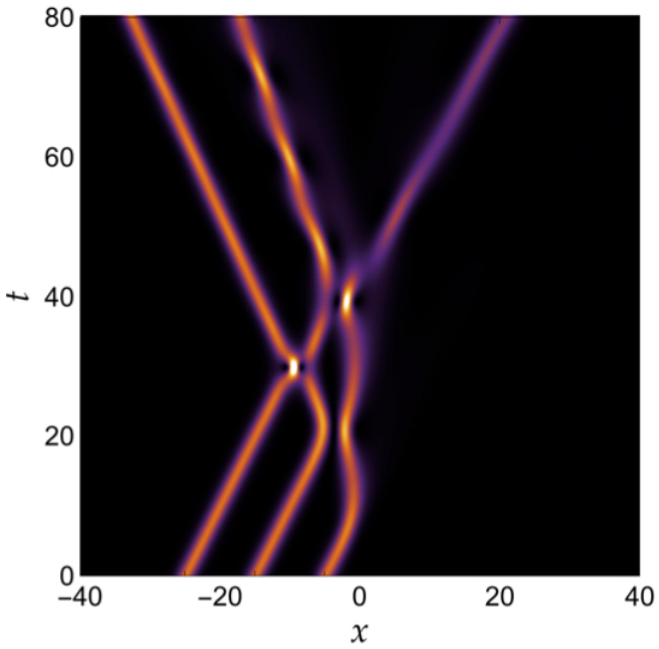

Figure 2.12: Scattering of a three-soliton molecule by a potential barrier for different values of v and $U_0 = 2$. Parameters are the same as in figure 2.9.

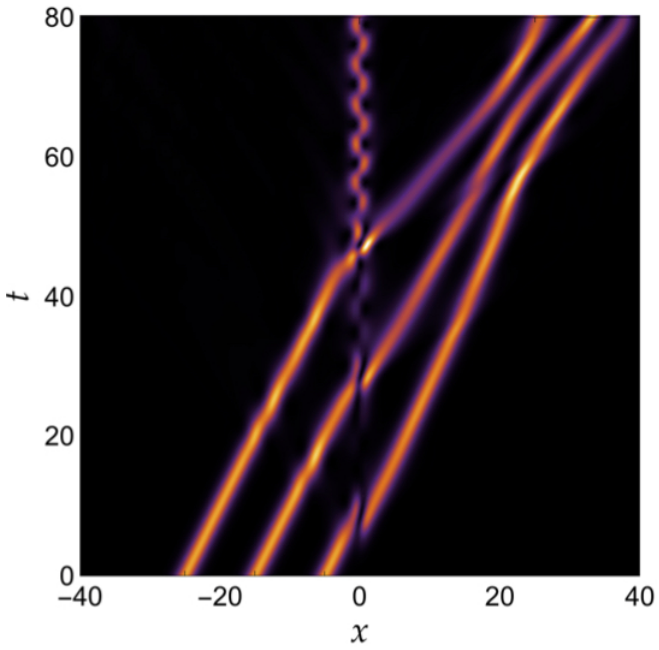

Figure 2.13: Scattering of a three-soliton molecule by a potential barrier for different values of v and $U_0 = 2$. Parameters are the same as in figure 2.9.

For the sake of completeness, we look here at how the soliton separation, Δ which

characterizes the kinetic energy of the incident solitons depends on the the barrier height, U_0 and its width, a. Figure 2.14 reveals that Δ increases with increasing U_0 regardless of the value of a. However, Δ decreases with augmenting a. For a narrow barrier, the dependence on U_0 is more pronounced.

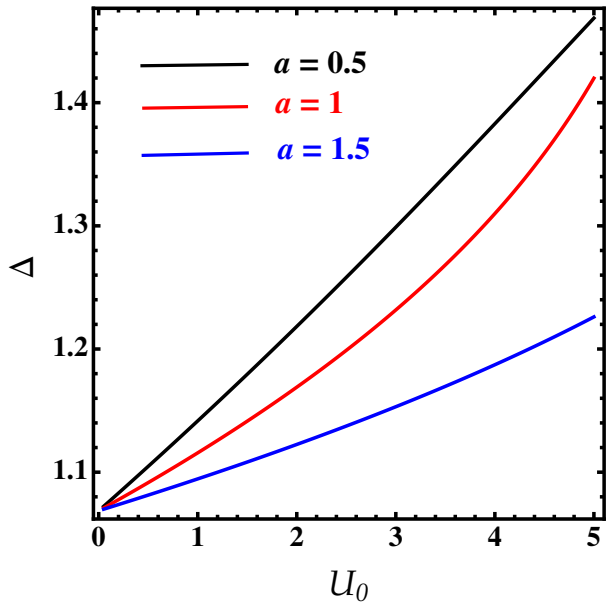

Figure 2.14: Separation between adjacent solitons as a function of the barrier height for various values of the barrier width. The parameters are the same as figure 2.9.

One can expect that the soliton width exhibits asymmetric oscillations during its time evolution due to the interaction with the potential barrier.

Chapter 3

Chapter 3

Interwires polar soliton molecules in a biwire system

Contents

3.1 Introduction

Recently, quantum degenerate dipolar gases placed in equidistant layers/wires have recieved a great deal of interest. These layered/wired structures which are connected with each other due to the long-range character of the DDI, exhibit remarkable interlayer effects such as interlayer bound states and superfluids of polar molecules [139–146]. In the nonlinear physics, the interlayer/interwire interaction leads to an effective potential between separated solitons, result in the formation of soliton molecules [75, 147]. Such molecules vitally depend on the interplay between contact and dipolar interactions [60, 75, 147].

In this chapter we consider dipolar BECs loaded in a biwire (tubes) system of a quasi-1D trap, where the two wires are separated by a distance λ much larger than the confinement length of the molecules within each wire ensuring vanishing hopping between wires. The dipole moments are assumed to be aligned perpendicularly to the tubes by an external field and in opposite directions in different wires (see figure 3.1). The long-range nature of the DDI affords an interaction in one BEC inside each wire. The most important feature of this setup is that the anisotropy of the DDI connects particles from each wires in a very specific form (different from the intrawire interaction) leading to a two-component BEC [141]. Experimentally, this biwire geometry can be created by optical lattices or atomic chip traps [148, 149].

In contrast to the arrangement used in [139–145], our biwire configuration makes the interwire interaction to be repulsive at short distance regime and attractive in the long-ranged regime. For repulsive contact interactions, it may open a new route to explore dark

soliton molecules due to the special interwire effects not considered in the configuration of [139–145]. This biwire pattern can also lead to the formation of matter-wave bright soliton molecules for both short- and long-range attractive interactions. In quasi-2D geometry, this type of system supports the formation of unconventional interlayer superfluids such as extended s-, p-, d-, and f-wave superfluids [138, 150, 151].

The numerical simulation of the underlying nonlocal GPE, reveals that the stability and properties of individual solitons, and soliton molecules in such a geometry crucially depend on the interwire distance and on the interplay between contact and dipolar interactions. We show that in such a biwire system, the excitation spectrum can acquire a roton-maxon structure. A detailed analysis of the nonlinear dynamics of these exotic soliton molecules is also carried out. It is found that near the roton instability, the solitons complexes exhibit oscillatory behavior with increasing the interaction stength and the interwire distance.

3.2 Model of the two biwire

Let us consider the quasi-1D biwire configuration of figure 3.1, where at each wire a dipolar BEC of N atoms with dipoles are head-to-tail across the wires. At zero temperature, the system is governed by the following dimensionless nonlocal two-coupled GP equations

$$i\frac{\partial \psi_j}{\partial t} = -\frac{\partial^2 \psi_j}{\partial x^2} - g_c|\psi_j|^2\psi_j + \int dx' V_{dd}(|x-x'|)\left(|\psi_1(x')|^2 + |\psi_{-1}(x')|^2\right)\psi_j,$$

where $j = \pm 1$ is the wire index, ψ_j is the wavefunction at each wire which is normalized to the number of atoms in the condensate $\int |\psi_j|^2 dx = N$, and $g = 2a/l_0$ is the strength of the

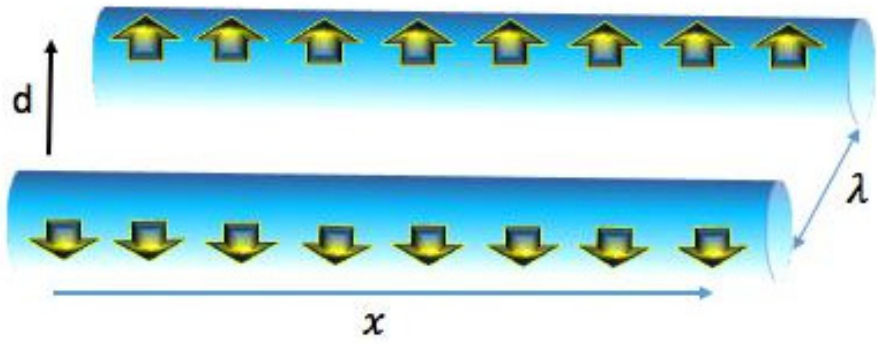

Figure 3.1: Biwire system of cold polar molecules with dipoles oriented in opposite directions in different wires.

local nonlinearity with $l_0 = \sqrt{\hbar/m\omega_\perp}$ being the harmonic oscillator length, $\omega_\perp$ corresponds to the frequency of radial confinement, and m is the particle mass. In system (3.1), lengths, time, density and energies are expressed in units of l_0, $\omega_\perp^{-1}$, l_0^{-1} and $\hbar\omega_\perp$, respectively.

We note here that the DDI potential $V_{dd}(x)$ appearing in equation (3.1) is composed of two parts: the interwire interaction potential which responsible for the interactions between the two wires

$$V_{\text{inter}}(x) = -g_d \frac{x^2 - 2\lambda^2}{(x^2+\lambda^2)^{5/2}}, \tag{3.1}$$

where $g_d = 2r_*/l_0$ with $r_* = md^2/\hbar^2$ being the characteristic of the distance between the two dipoles , and d is the scalar product of the average dipole moments of the molecules. The potential $V_{\text{inter}}(x)$ is repulsive for $x < \sqrt{2}\lambda$, while it is attractive at $x > \sqrt{2}\lambda$ which may open up the possibility of forming interwire soliton molecules.

The soliton-soliton potential (3.1), in contrast to that used in Refs [75, 147], is attractive at large distance x which may lead to the formation of an interwire bound state of two solitons in different wires (soliton dimer). When the interwire distance is increased, the

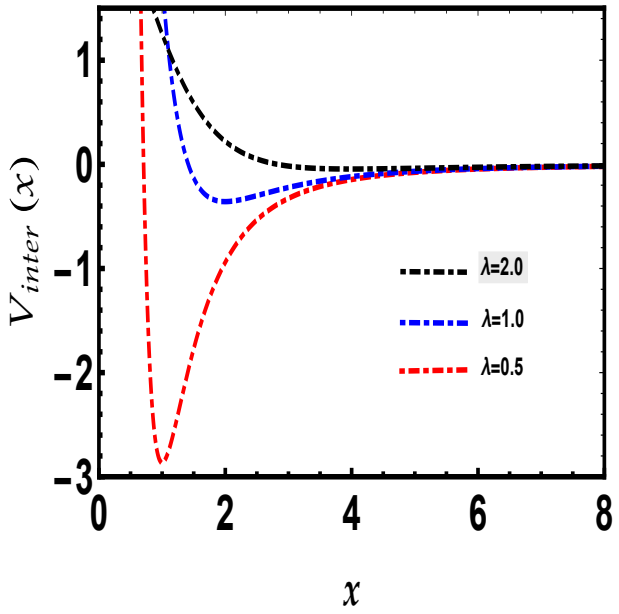

Figure 3.2: The interwire interaction potential versus sevral value of λ. (Red, Blue and Black for $\lambda = 0.5$, $\lambda = 1.0$ and $\lambda = 2.$) and $g_d = 10$. The figure show that this potential is more baounded when λ takes a small values.

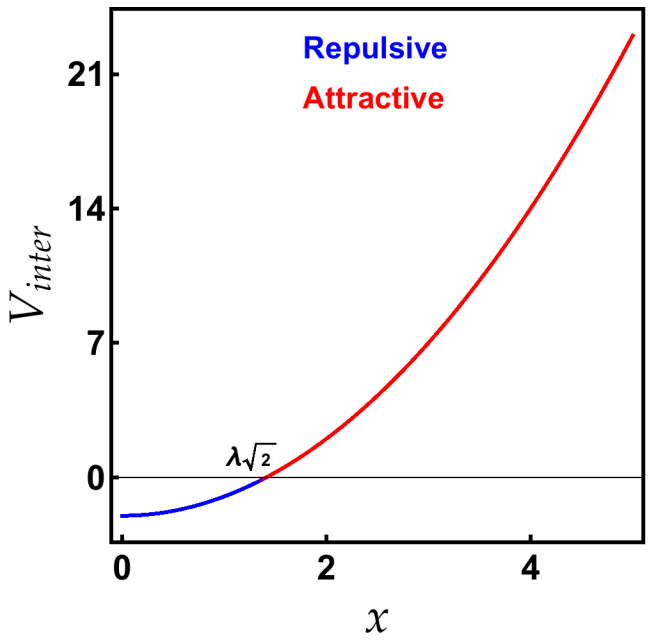

Figure 3.3: The interwire interaction potential versus x for $\lambda = 1$.

local minimum is shifted and thus, the molecular structure is modified. On the other hand, the intrawire interaction has a complicated form [47, 152].

However the most convenient form for analytical calculation is that proposed in Ref [40]

$$V_{\text{intra}}(x) = g_d \frac{\delta^3}{(x^2+\delta^2)^{3/2}}, \tag{3.2}$$

where $\delta = \pi^{-1/2}$ is a cutoff parameter, which regularizes the singularity problem. For $\lambda \gg l_0$, both $V_{\text{intra}}(x)$ and $V_{\text{inter}}(x)$ depend only on the interparticle distance along the wire direction x. In the absence of intertube interactions, the dynamics of solitons and soliton molecules in each 1D tube have been extensively investigated using the standard nonlocal GPE (see e.g. [40, 43, 46, 152]).

The soliton's energy functional corresponding to equation (3.1) reads

$$E = \sum_j \left\{ \frac{1}{2}|\nabla\psi_j|^2 - \frac{g_c}{2}\left(|\psi_j|^4 + \varepsilon_{dd}|\psi_j|^2 \times \int_{-\infty}^{+\infty} V_d(x-x') \left[|\psi_1(x')|^2 + |\psi_{-1}(x')|^2 \right] dx' \right) \right\}.$$

The first term represents the kinetic energy, the second term stands for the contact interactions energy, and the third term accounts for interaction energy due to DDI.

3.3 Stability of the uniform system

Here we analyze the stability of the interwires nonlinear modes associated with equation (3.1) which is affected by the excitations of the condensate. The elementary excitation energies ε_k can be obtained by considering small perturbations of the order parameter around the equilibrium solution ψ_{0j} namely: $\psi_j = \psi_{0j} + \delta\psi_j$, where $\delta\psi_j \ll \psi_{0j}$. This is the well

known Bogoliubov theory [31, 35, 109, 153, 154]. In the homogeneous case, the Fourier transform of the potential (3.1) reads

$$V_{\text{inter}}(k) = g_d k^2 [K_0(k\lambda) + K_2(k\lambda)], \tag{3.3}$$

where $K_0(y)$ and $K_2(y)$ are the modified Bessel functions. The small amplitude fluctuations are given via the Bogoliubov transformation (1.12):

$$\delta\psi_j = \left(u_k e^{-ikx+i\varepsilon_k t} + v_k e^{ikx-i\varepsilon_k t}\right) e^{-i\mu t}, \tag{3.4}$$

where μ is the chemical potential and u_k, v_k are the quasi-particle amplitudes. The Bogoliubov dispersion relation turns out to be given as

$$\varepsilon_k = k\sqrt{\frac{k^2}{4} + \mu_0 \left[1 + \varepsilon_{dd} k^2 \left(K_0(k\lambda) + K_2(k\lambda)\right)\right]}, \tag{3.5}$$

where $\mu_0 = g\psi_0^2$. Based on the sign of g_c and the strength of the DDI, the system sustains two types of instabilities namely, phonon instability (PI) and roton instability (RI). In the limit of low momenta ($k \to 0$), the PI occurs for $g < 0$ whatever the value of λ as is shown in figure 3.4. In nondipolar homogeneous BECs, the PI arises only for $g_c < 0$ (see e.g. [155]), while for BEC-impurity mixtures it originates even for repulsive short-range interaction [156]. In the case of 3D dipolar BECs, the PI comes from the anisotropy of DDI, resulting in a local collapse, see for review [31].

For $g_c > 0$ and under certain critical value of the interwire distance, the dipoles can modify the form of the dispersion relation exhibiting first a maximum and then a minimum

in spectrum as the momentum increases results in roton-maxon structure as is seen in figure 3.5 If the roton minimum touches the zero-energy axis, the Bose condensate suffers a RI. In this case, the energy and the position of the roton can be modified by changing ε_{dd}. The same behavior holds in quasi-2D dipolar BECs [60, 157]. The height of the roton is sensitive to λ; for sufficiently large intrawire space, the roton approaches zero which destroys the dimerization of solitons modeled initially by two dipolar BECs placed in a biwire system.

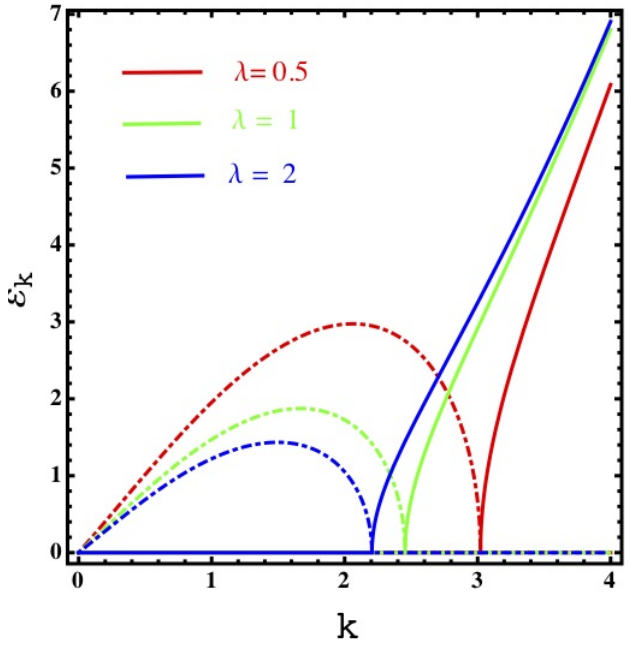

Figure 3.4: The Bogoliubov spectrum from equation (3.5) for $\varepsilon_{dd} = 1.5$. (a) $\mu_0 = -1$ (solid lines are the real part and dotdashed lines represent the imaginary part).

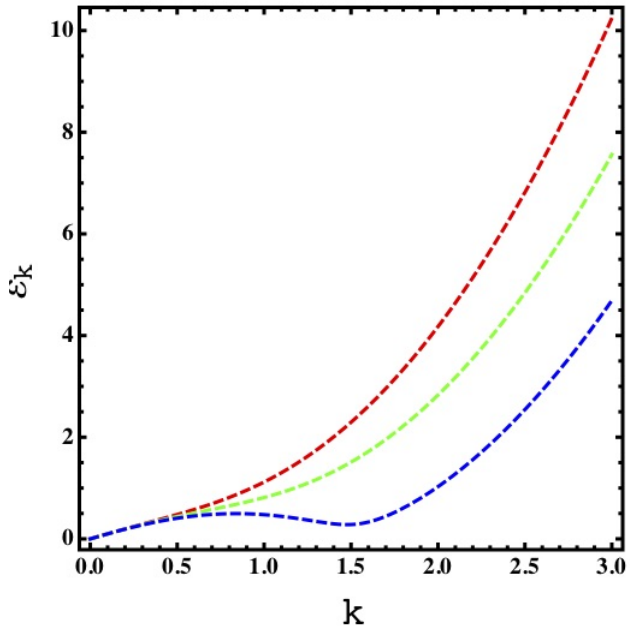

Figure 3.5: The Bogoliubov spectrum from equation (3.5) for $\varepsilon_{dd} = 1.5$. (a) $\mu_0 = 1$ (solid lines are the real part and dotdashed lines represent the imaginary part).

3.4 Dimer soliton molecules

3.4.1 Variation of the distance λ between the two wires

In this section we analyze the rudiments of dimer soliton molecules in biwire systems when with the variation of the distanse between the two wires λ where the interaction parameter stay constant the value of $g_d = 0.4$ correspond to the case figure 3.6 where the two solitons formed the molecule.

The results presented here rely on numerical simulation of the nonlocal GP equation (3.1), using a suitable initial condition envisaging solitonic solutions.

Here the potential interaction is calculated numericaly from the force of the interaction between the solitons, where we used the trajectories of the the solitons to found the force

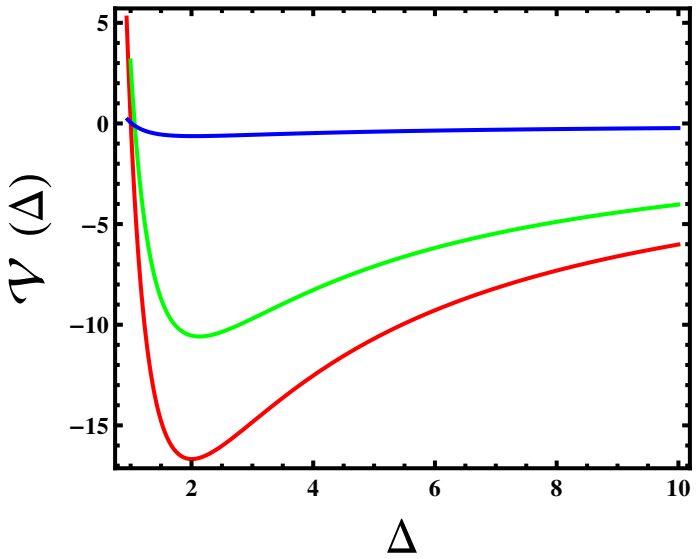

Figure 3.6: Soliton-soliton potential as a function of sepration Δ from numerical simulation of the nonlocal GP equation (3.1) for several values of λ. Parameters are: $g = 7.9$, $g_d = 0.4$. Red line: $\lambda = 0.5$. Green line: $\lambda = 1$. Blue line: $\lambda = 2$.

between them. The separation is calculated then differentiated numerically twice. finaly, the numerical integral of the force gives the potential interaction.

Figure 3.6 shows that the soliton-soliton potential $\mathcal{V}$ predicted by our numerical simulation has a local minimum at $\Delta = 2$ indicating the formation of a molecule of dimer solitons. The depth of the effective potential minimum is decreasing with increasing the interwire distance λ between the two wires i.e the two solitons become less bounded and hence, the molecule loss thir instability.

The numerical shape of the two-solitons molecule presented in the figure 3.7 is obtained by the numerical soliving of the nonlocal Gross-Pitaevskii (GP) equation (3.1) in the static case.

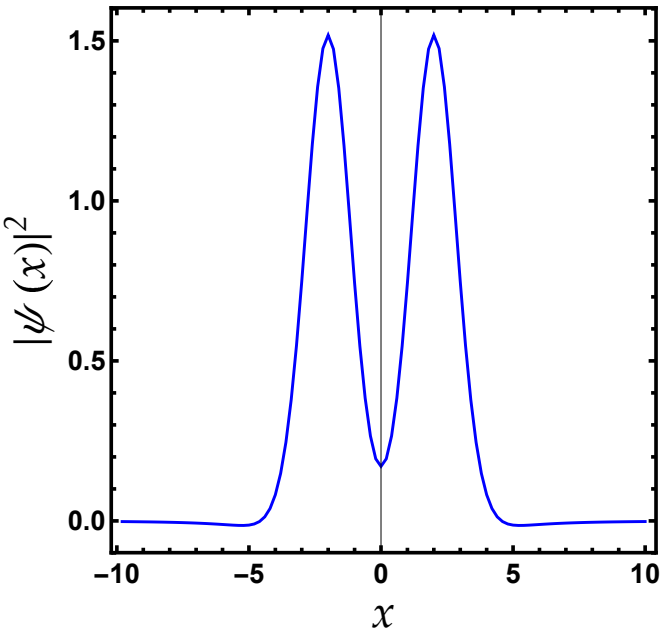

Figure 3.7: Stationary localized solutions of the nonlocal GP equation (3.1). Parameters are $g = 7.9$, $g_d = 0.4$ and $\lambda = 1$.

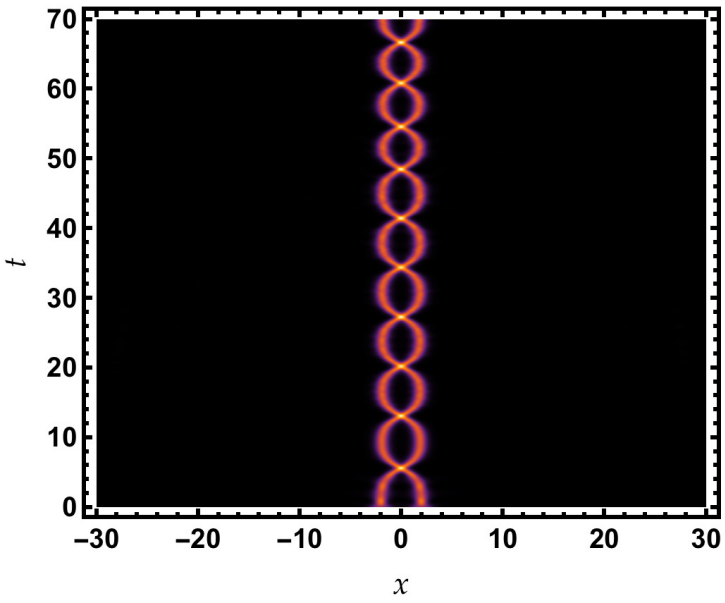

Figure 3.8: Spatiotemporal evolution of the interwire dimer soliton molecule. For $\lambda = 1$ the molecule is stable. Parameters are the same as in figure 3.6.

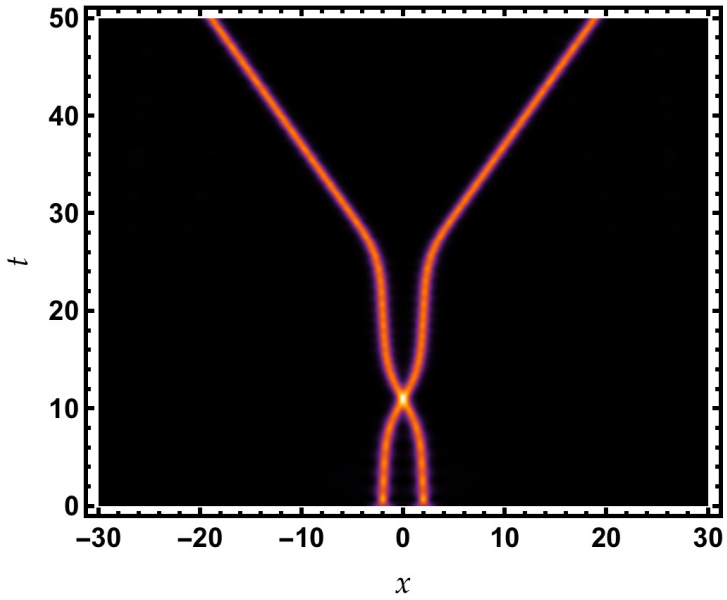

Figure 3.9: Spatiotemporal evolution of the interwire dimer soliton molecule. For $\lambda = 2$ the solitons repel. Parameters are the same as in figure 3.6.

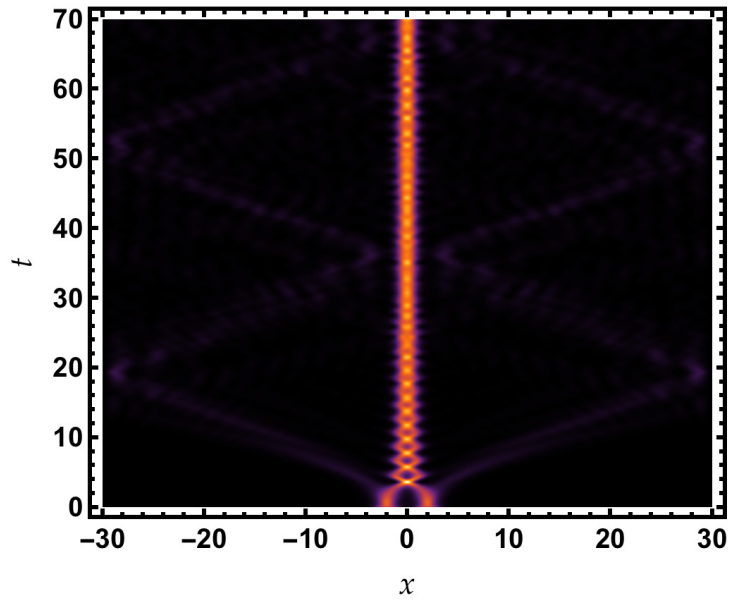

Figure 3.10: Spatiotemporal evolution of the interwire dimer soliton molecule. For $\lambda = 0.5$ molecule vibrations are clear. Parameters are the same as in figure 3.6.

Figures.3.8, 3.9 and 3.10 depicts the density profiles which were calculated using the equilibrium conditions found by minimizing the energy functional (3.3). For small

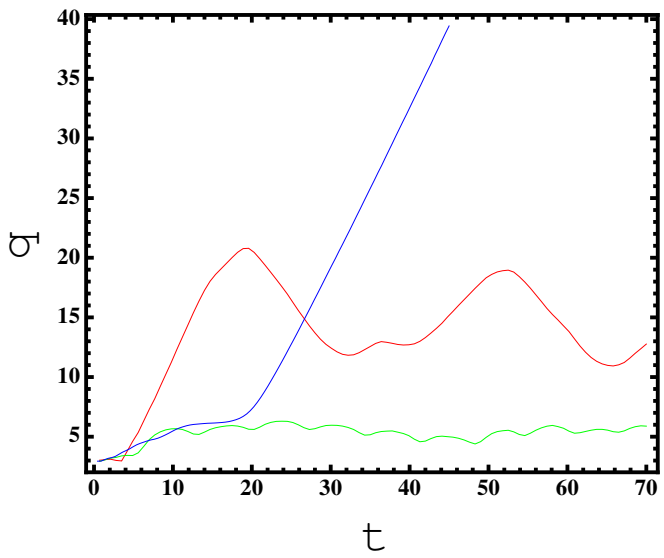

Figure 3.11: Time evolution of the width of the soliton along x direction, forming the molecule placed in opposite directions. Red line: $\lambda = 0.5$. Green line: $\lambda = 1$. Blue line: $\lambda = 2$. Parameters are the same as in figure 3.6.

separation, the solitons attract each other undergoing fusion and eventually becoming a single big soliton (see the 3.10).

If solitons are well separated ($\lambda > 1$), they can be approximated as point-like solitons [158]. In this case, the solitons repel and acquire sufficient kinetic energy to diverge to infinity at larger time as is shown in the middle pannel. When $\lambda = 1$, the molecule exhibits periodic oscillations around the equilibrium during its propagation analogous to vibrational modes of a diatomic molecule (see the figure 3.8).

Figure 3.11 that the width of the soliton exhibit breathing (contraction and expansion) oscillations. For large interwire speration ($\lambda \geq 2$), process of oscillation of the solitons goes on for some time ($t < 30$) due to the roton instability where the molecule disintegrates into individual freely solitons. The width of soliton can be extracted from the GP equation (3.1) using $q_j(t) = \sqrt{\int_{-\infty}^{+\infty} dx x^2 |\psi_j(x,t)|^2}$.

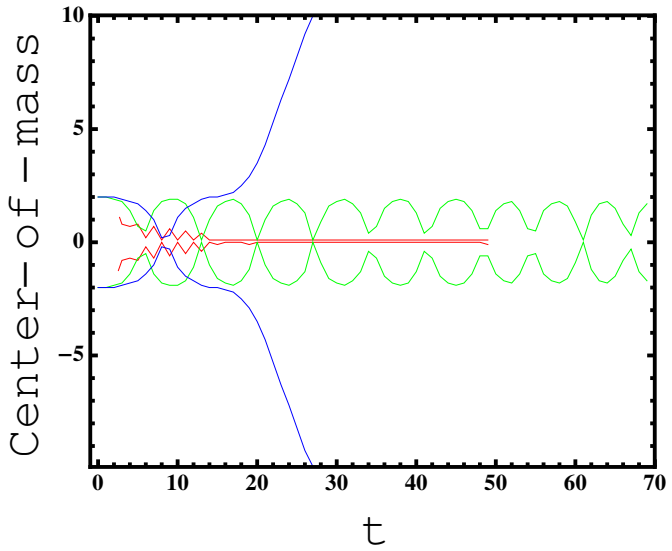

Figure 3.12: Time evolution of the centers of masses of the soliton along x direction of two solitons, forming the molecule placed in opposite directions . Red line: $\lambda = 0.5$. Green line: $\lambda = 1$. Blue line: $\lambda = 2$. Parameters are the same as in figure 3.6.

Figures 3.12 reveals te same edea as the figure 3.11 the center-of-mass of the soliton. The center-of-mass of soliton can be extracted from the GP equation (3.1) using $\eta_j(t) = \int_{-\infty}^{+\infty} dx\, x|\psi_j(x,t)|^2$.

3.4.2 Variation of the constant g_d

We now examine the role of the interaction strength in the behavior dimer soliton molecules exactly the cases of his width and his center-of-mass.

The figures (3.13), (3.14)and (3.15) translate the influence of the strength interaction on the dimer soliton molecules g_d. the first figure show the two solitons in the absence of the strength interaction $g_d = 0$, the second figure wherre $g_d = 1.4$ present thecase when there a strength interaction on the dimer soliton molecules,so the the two solitons will be merged, and the last figure show the that the two solitons formed a molecule from ($t = 0$ to

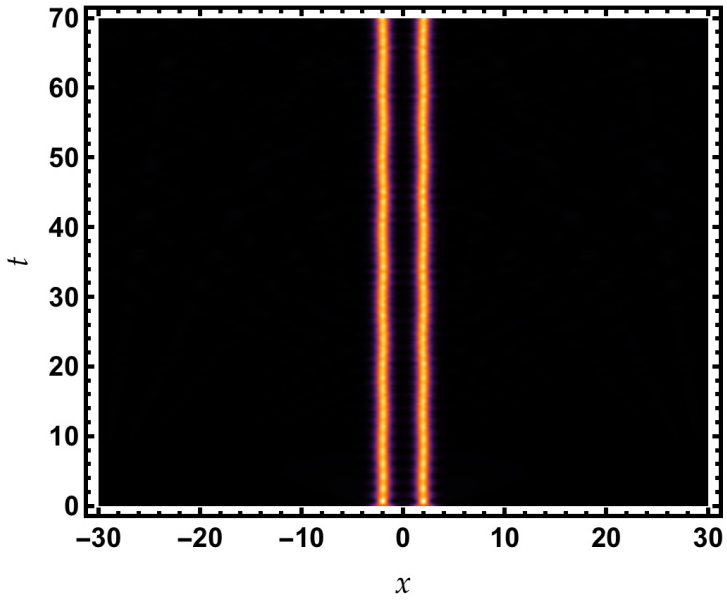

Figure 3.13: Spatiotemporal evolution of the interwire dimer soliton molecule. For $\lambda = 1$, $g = 7.9$ and $g_d = 0$.

$t = 30$) and from the $t = 30$ the two solitons will be separated. By increasing the interaction strength ($g_d \simeq 1.4$), the two solitons become very close to each other and the modulation of oscillations of width and the center-of-mass of the solitons becomes stronger as is seen in figure 3.16 and figure 3.17 . The oscillations decay at larger time. This can be understood from the fact that for strong interaction, the atoms scattered with high energy leave the condensate due to the absence of an external trap. For $g_d = 0.4$, the solitons continue to oscillate periodically forever. For $g_d = 0$, the two solitons undergo very slow oscillations and the molecule cannot be formed in such a situation.

With a comparison the figure (3.8) with the two figures (3.14) and (3.15) we see that the constant of the interaction between the two wires g_d plays an important role where if this constant takes a values higher than $g_d = 0.4$, the two-solitons will be merged so it's mean the interaction between the two solitons are stronger. Also, if this constant g_d takes

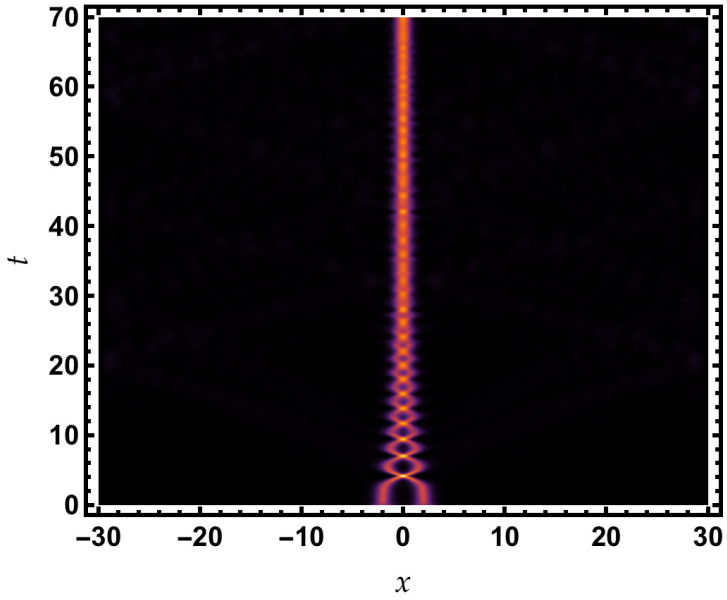

Figure 3.14: Spatiotemporal evolution of the interwire dimer soliton molecule. For $\lambda = 1$, $g = 7.9$ and $g_d = 1.4$.

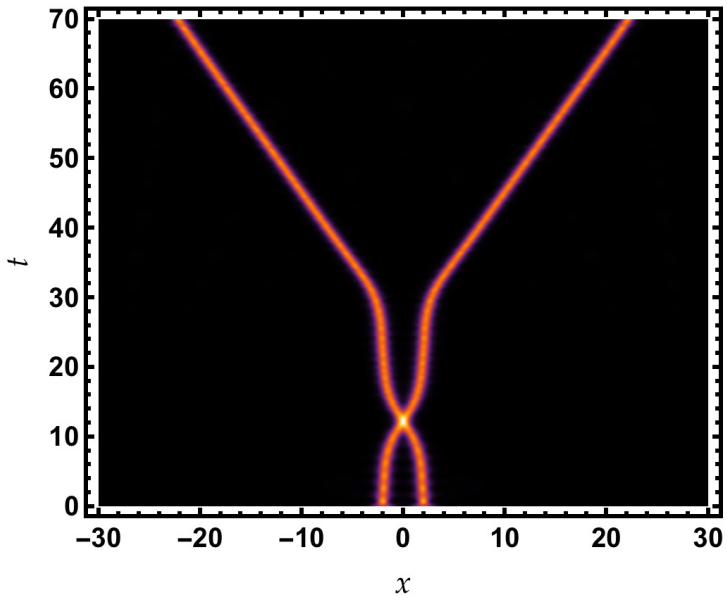

Figure 3.15: Spatiotemporal evolution of the interwire dimer soliton molecule. For $\lambda = 1$, $g = 7.9$ and $g_d = 0.05$.

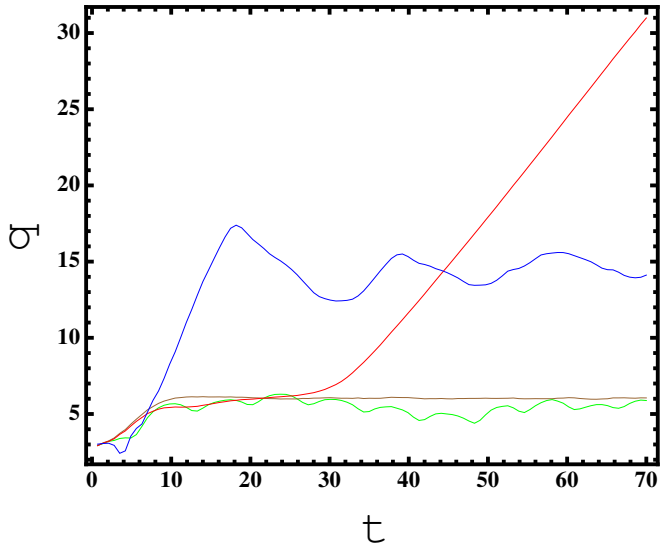

Figure 3.16: Time evolution of the width of the soliton along x direction of two solitons for different values of g_d. Brown line: $g_d = 0$. Red line: $g_d = 0.05$. Green line: $g_d = 0.4$. Blue line: $g_d = 1.4$. Parameters are $g = 7.9$, and $\lambda = 1$.

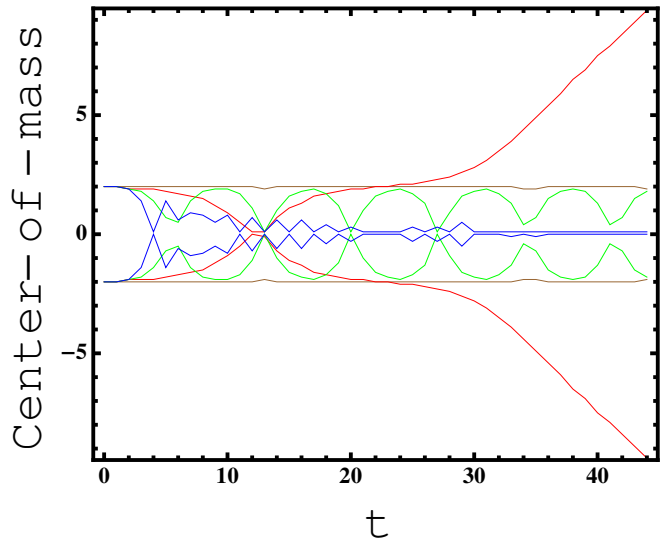

Figure 3.17: (Color online) Time evolution of the centers of masses of the soliton along x direction of two solitons for different values of g_d. Brown line: $g_d = 0$. Red line: $g_d = 0.05$. Green line: $g_d = 0.4$. Blue line: $g_d = 1.4$. Parameters are $g = 7.9$, and $\lambda = 1$.

a lawer values than $g_d = 0.4$ the solitons will separated, this second case mean that the interaction between the solitons which formed the molecule become very weak figure (3.15) after ($t > 30$), if g_d goes to zero, the two solitons will be really separated.

The realization of such polar soliton molecules in a quasi-1D biwire system is less challenging and can be probed in current Cr, Dy and Er experiments. For instance, for ^{164}Dy atoms which are characterized by $r_* = 131a_0$, where a_0 is the Bohr radii and $\omega_\perp = 60 \times 2\pi$ Hz placed in a biwire system, a stable soliton molecule can be nucleated for interwire separation $\lambda \simeq 400$ nm.

Chapter 4

Chapter 4

Singular Soliton Molecules of the Nonlinear Schrodinger Equation

Contents

4.1 Introduction

The fundamental NLSE or GPE is one of the most investigated equations in describing the dynamics of multiple physical phenomena, in both discrete and continuous systems. One important admitted solution to this equation is soliton. Many successful techniques have been developed to solve the NLSE. Among them are Painlevé analysis [134, 159, 160], Hirota method [161], similarity transformation method [162], Lax Pair (LP) and Darboux transformation (DT) method [163–165], Miura transformation [166, 167], inverse scattering transform and Hamiltonian approach [168], homotopy analysis method [169], Exp-function method [170], the tanh-function method [171, 172], the homogeneous balance method [173], and the F-expansion method [174].

Currently, there is a considerable interest in finding exact solutions to the non-local NLSE [175–178]. This non-Hermitian and PT-symmetric equation with the potential $V(x,t) = u(x,t)u^*(-x,t)$, where $u(x,t)$ is the mean-field wave-function, satisfies the PT-symmetric condition, $V(x,t) = V^*(-x,t)$. Several efforts were devoted in showing that this equation admits a soliton solution as well [175–178].

Prominent among the solutions of the NLSE is the two-soliton solution which can be obtained using the LP and DT method [78, 79]. Employing the trivial seed solution, $u_0(x,t) = 0$, the DT generates a single soliton solution. Using the latter as seed, generates the two-soliton solution [179]. The binding energy, the force, and potential of interaction between solitons have been calculated and studied extensively [78–80, 180–184].

In this chapter, we use the LP and DT method with a seed solution of the form $u_0(x,t) = 1/x$ to generate a new two-soliton solution that is characterized by two diverging peaks. Dispite this divergence, the new solution describe a soliton molecule with a binding energy. We calculate the potential of the interaction between the two solitons to show that it is of molecular type. Furthermore, we have considered the nonlocal NLSE and used the same procedure to generate a new solution out of the $u_0(x,t) = 1/x$ seed. It turned out that the new solution is much richer than the local case. Here, the new solution corresponds to the scattering of stationary soliton and two breathers on a finite background at half of space and inclined backgruond at the other half.

4.2 Lax Pair and Darboux transformation method

The LP and DT method is an exercisable way to generate soliton solutions of NLSE and GPE. Briefly, the LP and DT method is based on searching for an appropriate pair of matrices that associates the nonlinear system to a linear system. The LP should be associated with the nonlinear model through what is called a compatibility condition. The obtained linear system is solved using a seed solution, $\psi_0(x,t)$, which is a known exact solution of the nonlinear system. Each seed solution generates a family of exact solutions.

4.2.1 Basic ideas

In this section we give a review of the basic concepts regarding the LP and DT method. Let us recall the dimensionless 1D NLSE:

$$i\psi_t + \frac{1}{2}\psi_{xx} - c|\psi|^2\psi = 0, \tag{4.1}$$

where c is a complex constant parameter .

We associate to the equation (4.1) with an auxiliary field Φ which is a linear system as follow:

$$\Phi(x,t) = \begin{pmatrix} \psi_1(x,t) & \psi_2(x,t) \\ \phi_1(x,t) & \phi_2(x,t) \end{pmatrix}. \tag{4.2}$$

All the components of this matrice are being complex function of x and t.

The well known Lax Pair of (4.1) is defined as

$$\Phi_x = J \cdot \Phi \cdot \Lambda + U_0 \cdot \Phi, \tag{4.3}$$

$$\Phi_t = iJ \cdot \Phi \cdot \Lambda^2 + iU_0 \cdot \Phi \cdot \Lambda + V_0 \cdot \Phi. \tag{4.4}$$

Where Φ_x and Φ_t are the derivative of Φ with respect to x and with respect to t respectively. We note here that

$$U_0 = c^{1/2} \begin{pmatrix} 0 & \psi(x,t) \\ -\psi^*(x,t) & 0 \end{pmatrix}, \tag{4.5}$$

$$V_0 = \frac{i}{2} \begin{pmatrix} -c\,|\psi(x,t)|^2 & i\,c^{1/2}\,\psi_x(x,t) \\ i\,c^{1/2}\,\psi_x^*(x,t) & -c\,|\psi(x,t)|^2 \end{pmatrix}, \tag{4.6}$$

$$J = \begin{pmatrix} 1 & 0 \\ 0 & -1 \end{pmatrix}, \tag{4.7}$$

$$\Lambda = \begin{pmatrix} \lambda_1 & 0 \\ 0 & \lambda_2 \end{pmatrix}, \tag{4.8}$$

where $\psi^*(x,t)$ is the complex conjugate of $\psi(x,t)$, J and Λ are constant matrices, and λ_1 and λ_2 are complex constants called the *spectral parameters*, $\lambda_{1,2} = \lambda_{(1,2)r} + i\lambda_{(1,2)i}$ $\lambda_{(1,2)r}$ and $\lambda_{(1,2)i}$ are real constants. We note here also that $|\psi(x,t)|^2 = \psi(x,t)\,\psi^*(x,t)$.

We refer to the equations (4.3 et 4.4) as the LP. It refers also sometimes to the two marices U and V.

4.2.2 Compatibility condition

The link between the NLSE and the LP is called the ***compatibility condition*** which is given by

$$\Phi_{xt} - \Phi_{tx} = 0, \tag{4.9}$$

where Φ_x and Φ_t are the derivative of Φ with respect to x and with respect to t, respectively. Also, Φ_{xt} is the derivative of Φ_x with respect to t, and Φ_{tx} is the derivative of Φ_t with respect to x.

The last equation (4.9) requires the equation

$$U_x - V_t + [U,V] = 0, \tag{4.10}$$

where the $[U,V]$ is the commutator of $U$and V where $[U,V] = UV - VU$. Using the expressions of U_0 from equation (4.3), we get

$$\Phi_x(x,t) = \begin{pmatrix} i\,c^{1/2}\psi(x,t)\phi_1(x,t) + \lambda_1\psi_1(x,t) & i\,c^{1/2}\psi(x,t)\phi_2(x,t) + \lambda_2\psi_2(x,t) \\ -\lambda_1\phi_1(x,t) - i\,c^{1/2}\psi_s(x,t)\psi_1(x,t) & -\lambda_2\phi_2(x,t) - i\,c^{1/2}\psi_s(x,t)\psi_2(x,t) \end{pmatrix}. \tag{4.11}$$

and the two expressions of U_0 and V_0 from equation (4.4) give

$$\Phi_t(x,t) = \begin{pmatrix} A & B \\ C & D \end{pmatrix}, \tag{4.12}$$

where $A = -\sqrt{c}\,\lambda_1\psi(x,t)\phi_1(x,t) + i\,\lambda_1^2\psi_1(x,t) - \frac{1}{2}i\,c\psi(x,t)\psi_1 - \frac{1}{2}\,\sqrt{c}\,\phi_1(x,t)\psi_{1t}(x,t)$,

$B = -\sqrt{c}\,\lambda_2\psi(x,t)\phi_2 + i\,\lambda_2^2\psi_2(x,t) - \frac{1}{2}\,i\,c\,\psi_s(x,t)\psi_2 - \frac{1}{2}\,\sqrt{c}\,\phi_2(x,t)\psi_{1t}(x,t)$,

$C = -i\,\lambda_1^2 + \frac{1}{2}\,i\,c\,\psi(x,t)\,u_s(x,t)\phi_1 + \sqrt{c}\,\lambda_1\psi_s(x,t)\psi_1 - \frac{1}{2}\sqrt{c}\,\psi_1\,\psi_{sx}(x,t)$

and

$D = -i\,\lambda_2^2 + \frac{1}{2}\,i\,c\,\psi(x,t)\,\psi_s(x,t)\phi_2 + \sqrt{c}\,\lambda_2\psi_s(x,t)\psi_2 - \frac{1}{2}\,\sqrt{c}\psi_2\,\psi_{sx}(x,t)$.

To use the compatibility condition (4.9), we derive the formula (4.11) with respect to t and we derive the formula (4.12) with respect to x, the result become

$$\Phi_t(x,t) = \begin{pmatrix} a_{11} & a_{12} \\ a_{21} & a_{22} \end{pmatrix}. \tag{4.13}$$

$a_{11} = \frac{1}{2}\sqrt{c}\,\phi_1(x,t)\left(-2\,c\,\psi^2(x,t)\,\psi_s(x,t) + 2\,i\,\psi_t(x,t) + \psi_{xx}(x,t)\right)$,

$a_{12} = \frac{1}{2}\sqrt{c}\,\phi_2(x,t)(-2\,c\,\psi^2(x,t)\,\psi_s(x,t) + 2\,i\,\psi_t(x,t) + \psi_{xx}(x,t))$,

$a_{21} = \frac{1}{2}\sqrt{c}\,\psi_1(x,t)(-2\,c\,\psi(x,t)\psi_s^2(x,t) - 2\,i\,\psi_{s_t}(x,t) + \psi_{s_{xx}}(x,t))$

and

$a_{22} = \frac{1}{2}\,\sqrt{c}\,\psi_2(x,t)(-2\,c\,\psi(x,t)\,\psi_s^2(x,t) - 2\,i\,\psi_{s_t} + \psi_{s_{xx}}(x,t))$.

The compatibility condition is nothing but the NLSE and its complex conjugate, i.e. we see

that the four terms of this matrice present the equation (4.1) also its conjugate. It requires that $\psi(x,t)$ is a solution to the NLSE and $\psi^*(x,t)$ is the solution of its the complex conjugate. This matrice gives the link between the NLSE equation and the linear system of the LP.

4.2.3 Darboux Transformation

We use as seed zero solution $\psi_0(x,t)$, so the linear system will take as a solutions Φ_0.
The Darboux Transformation is defined as :

$$\Phi[1] = \Phi \cdot \Lambda - \sigma\Phi, \tag{4.14}$$

where

$$\sigma = \Phi_0 \cdot \Lambda \cdot \Phi_0^{-1}. \tag{4.15}$$

We note that Φ_0 is a seed solution of the linear system for a given seed solution of the NLSE, Φ denotes any solution of the linear system, and $\Phi[1]$ is the new solution of the linear system.
The equations (4.5) and (4.6) under the DT

$$\Phi[1]_x = J \cdot \Phi[1] \cdot \Lambda + U[1] \cdot \Phi[1], \tag{4.16}$$

and

$$\Phi[1]_t = iJ \cdot \Phi[1] \cdot \Lambda^2 + iU[1] \cdot \Phi[1] \cdot \Lambda + V \cdot \Phi[1]. \tag{4.17}$$

By substituting in this system for Φ_1 from equation (4.14) and using the LP, equations (4.5) and (4.6), the transformed LP matrices $U[1]$ and $V[1]$ must satisfy the two following formula

$$U[1] = U_0 + \Big[J, \sigma\Big] = 0, \tag{4.18}$$

$$V[1] = V_0 + i\Big[U_0, \sigma\Big] = 0, \tag{4.19}$$

where U_0 and V_0 are the Lax Pair in terms of the seed solution zero.
We no that the DT applies only for the linear system (equations) and that the two matrices

(4.7) and (4.8) are constant under the DT and are and do not change. So the new seed solution becomes $U[1]$ where its obtained from the last equation (4.18) and its takes the following form:

$$\begin{aligned} U[1] &= \begin{pmatrix} 0 & \psi[1](x,t) \\ -\psi^*[1](x,t) & 0 \end{pmatrix} \\ &= \begin{pmatrix} 0 & \psi_0(x,t) \\ -\psi_0^*(x,t) & 0 \end{pmatrix} + \begin{pmatrix} 0 & \frac{2(\lambda_1-\lambda_2)\psi_1\psi_2}{\phi_1\psi_2-\phi_2\psi_1} \\ \frac{2(\lambda_1-\lambda_2)\phi_1\phi_2}{\phi_1\psi_2-\phi_2\psi_1} & 0 \end{pmatrix} \end{aligned} \tag{4.20}$$

For the $V_0[1]$ its will takes

$$V[1] = \frac{i}{2}\begin{pmatrix} -|\psi[1](x,t)|^2 & \psi[1]_x(x,t) \\ i\psi[1]_x^*(x,t) & -|\psi[1](x,t)|^2 \end{pmatrix}, \tag{4.21}$$

in this situation the compatibility condition takes form

$$U[1]_t - V[1]_x = \Big[V[1], U[1]\Big]. \tag{4.22}$$

This means that $\psi[1]$ is a solution of the NLSE

$$i\psi[1]_t + \frac{1}{2}\psi[1]_{xx} - |\psi[1]|^2\psi[1] = 0. \tag{4.23}$$

Thus, we see that from the solution zero $\psi_0(x,t)$ to NLSE we obtained a new solution $\psi[1]$ to the same equation NLSE whre this new solution takes the following expression

$$\psi[1] = \psi_0 + \frac{2(\lambda_1-\lambda_2)\psi_1\psi_2}{\phi_1\psi_2-\phi_2\psi_1}, \tag{4.24}$$

and for the complex conjugate of $\psi[1]$:

$$\psi[1]^* = \psi_0^* - \frac{2(\lambda_1-\lambda_2)\phi_1\phi_2}{\phi_1\psi_2-\phi_2\psi_1}, \tag{4.25}$$

Here, the second term on the right side of the to equations 4.24 and 4.25 is called the *Darboux Dressing*.

4.2.4 Symmetry Reduction

In this section we will obtain eight equations by equating the two matrices (4.3) and (4.4), the derivatives of the auxiliary field with respect to x and t gives

For the x-**equations**

$$-i\sqrt{c}\,\psi(x,t)\,\phi_1-\lambda_1\,\psi_1+\psi_{1x}=0, \tag{4.26}$$

$$-i\sqrt{c}\,\psi(x,t)\,\phi_2-\lambda_2\,\psi_2+\psi_{2x}=0, \tag{4.27}$$

$$\lambda_1\,\phi_1(x,t)+i\sqrt{c}\,\psi_s(x,t)\psi_1+\psi_{1x}=0, \tag{4.28}$$

$$\lambda_2\,\phi_2(x,t)+i\sqrt{c}\,\psi_s(x,t)\psi_2+\psi_{2x}=0. \tag{4.29}$$

And for the t-**equations**

$$-i\lambda_1^2\,\psi_1(x,t)+\psi(x,t)(\sqrt{c}\,\lambda_1\phi_1(x,t)+\frac{1}{2}\,i\,c\,\psi_s(x,t)\psi_1(x,t))+\psi_{1t}+\frac{1}{2}\sqrt{c}\,\phi_1(x,t)\psi_x(x,t)=0, \tag{4.30}$$

$$-i\,\lambda_2^2\,\psi_2(x,t)+\psi(x,t)(\sqrt{c}\,\lambda_2\,\phi_2(x,t)+\frac{1}{2}i\,c\,\psi_s(x,t)\psi_2(x,t))+\psi_{2t}+\frac{1}{2}\sqrt{c}\,\phi_2(x,t)\psi_x(x,t)=0, \tag{4.31}$$

$$\frac{1}{2}\,i(2\lambda_1^2-c\,\psi(x,t))\phi_1(x,t)-\sqrt{c}\,\lambda_1\psi_s(x,t)\psi_1+\phi_{1t}(x,t)+\frac{1}{2}\,\sqrt{c}\,\psi_1(x,t)\psi_{s_t}(x,t)=0, \tag{4.32}$$

$$\frac{1}{2}\,i\,(2\lambda_2^2-c\,\psi_s(x,t))\phi_2(x,t)-\sqrt{c}\,\lambda_2\,\psi_s(x,t)\psi_2+\phi_{2t}(x,t)+\frac{1}{2}\,\sqrt{c}\,\psi_1(x,t)\psi_{s_t}(x,t)=0. \tag{4.33}$$

The solution of the eight equations (4.26-4.33), t-**equations** and t-**equations** gives the

expressions of the four functions ψ_1, ϕ_1, ψ_2 and ϕ_2.

We note also that we the eight equations can be reduced to four equations by using the following conditions:

$$\lambda_2{}^* = -\lambda_1, \qquad \phi_2{}^* = \psi_1, \qquad \psi_2{}^* = -\phi_1, \tag{4.34}$$

where after applying the symmetry conditions we can solve only the four equations 4.26 , 4.28, 4.30and 4.32 to get the solution of NLSE equation 4.23. The solution of equation (4.23) will be given by the following formula :

$$\psi(x,t) = \psi_0(x,t) - \frac{i}{\sqrt{c}} \frac{2(\lambda_1 - \lambda_2)\psi_1(x,t)\psi_2(x,t)}{-\phi(x,t)_2\psi_1(x,t) + \phi_1(x,t)\psi_2(x,t)}. \tag{4.35}$$

We can do the reduction of the eight equations to four equations according to the constant c, so two cases will be presented for the $u(x,t)$:

(i) positive constant, $c > 0$

the symmetry condition here are: $\phi_{2s}(x,t) = \psi_1$,$\phi_{2s}(x,t) = \phi_1$ and $\lambda_{2s} = -\lambda_1$.

$$\psi(x,t) = \psi_0(x,t) - \frac{i}{\sqrt{c}} \frac{2(\lambda_1 + \lambda_{1s})\psi_1(x,t)\psi_{1s}(x,t)}{-\psi(x,t)_{1s}\psi_1(x,t) + \phi_1(x,t)\psi_{1s}(x,t)}. \tag{4.36}$$

(ii) negative constant, $c < 0$

for this case , we use the symmetry: $\phi_{2s}(x,t) = \psi_1$,$\phi_{2s}(x,t) = -\phi_1$ and $\lambda_{2s} = -\lambda_1$.

$$\psi(x,t) = \psi_0(x,t) + \frac{i}{\sqrt{c}} \frac{2(\lambda_1 + \lambda_{1s})\psi_1(x,t)\psi_{1s}(x,t)}{\psi(x,t)_{1s}\psi_1(x,t) + \phi_1(x,t)\psi_{1s}(x,t)}. \tag{4.37}$$

4.2.5 Solution of the linear system for the fundamental NLSE for zero seed

In this section, we solve the NLSE for the constant $c = -1$, so the equation (4.1) reads

$$i\psi_t + \frac{1}{2}\psi_{xx} + |\psi|^2\psi = 0, \tag{4.38}$$

where we take as seed solution zero the function $\psi(x,t) = 0$.

The correponding Lax pair terms of this solution read

$$\psi_0 = \begin{pmatrix} 0 & 0 \\ 0 & 0 \end{pmatrix}. \tag{4.39}$$

$$V_0 = \frac{i}{2}\begin{pmatrix} 0 & 0 \\ 0 & 0 \end{pmatrix}. \tag{4.40}$$

Because λ_1 and λ_2 are complex constant, we can write equation (4.8) for the constant Λ as

$$\Lambda = \begin{pmatrix} \lambda_{1r} + i\,\lambda_{1i} & 0 \\ 0 & \lambda_{2r} + i\,\lambda_{2i} \end{pmatrix}. \tag{4.41}$$

From equations (4.3) and (4.4), we have

$$\Phi_x(x,t) = \begin{pmatrix} (i\lambda_{1i} + \lambda_{1r})\psi_1 & (i\lambda_{2i} + \lambda_{2r})\psi_2 \\ -(i\lambda_{1i} + \lambda_{1r})\phi_1 & -(i\lambda_{2i} + \lambda_{2r})\phi_2 \end{pmatrix}, \tag{4.42}$$

and

$$\Phi_t(x,t) = \begin{pmatrix} i(i\lambda_{1i} + \lambda_{1r})^2\psi_1 & i(i\lambda_{2i} + \lambda_{2r})^2\psi_2 \\ -i(i\lambda_{1i} + \lambda_{1r})^2\phi_1 & -i(i\lambda_{2i} + \lambda_{2r})^2\phi_2 \end{pmatrix}. \tag{4.43}$$

Equating these two matrices with the derivatives of the auxiliary field with respect to x and t, respectively to applying the compatibility condition $\Phi_{tx} = \Phi_{xt}$, we get the following eight equations

$$\psi_{1x} = (i\lambda_{1i} + \lambda_{1r})\psi_1, \tag{4.44}$$

$$\psi_{2x} = (i\lambda_{2i} + \lambda_{2r})\psi_2, \tag{4.45}$$

$$\phi_{1x} = -(i\lambda_{1i} + \lambda_{1r})\phi_1, \tag{4.46}$$

$$\phi_{2x} = -(i\lambda_{2i} + \lambda_{2r})\phi_2, \tag{4.47}$$

$$\psi_{1t} = i(i\lambda_{1i} + \lambda_{1r})^2\psi_1, \tag{4.48}$$

$$\psi_{2t} = i(i\lambda_{2i} + \lambda_{2r})^2\psi_2, \tag{4.49}$$

$$\phi_{1t} = -i(i\lambda_{1i} + \lambda_{1r})^2\phi_1, \tag{4.50}$$

$$\phi_{2t} = -i(i\lambda_{2i} + \lambda_{2r})^2\phi_2, \tag{4.51}$$

Solving the above eight equations for the two variables x and t, we find

$$\psi_1(x,t) = C_1 e^{(\lambda_{1i} - i\lambda_{1r})x} e^{-i(\lambda_{1i}^2 - 2i\lambda_{1i}\lambda_{1r} - \lambda_{1r}^2)t}, \tag{4.52}$$

$$\psi_2(x,t) = C_2 e^{(\lambda_{2i} - i\lambda_{2r})x} e^{-i(\lambda_{2i}^2 - 2i\lambda_{2i}\lambda_{2r} - \lambda_{2r}^2)t}, \tag{4.53}$$

$$\phi_1(x,t) = C_3 e^{-i(\lambda_{1i} - i\lambda_{1r})x} e^{(i\lambda_{1i}^2 + 2i\lambda_{1i}\lambda_{1r} - i\lambda_{1r}^2)t}, \tag{4.54}$$

$$\phi_2(x,t) = C_4 e^{-i(\lambda_{2i} - i\lambda_{2r})x} e^{(i\lambda_{2i}^2 + 2i\lambda_{2i}\lambda_{2r} - i\lambda_{2r}^2)t}, \tag{4.55}$$

where C_1, C_2, C_3 and C_4 are real constants.

From equations (4.52), (4.53), (4.54) and (4.55), we construct the seed of the aixiliary field as

$$\Phi_0 = \frac{i}{2}\begin{pmatrix} C_1 e^{(\lambda_{1i} - i\lambda_{1r})x} e^{-i(\lambda_{1i}^2 - 2i\lambda_{1i}\lambda_{1r} - \lambda_{1r}^2)t} & C_2 e^{(\lambda_{2i} - i\lambda_{2r})x} e^{-i(\lambda_{2i}^2 - 2i\lambda_{2i}\lambda_{2r} - \lambda_{2r}^2)t} \\ C_3 e^{-i(\lambda_{1i} - i\lambda_{1r})x} e^{(i\lambda_{1i}^2 + 2i\lambda_{1i}\lambda_{1r} - i\lambda_{1r}^2)t} & C_4 e^{-i(\lambda_{2i} - i\lambda_{2r})x} e^{(i\lambda_{2i}^2 + 2i\lambda_{2i}\lambda_{2r} - i\lambda_{2r}^2)t} \end{pmatrix}. \tag{4.56}$$

Using the definition of the DT (4.14) and equation (4.18). After inserting the expression of

σ in equation (4.15) we get

$$U_0[1] = \begin{pmatrix} 0 & U_0[1]_{12} \\ U_0[1]_{21} & 0 \end{pmatrix}, \tag{4.57}$$

where

$$U_0[1]_{12} = \frac{2C_1C_2(-i\lambda_{1i} - \lambda_{1r} + i\lambda_{2i} + \lambda_{2r})e^{2(i\lambda_{1i}+\lambda_{1r}+i\lambda_{2i}+\lambda_{2r})x}}{C_1C_4e^{2(i\lambda_{1i}+\lambda_{1r})x+2i(\lambda_{2i}-i\lambda_{2r})^2t} - C_2C_3e^{2(i\lambda_{2i}+\lambda_{2r})x+2i(\lambda_{1i}-i\lambda_{1r})^2t}}, \tag{4.58}$$

$$U_0[1]_{21} = \frac{2C_3C_4(i\lambda_{1i} + \lambda_{1r} - i\lambda_{2i} - \lambda_{2r})e^{2i(\lambda_{1i}^2-2i\lambda_{1r}\lambda_{1i}-\lambda_{1r}^2+(\lambda_{2i}-i\lambda_{2r})t}}{-C_1C_4e^{2(i\lambda_{1i}+\lambda_{1r})x+2i(\lambda_{2i}-i\lambda_{2r})^2t} + C_2C_3e^{2(i\lambda_{2i}+\lambda_{2r})x+2i(\lambda_{1i}-i\lambda_{1r})^2t}}, \tag{4.59}$$

where here, the element $U_0[1]_{12}$ represents $\psi[1]$ and the $U_0[1]_{21}$ represents $-\psi[1]^*$. Also, $\psi[1]$ is the new solution that we search of the NLSE for zero seed, $\psi_0 = 0$.

4.2.6 Representation of the new exact solution to the local NLSE

To simplify the solution represented in the equation (4.58), we take:

$$C_1 = \frac{-C_3C_4}{C_2} \tag{4.60}$$

and

$$\lambda_{1r} = -\lambda_{2r} \tag{4.61}$$

if we put that $\alpha = C_4/C_2$, so equation (4.58) becomes

$$\psi[1](x,t) = \frac{2(-i\lambda_{1i} + i\lambda_{2i} + 2\lambda_{2r})}{e^{-2i\lambda_{1i}x+2i\lambda_{1i}^2t+2\lambda_{2r}x-4\lambda_{1i}\lambda_{2r}t-2i\lambda_{2r}^2-ln\alpha} + e^{-2i\lambda_{2i}x+2i\lambda_{2i}^2t-2\lambda_{2r}x-4\lambda_{2i}\lambda_{2r}t-2i\lambda_{2r}^2+ln\alpha}}. \tag{4.62}$$

Note that the solitonic solution is achieved when the following condition is satisfied

$$\lambda_{1i} = \lambda_{2i}, \tag{4.63}$$

thus, the solution in equation (4.62) becomes

$$\psi[1](x,t) = \frac{4\lambda_{2r}e^{2i\lambda_{2i}x-2i\lambda_{2i}^2t+2i\lambda_{2r}^2t}}{e^{2\lambda_{2r}x-4\lambda_{2i}\lambda_{2r}t-ln\alpha}+e^{-2\lambda_{2r}x+4\lambda_{2i}\lambda_{2r}t+ln\alpha}}, \tag{4.64}$$

we can write also the last equation (4.64) in the following form:

$$\psi[1](x,t) = 2\lambda_{2r}e^{2i\lambda_{2i}x-2i\lambda_{2i}^2t+2i\lambda_{2r}^2t}\,\mathrm{sech}[2\lambda_{2r}(x-2\lambda_{2i}t-\frac{\ln\alpha}{2\lambda_{2r}})]. \tag{4.65}$$

We clearly see that in 4.65, the factor $2\lambda_{2r}$ plays the role of the pulse speed of the soliton. In general, we can put $\lambda_{2r}\to A$, $\ln\alpha/2\lambda_{2r}\to x_0$ and $2\lambda_2 i\to -v$. The solution (4.65) can be written as:

$$\psi[1](x,t) = A\,e^{-ivx-\frac{iv^2}{2}t+\frac{iA^2}{2}t}\,\mathrm{sech}[A(x-x_0-+vt)]. \tag{4.66}$$

Finaly, the solution becomes

$$\psi[1](x,t) = Ae^{i\Phi(x,t)}\,\mathrm{sech}[A(x-x_0+vt)], \tag{4.67}$$

where $\Phi(x,t) = -vx-(A^2/2-v^2/2)t$. The solution (4.67) is similar to the exact solution (1.38) found in Chapter 1 using the hydrodynamic approach.

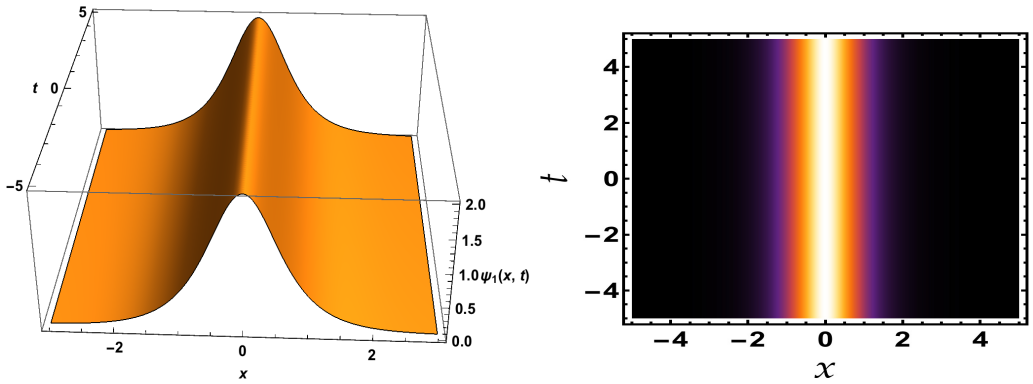

Figure 4.1: Soitonic solution of the fundamental NLSE with a zero velocity $v=0$, $A=2$, and $x_0=0$.

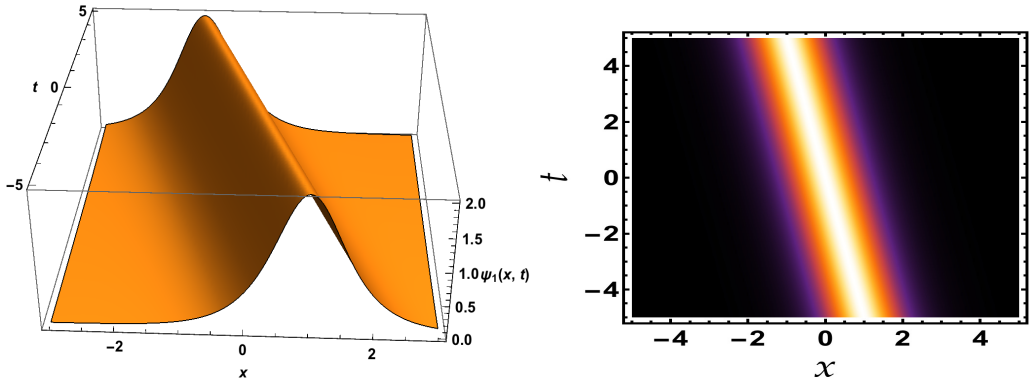

Figure 4.2: Movable solitonic solution of the fundamental NLSE with a velocity $v = 0.2$, $A = 2$ and $x_0 = 0$. Evolution of the movable soliton (left). Contour plot of the solution (right).

If we take a negative velocity, the soliton moves in the opposite direction of the case when the velocity is positive as shown in figure 4.3.

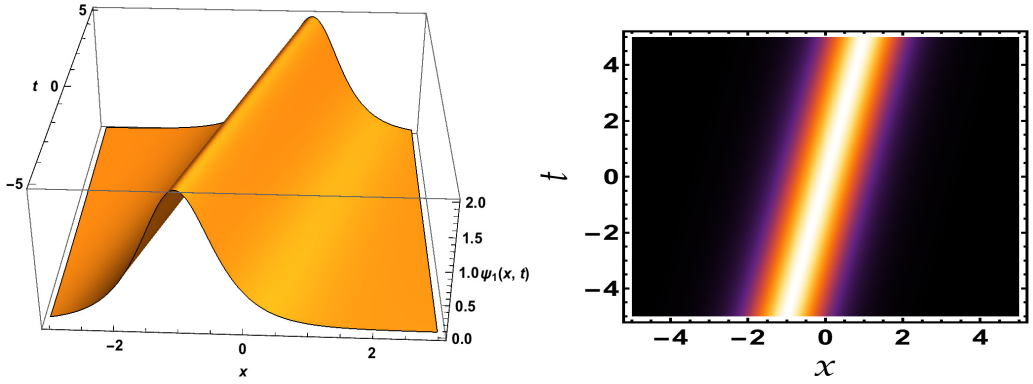

Figure 4.3: Movable solitonic solution of the fundamental NLSE with a velocity $v = -0.2$, $A = 2$ and $x_0 = 0$. Evolution of the movable soliton (left). Contour plot of the solution (right).

4.3 New exact solution to the local NLSE

In this section, we apply the LP and DT method with the rational seed solution, $\psi_0 = 1/x$, to get a new solution to the local NLSE equation 4.1 when the constant $c = +1$. We get

$$i\psi_t + \frac{1}{2}\psi_{xx} - |\psi|^2\psi = 0, \tag{4.68}$$

The LP in the case of equation (4.68) is the same used in equation (4.3) and equation (4.4) [165].

The auxiliary field $\Phi(x,t)$ is given by (the same 4.2). The field $\Phi(x,t)$ represents any solution of the linear system and $\Phi[1]$ is the new solution of this system which obeys the two equations (4.16) and (4.17).

Using the three equations (4.5), (4.6) and (4.14), the solution of the NLSE (4.68)becomes

$$\psi[1] = \psi_0 + Q(\psi_1, \phi_1), \tag{4.69}$$

where the Darboux dressing is given by the expression (4.25). The use the compatibility condition referenced with (4.9) in our case gives

$$\Phi_x(x,t) = \begin{pmatrix} i\psi(x,t)\phi_1(x,t) + \lambda_1\psi_1(x,t) & i\psi(x,t)\phi_2(x,t) + \lambda_2\psi_2(x,t) \\ -\lambda_1\phi_1(x,t) - i\psi_s(x,t)\psi_1(x,t) & -\lambda_2\phi_2(x,t) - i\psi_s(x,t)\psi_2(x,t) \end{pmatrix}. \tag{4.70}$$

and

$$\Phi_t(x,t) = \begin{pmatrix} \Phi_{t_{11}}(x,t) & \Phi_{t_{12}}(x,t) \\ \Phi_{t_{21}}(x,t) & \Phi_{t_{22}}(x,t) \end{pmatrix}. \tag{4.71}$$

$$\Phi_{t_{11}}(x,t) = -\tfrac{1}{2}\psi_x(x,t)\phi_1(x,t) - \tfrac{1}{2}i\psi(x,t)\psi_s(x,t)\psi_1(x,t) - \lambda_1\psi(x,t)\phi_1(x,t) + i\lambda_1^2\psi_1(x,t),$$
$$\Phi_{t_{12}}(x,t) = -\tfrac{1}{2}v_x(x,t)\phi_2(x,t) - \tfrac{1}{2}i\psi(x,t)\psi_s(x,t)\psi_2(x,t) - \lambda_2\psi(x,t)\phi_2(x,t) + i\lambda_2^2\psi_2(x,t),$$
$$\Phi_{t_{21}}(x,t) = \tfrac{1}{2}i\psi(x,t)\psi_s(x,t)\phi_1(x,t) - \tfrac{1}{2}\psi_{s_x}(x,t)\psi_1(x,t) + \lambda_1\psi_s(x,t)\psi_1(x,t) - i\lambda_1^2\phi_1(x,t),$$
$$\Phi_{t_{22}}(x,t) = \tfrac{1}{2}i\psi(x,t)\psi_s(x,t)\phi_2(x,t) - \tfrac{1}{2}\psi_{s_x}(x,t)\psi_2(x,t) + \lambda_2\psi_s(x,t)\psi_2(x,t) - i\lambda_2^2\phi_2(x,t).$$

Equating the two matrices with the derivatives of the auxiliary field with respect to x and t, resperctively, we get eight equations in the folowing form:

$$-i\,\psi(x,t)\,\phi_1(x,t) - \lambda_1\,\psi_1(x,t) + \psi_{1_x}(x,t) = 0, \tag{4.72}$$

$$-i\,\psi(x,t)\,\phi_2(x,t) - \lambda_2\,\psi_2(x,t) + \psi_{2_x}(x,t) = 0, \tag{4.73}$$

$$i\,\psi_s(x,t)\psi_1(x,t) + \lambda_1\,\phi_1(x,t) + \varphi_{1_x}(x,t) = 0, \tag{4.74}$$

$$i\,\psi_s(x,t)\,\psi_2(x,t)+\lambda_2\,\phi_2(x,t)+\phi_{2_x}(x,t)=0, \tag{4.75}$$

$$\frac{1}{2}\psi_x(x,t)\phi_1(x,t)+\psi(x,t)\left(\lambda_1\phi_1(x,t)+\frac{1}{2}\,i\,\psi_s(x,t)\psi_1(x,t)\right)-i\,\lambda_1^2\,\psi_1(x,t)+\psi_{1_t}(x,t)=0, \tag{4.76}$$

$$\frac{1}{2}\psi_x(x,t)\phi_2(x,t)+\psi(x,t)\left(\lambda_2\phi_2(x,t)+\frac{1}{2}\,i\,\psi_s(x,t)\psi_2(x,t)\right)-i\,\lambda_2^2\,\psi_2(x,t)+\psi_{2_t}(x,t), \tag{4.77}$$

$$\frac{1}{2}\,i\,\phi_1(x,t)\left(2\lambda_1^2-u(x,t)\,\psi_s(x,t)\right)+\frac{1}{2}\psi_{s_x}(x,t)\psi_1(x,t)-\lambda_1\,\psi_s(x,t)\psi_1(x,t)+\phi_{1_t}(x,t), \tag{4.78}$$

$$\frac{1}{2}i\phi_2(x,t)\left(2\lambda_2^2-\psi(x,t)\,\psi_s(x,t)\right)+\frac{1}{2}\psi_{s_x}(x,t)\psi_2(x,t)-\lambda_2\,\psi_s(x,t)\psi_2(x,t)+\phi_{2_t}(x,t). \tag{4.79}$$

Using the following symmetry reductions:

$$\lambda_2^*=-\lambda_1, \qquad \phi_2^*=\psi_1, \qquad \psi_2^*=\phi_1, \tag{4.80}$$

The eights equations from equations (4.72)-(4.79) become

$$-\lambda_1\psi_1-\psi\phi_1+\psi_{1_x}=0, \tag{4.81}$$

$$\lambda_1\phi_1+\psi^*\psi_1+\phi_{1_x}=0, \tag{4.82}$$

$$i\psi_{1_t}+\psi_1\left(\lambda_1^2+\frac{|\psi|^2}{2}\right)+\phi_1\left(\lambda_1\psi+\frac{\psi_x}{2}\right)=0, \tag{4.83}$$

$$i\phi_{1_t} + \psi_1\left(\frac{(\psi_x)^*}{2} - \lambda_1\psi^*\right) - \phi_1\left(\lambda_1^2 + \frac{|\psi|^2}{2}\right) = 0, \tag{4.84}$$

where $|\psi|^2 = \psi.\psi_s$.

Substituting the seed zero $\psi_0 = 1/x$ in (4.81)-(4.84) and solving for ψ_1 and ϕ_1 we find the solutions

$$\psi_1(x,t) = \frac{e^{-x\lambda_1}}{4x}(4c_{10}e^{-i\lambda_1^2 t} + \frac{c_{20}(2\lambda_1 x - 1)e^{2\lambda_1 x + i\lambda_1^2 t}}{\lambda_1^2}), \tag{4.85}$$

$$\phi_1(x,t) = \frac{ie^{-\lambda_1(x+i\lambda_1 t)}}{4\lambda_1^2 x}(4c_{10}\lambda_1^2(2\lambda_1 x + 1) - c_{20}e^{2\lambda_1(x+i\lambda_1 t)}), \tag{4.86}$$

where c_{10} and c_{20} are arbitrary complex constants.

Substituting (4.85) and (4.86) into (4.69), we obtain a new exact solution to the local NLSE, equation (4.68) namely:

$$\psi[1](x,t) = \frac{U_{1n}}{U_{1d}}, \tag{4.87}$$

where

$U_{1n} = 16A_1 x_1^2 + 2A_1[2A_1 x_0(\lambda_1 - \lambda_1^* + 2x x_1) - A_0\lambda_1^2 e^{2\lambda_1^*(x-i\lambda_1^* t)}]e^{2\lambda_1(x+i\lambda_1 t)}$,

$U_{1d} = 4A_0\lambda_1^2 x_0 e^{2\lambda_1^*(x-i\lambda_1^* t)} + A_1[2A_1 x_0 + A_0(2x x1 - x0)e^{2\lambda_1^*(x-i\lambda_1^* t)}]e^{2\lambda_1(x+i\lambda_1 t)} - 8A_1\lambda_1^2(2x x1 + x0)$

, and $x_0 = \lambda_1 + \lambda_1^*$, $x_1 = \lambda_1\lambda_1^*$, $A_0 = c_{20}c_{20}^*/2\lambda_1^{*2}c_{10}c_{10}^*$, and $A_1 = c_{20}/c_{10}$.

According to the previous parameters, we can separate three cases, where will change the value of constants c_i and λ_i to obtain the physical discipline of the function $u_1(x,t)$, distinguish three different regimes of the molecule of the two solitons molecule, namely:

(i) Symmetric coalescing solitons:

For $\lambda_1 = \lambda_{1r} = 1/2$, $c_{10} = 10 + 10i$ and $c_{20} = 10 - 10i$, the solution (4.87) reduces to

$$\psi[1](x,t) = \frac{e^{\frac{it}{2}}\left(2xe^{x+\frac{it}{2}} - ie^{2x} + i\right)}{i(x-2)e^{2x+\frac{it}{2}} + 2e^{x+it} - ie^{\frac{it}{2}}(x+2) - 2e^x}, \tag{4.88}$$

which is displayed in figure 4.4. Here, we observe that the two solitons collide periodically.

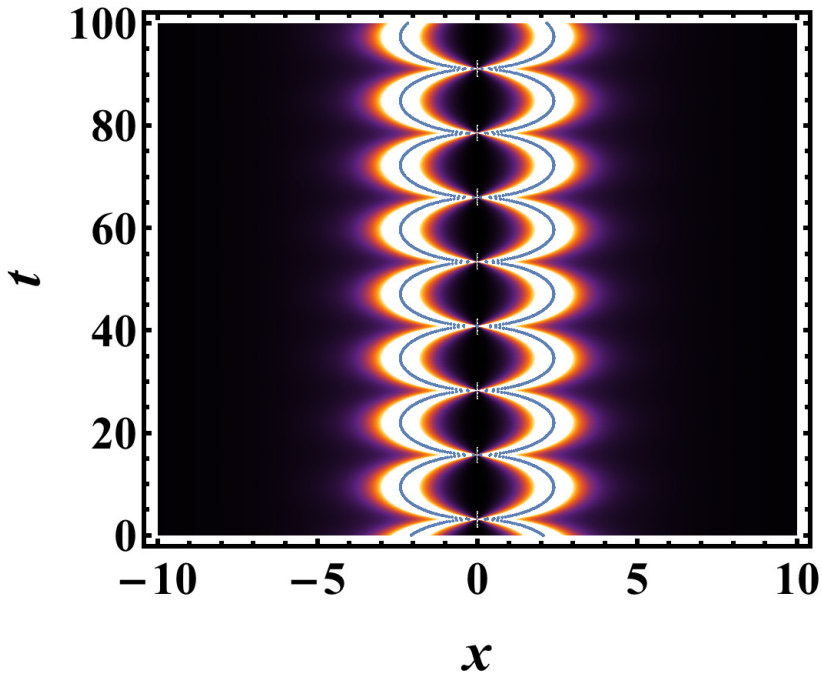

Figure 4.4: Singular solitons molecules with zero relative velocity. Symmetric coalescing solitons from (4.88) for $\lambda_1 = \lambda_{1r} = 1/2$, $c_{10} = 10 + 10i$ and $c_{20} = 10 - 10i$.

(ii) Asymmetric noncoalescing solitons:

For $\lambda = 1/4$, $c_{10} = 2i$ and $c_{20} = -4i$, we get

$$\psi[1](x,t) = \frac{e^{\frac{it}{8}}\left(8xe^{\frac{x}{2}+\frac{it}{8}} + 64e^{x} - 1\right)}{-64(x-4)e^{x+\frac{it}{8}} + 32e^{\frac{x}{2}+\frac{it}{4}} + e^{\frac{it}{8}}(x+4) + 32e^{x/2}}. \tag{4.89}$$

Here the two solitons still form a molecule but they do not coalesce, stay separated as shown in figure 4.5 .

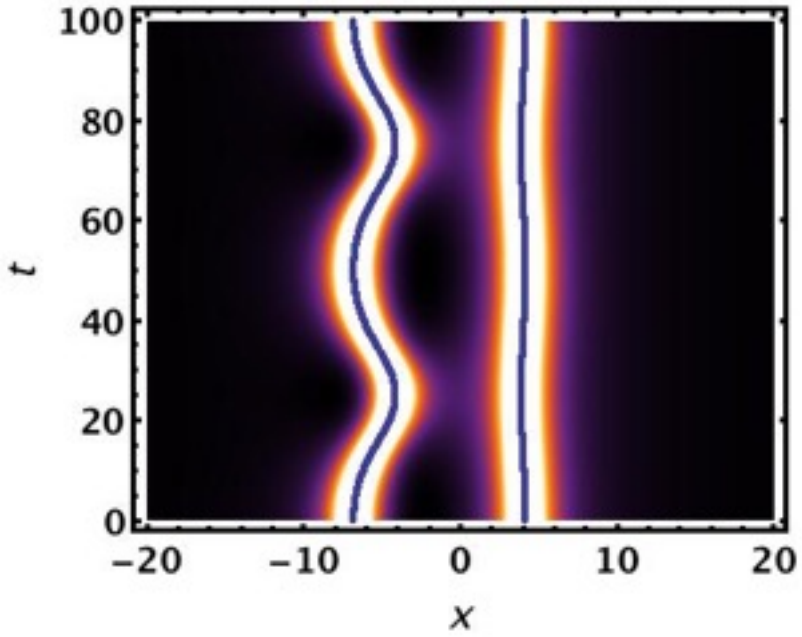

Figure 4.5: Singular solitons molecules with zero relative velocity. Asymmetric non coalescing solitons from (4.89) for$\lambda = 1/4$, $c_{10} = 2i$ and $c_{20} = -4i$.

(iii) Asymmetric coalescing solitons:

For small intersoliton distance, i.e, $\lambda = 1$, $c_{10} = 1+1i$ and $c_{20} = 1+1i$, equation (4.85) simplifies to

$$\psi[1](x,t) = \frac{e^{2it}\left(16xe^{2x+2it} - e^{4x} + 16\right)}{(x-1)e^{4x+2it} + 4e^{2x+4it} - 16e^{2it}(x+1) + 4e^{2x}}. \tag{4.90}$$

In this case the solitons coalesce, as in the first case, but the inter-soliton oscillation in performed mainly by one soliton, as in the second case. This is shown in figure (4.6) .

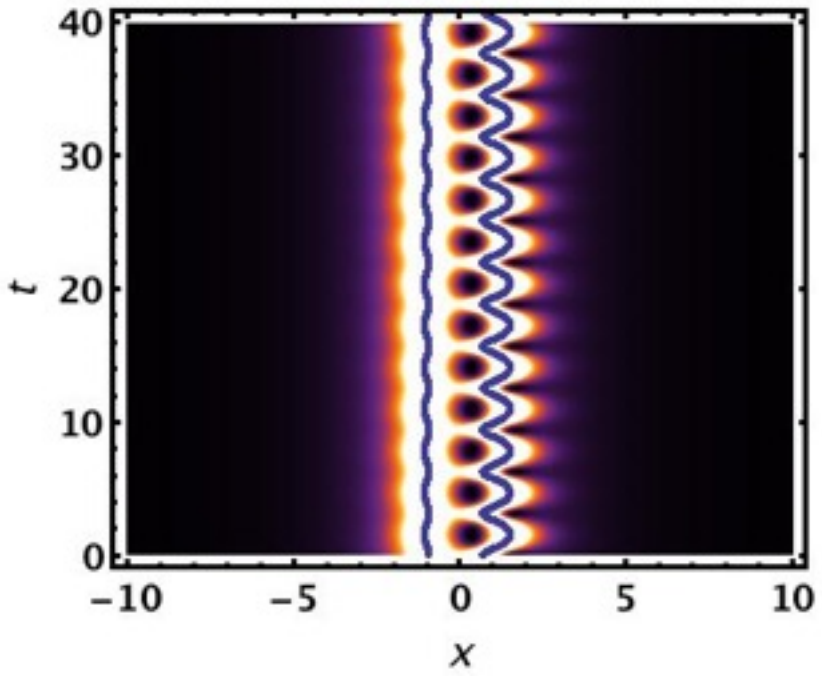

Figure 4.6: Singular solitons molecules with zero relative velocity. Asymmetric coalescing solitons from (4.90) for$\lambda = 1$, $c_{10} = c_{20} = 1 + 1i$.

The blue line in the three figures (4.4), (4.5) and (4.6) present the trajectory of solitons.

4.3.1 Determination of the force between the two solitons

To determine the forces of interaction between the two solitons , we calculate first the acceleration , a_r of the right soliton and a_l od the left soliton, this performed by extracting the center of mass of each soliton. x_r for the right soliton and x_l for the left soliton, and taking the second derivative , $a_r = \ddot{x}_r$ and $a_l = \ddot{x}_l$. The forces of interaction between the two solitons is proportional to the second derivative of their separation $F = m(a_r - a_l)$, where $m = \int_{-\infty}^{\infty} |u_1(x,t)|^2 dx$. Then, the integration of the force gives the potential $V = -\int F dx$.

When the two solitons are well-separated from each over, analytic expression for their positions can be extracted from the exact solutions, equation (4.87), which lead to the following expression for their accelerations

$$a_r = \frac{-x^3 + 4x^2 - 13x + 64e^x(4-x) - 4}{8e^x(x^3 - 6x^2 + 12x - 8) + 1536(x^3 - 2x^2 - 4x + 8)}, \tag{4.91}$$

and

$$a_l = \frac{64\left(x^3-4x^2+13x+4\right)+e^x(x-4)}{512e^x\left(x^3-6x^2+12x-8\right)+48\left(x^3-2x^2-4x+8\right)}, \tag{4.92}$$

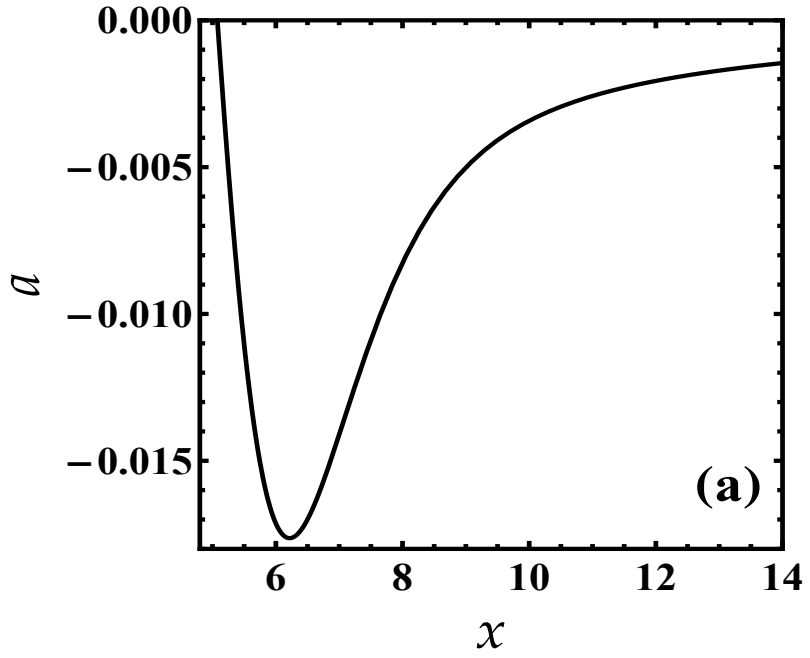

Figure 4.7: Presentation of the force from equations (4.91) and (4.92) when the solitons are well-separated. The acceleration of the solitons separation, $a_r - a_l$ as given by the equations (4.91) and (4.92), which is proportional to the mutuel force of interaction, F. Parameters are: $\lambda_1 = 1/4$, $c_{10} = 2\,i$ and $c_{20} = -4\,i$.

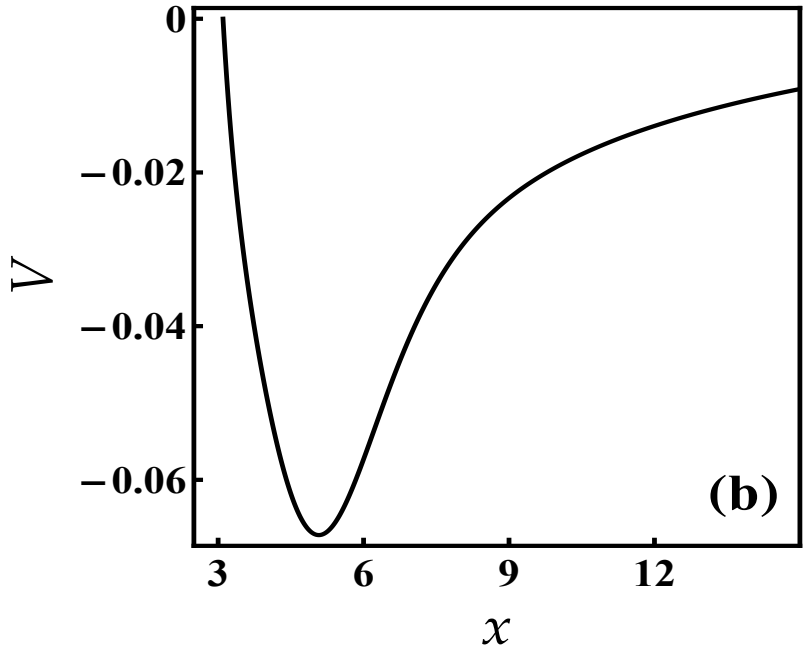

Figure 4.8: The interaction potential energy when the solitons are well-separated for $\lambda_1 = 1/4$, $c_{10} = 2i$ and $c_{20} = -4i$.

Similarty, when the solitons are close to each other, the acceleration read

$$a_r = \frac{64\left(-16x^3-16x^2-13x+1\right)+4e^{-x}(-x-1)}{-384x^3-192x^2+e^{-4x}\left(-8x^3-12x^2-6x-1\right)+96x+48}, \tag{4.93}$$

and

$$a_l = \frac{4\left(-16x^3-16x^2-13x+1\right)+64e^{-4x}(-x-1)}{16e^{-4x}\left(-8x^3-12x^2-6x-1\right)+3\left(-8x^3-4x^2+2x+1\right)}. \tag{4.94}$$

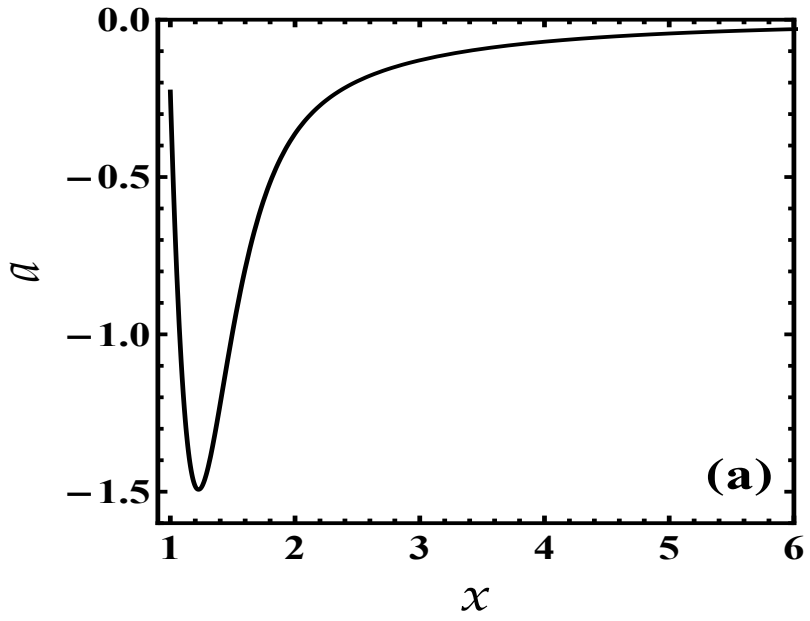

Figure 4.9: Presentation of the force , from equations (4.93) and (4.94) when the solitons are coalescing case. The acceleration of the solitons in fusion, $a_r - a_l$ as given by the equations (4.93) and (4.93), which is proportional to the mutuel force of interaction, F. Parameters are : $\lambda_1 = 1$, $c_{10} = 1 + i$ and $c_{20} = 1 + i$.

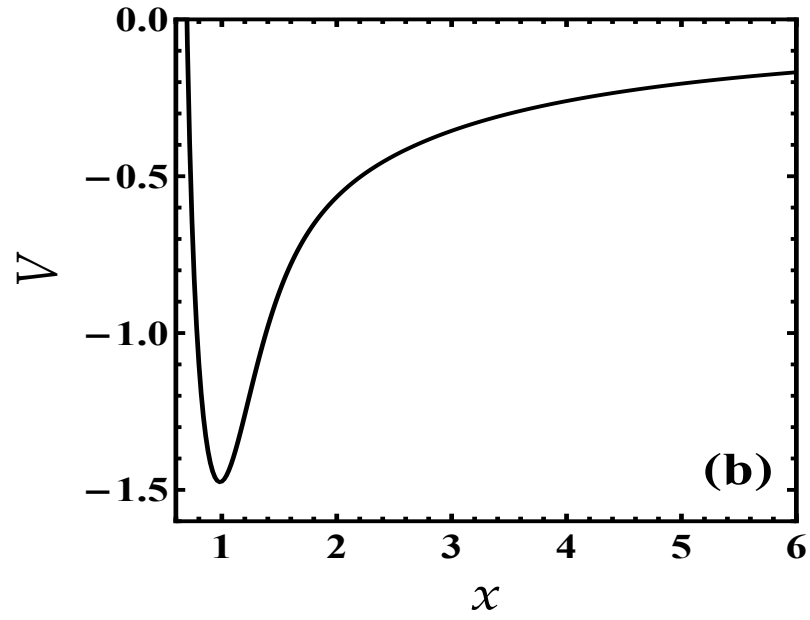

Figure 4.10: The interaction potential energy for $\lambda_1 = 1$, $c_{10} = 1 + i$ and $c_{20} = 1 + i$.

IIt is clearly apparent from figure (4.8) that for large separation, the interaction potential is nefative showing the instability and the robustness of the bond between the solitons. It is noticed that while each of the two solitons experiences the same force of interaction, they

have different acceleraction due their different masses, as is shown of figure (4.7) and figure (4.5). The situation is quite different when the two solitons are placed close to each other, the acceleration and the interaction potential well become narrower and deeper a fact that influences the formation of the bound state as is seen in figures (4.9) and (4.10). respectively. Figures (4.7), (4.8)(4.9) and (4.10) clearly show molecular type of potential between the two singular solitons.

4.3.2 Interaction of singular solitons

Let us now discuss the interaction of the two local solitons given by (4.87). Figures (4.11) and (4.12) show the scattering of the two solitons where they preserve their integrity after collision.

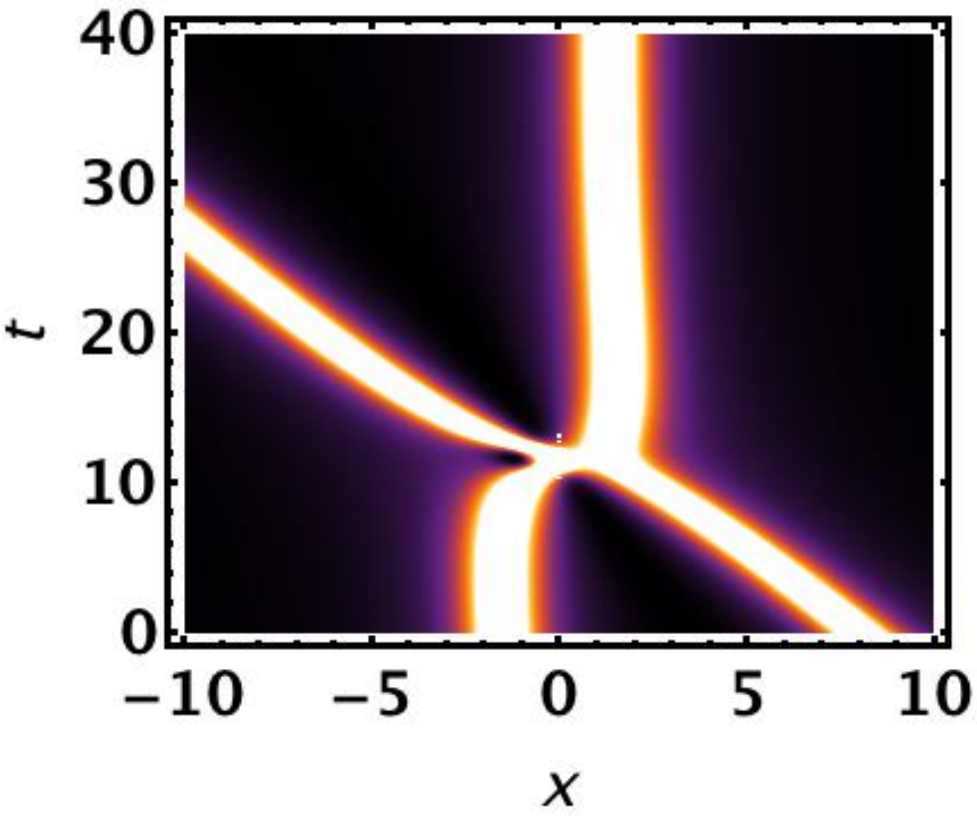

Figure 4.11: Transmission of one solitons with known speed λ_i, through a stationary soliton. Parameters used $\lambda_1 = -0.15 - 0.3i$, $c_1 = -10 - 10i$ and $c_2 = 10 + 50i$.

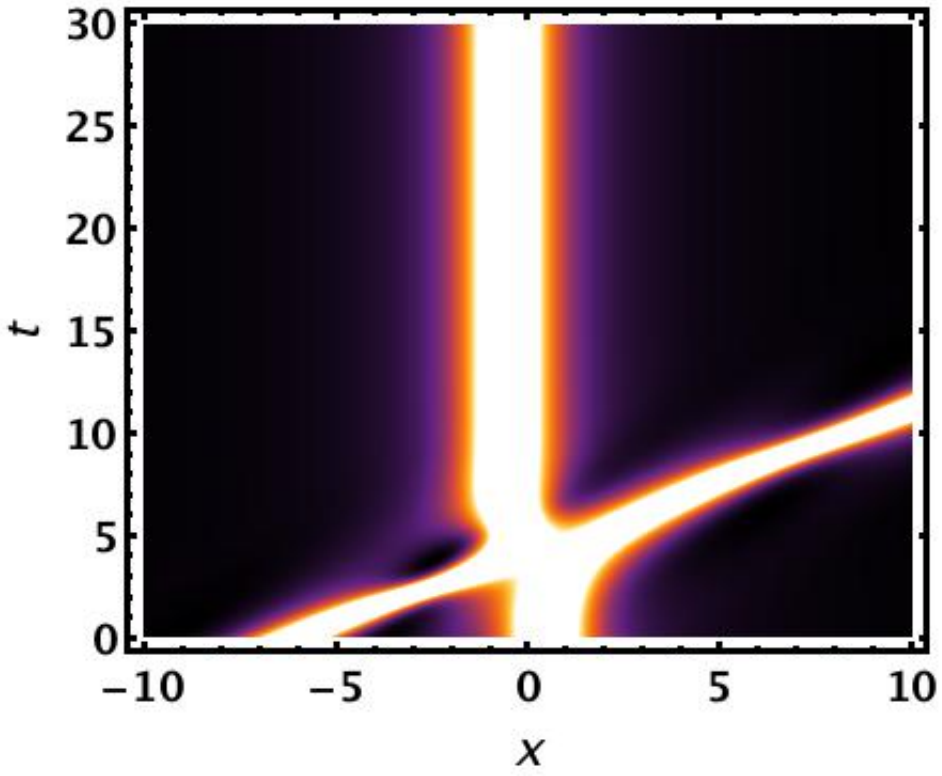

Figure 4.12: Transmission of one solitons with known speed λ_i, through a stationary soliton. Parameters used $\lambda_1 = -0.15 + 0.7i$, $c_1 = -10 + 10i$ and $c_2 = -1$.

4.4 New exact solution to the nonlocal NLSE

In this section, we apply the LP and DT method with the same rational seed solution, $\psi_0(x,t) = 1/x$, to the nonlocal NLSE can be written as:

$$i\psi_t + \frac{1}{2}\psi_{xx} + \psi^2\bar{\psi} = 0, \tag{4.95}$$

where $\bar{\psi} = \psi^*(-x,t)$. The Lax pair of (4.95) can found to be (4.3) and (4.4) with the following operators

$$U = \begin{pmatrix} 0 & -\psi \\ -\bar{\psi} & 0 \end{pmatrix}, \tag{4.96}$$

$$V = \frac{i}{2}\begin{pmatrix} \psi\bar{\psi} & \psi_x \\ \bar{\psi} & -\psi\bar{\psi} \end{pmatrix}, \tag{4.97}$$

The system of the two equations (4.16) and (4.17) translate into eight equations:

$$\psi(x,t)\phi_1(x,t) - \lambda_1\psi_1(x,t) + \psi_{1_x}(x,t) = 0, \tag{4.98}$$

$$\psi(x,t)\phi_2(x,t) - \lambda_2\psi_2(x,t) + \psi_{2_x}(x,t) = 0, \tag{4.99}$$

$$-\psi_s(-x,t)\psi_1(x,t) + \lambda_1\phi_1(x,t) + \phi_{1_x}(x,t) = 0, \tag{4.100}$$

$$-\psi_s(-x,t)\psi_2(x,t) + \lambda_2\phi_2(x,t) + \phi_{2_x}(x,t) = 0, \tag{4.101}$$

$$\frac{1}{2}i\psi_x(x,t)\phi_1(x,t) + \psi(x,t)\left(i\lambda_1\phi_1(x,t) - \frac{1}{2}i\psi_s(-x,t)\psi_1(x,t)\right) - i\lambda_1^2\psi_1(x,t) + \psi_{1t}(x,t) = 0, \tag{4.102}$$

$$\frac{1}{2}i\psi_x(x,t)\phi_2(x,t) + \psi(x,t)\left(i\lambda - 2\phi_2(x,t) - \frac{1}{2}i\psi_s(-x,t)\psi_2(x,t)\right) - i\lambda_2^2\psi_2(x,t) + \psi_{2t}(x,t) = 0, \tag{4.103}$$

$$\frac{1}{2}i\phi_1(x,t)\left(\psi(x,t)\psi_s(-x,t) + 2\lambda_1^2\right) - \frac{1}{2}i\psi_{s_x}(-x,t)\psi_1(x,t) - i\lambda_1\psi_s(-x,t)\psi_1(x,t) + \phi_{1t}(x,t) = 0, \tag{4.104}$$

$$\frac{1}{2}i\phi_2(x,t)\left(\psi(x,t)\psi_s(-x,t) + 2\lambda_2^2\right) - \frac{1}{2}i\psi_{s_x}(-x,t)\psi_2(x,t) - i\lambda_2\psi - s(-x,t)\psi_2(x,t) + \phi_{2t}(x,t) = 0, \tag{4.105}$$

Using the symmetry reductions in (4.80), the eight equations reduced to four equations in

the following

$$\psi\,\phi_1 - \lambda_1\,\psi_1 + \psi_{1_x} = 0, \tag{4.106}$$

$$\bar{\psi}\,\psi_1 - \lambda_1\,\phi_1 - \phi_{1_x} = 0, \tag{4.107}$$

$$-i\,\lambda_1^2\,\psi_1 + \frac{i}{2}\,\psi\,(2\,\lambda_1\,\phi_1 - \bar{\psi}\,\psi_1) + \psi_{1_t} + \frac{i}{2}\,\phi_1\,\psi_x = 0, \tag{4.108}$$

$$\frac{i}{2}(2\,\lambda_1^2 + \psi\,\bar{\psi})\,\phi_1 - i\,\lambda_1\,\bar{\psi}\,\psi_1 + \phi_{1_t} - \frac{i}{2}\,\psi_1\,\bar{\psi}_x = 0. \tag{4.109}$$

Applying the seed $\psi_0 = 1/x$ in (4.106)-(4.109) and solving for ψ_1 and ϕ_1, so

$$\psi_1(x,t) = \frac{1}{x}\left[c_1 - c_2\,(2\,\lambda_1\,x - 1)\,e^{2\,\lambda_1\,(x + i\,\lambda_1\,t)}\right] e^{-\lambda_1\,(x + i\,\lambda_1\,t)}, \tag{4.110}$$

$$\phi_1(x,t) = \frac{1}{x}\left[c_1 + c_2\,e^{2\,\lambda_1\,(x + i\,\lambda_1\,t)} + 2\,c_1\,\lambda_1\,x\right] e^{-\lambda_1\,(x + i\,\lambda_1\,t)}, \tag{4.111}$$

and hence, the new exact solution to the nonlocal NLSE, (4.95) is obtained by substituting (4.110) and (4.111) into (4.69)

$$\psi[1](x,t) = \frac{z_1(x,t)}{z_2(x,t)}, \tag{4.112}$$

where

$z_1(x,t) = c_1^2\,(-2\,\lambda_2\,x + e^{2\,\lambda_2\,(x + i\lambda_2 t)}) + c_1\,c_2\,((4\,\lambda_2^2\,x^2 - 1)\,e^{2\,\lambda_2\,(x + i\,\lambda_2\,t)}$
$+ (1 - 2\,\lambda_1\,x)e^{2x(\lambda_1 + \lambda_2) + 2it(\lambda_1 * 2 + \lambda_2 * 2)} - 2x(\,\lambda_2 + 2\,\lambda_1\,x(\,\lambda_1 - \lambda_2))\,e^{2\,\lambda_1 (x + i\,\lambda_1 t)}$
$+ 2\,\lambda_2\,x + c_2^2\,(2\,\lambda_2\,x\,(1 - 2\,\lambda_1\,x))e^{2\,\lambda_1 (x + i\,\lambda_1 t)} + (2\,\lambda_2\,x - 1)(4\,\lambda_1\,x^2\,(\,\lambda_1 - \lambda_2)$
$- 2x\,(\,\lambda_1 - \lambda_2) + 1)),$

and

$z_2(x,t) = x\,(-2\,c_1^2\,x\,(\,\lambda_1 - c_2\,\lambda_2\,e^{\,\lambda_2 (2x + i\lambda_2 t)} + c_2^2\,(-1 + 2\,x\,\lambda_2)\,e^{2x(\lambda_1 + \lambda_2) + 2it\,(\lambda_1^2 + \lambda_2^2)}$
$- c_1\,c_2\,(2\,x\,\lambda_1\,e^{2\,\lambda_1\,(x + it\,\lambda_1)} + 2\,c_2\,x\,\lambda_2\,(-1 + 2\,x\,\lambda_1)\,e^{2x(\lambda_1 + \lambda_2) + it\,(2\,\lambda_1^2 + \lambda_2^2)}$
$- (1 + 2\,x\,\lambda_1)(-1 + 2\,x\,\lambda_2)\,e^{2\,\lambda_2 (x + it\lambda_2)}))),$

where c_1 and c_2 are arbitrary real constants. For simplicity, we take $c_1 = c_2 = 1$, so the solution $u_1(x,t)$ takes the following form

$$\psi[1](x,t) = \frac{-4\,i\,\lambda_{1i}(x|\lambda_1|^2 - \lambda_{1r}^2)e^{2q_3(x,t)} - \lambda_1^{*2}e^{q_1(x,t)} + \lambda_1^2 e^{q_2(x,t)}}{2\,i\left\{\lambda_{1i}\cos[q_4(x,t)] + \lambda_{1i}\cosh[2\,\lambda_{1r}x - 2\,i\,(\lambda_{1i}{}^2 - \lambda_{1r}{}^2)t] + |\lambda_1|^2 x\sin[q_4(x,t)]\right\}e^{q_3(x,t)}}, \tag{4.113}$$

where

$q_1(x,t) = 2\,\lambda_1^*\,(x + i\,\lambda_1 t)$,

$q_2(x,t) = 2\,\lambda_1\,(x + i\,\lambda_1^* t)$,

$q_3(x,t) = 2\,x\,\lambda_{1r} - 2\,i\,(\lambda_{1i}{}^2 - \lambda_{1r}{}^2)\,t$,

and

$q_4(x,t) = 2\,\lambda_{1i}\,(x + 2\,i\,\lambda_{1r})$.

The solution (4.113) corresponds to the scattering of a stationary soliton and two breathers; one on a flat background and the other is on a inclined backgroud as in shown in figure 4.13.

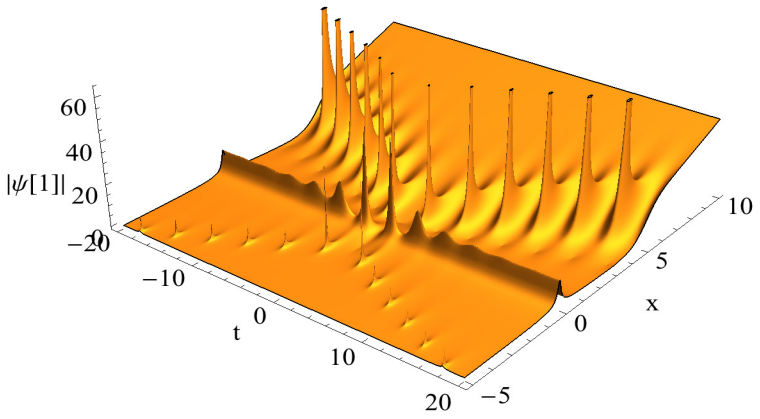

Figure 4.13: Solution (4.113) of the nonlocal NLSE (4.95) . It shows the interaction between a stationary solitons and two breathers, the breather soliton on the right side is in an inclined background and the left breather is in flat background. Parameters used: $\lambda_{1i} = 0.08$ and $\lambda_{1r} = 1$.

4.4.1 Variation of the constant λ_{1r}

Here, we show the effect of λ_{1r} on the middle soliton and the two breathers.

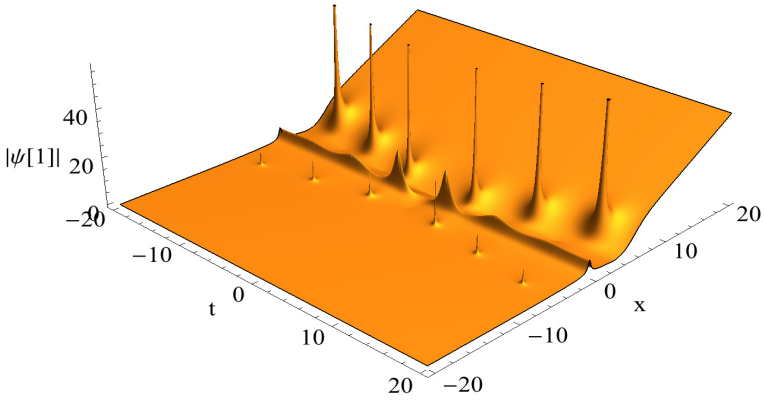

Figure 4.14: Temporal Spatial representation of the soliton breather envelope $\psi[1](x,t)$, parameters $\lambda_{1i} = 0.08$ and $\lambda_{1r} = 0.7$.

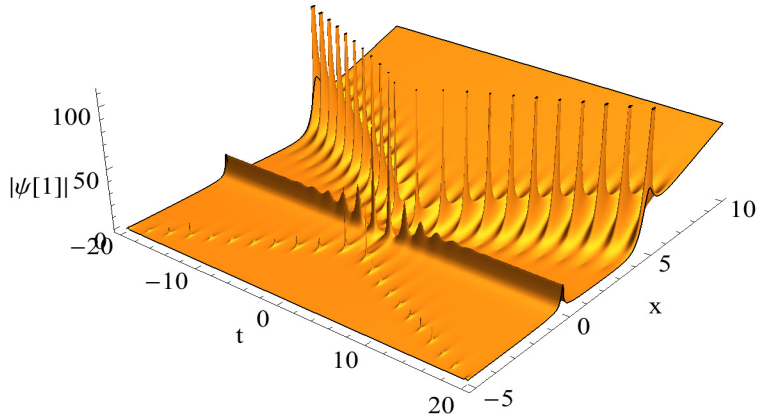

Figure 4.15: Temporal Spatial representation of the soliton breather envelope u_1, parameters $\lambda_{1i} = 0.08$ and $\lambda_{1r} = 1.3$.

Figures (4.14) and (4.15) show the role of λ_{1r} in our nonlocal solution of the NLSE (4.95). We see that the constant λ_{1r} tends to increase/decrease the trains waves of the two solitons breather.

4.5 New Exact Solution to the Reverse-Time NLSE

Another interesting possibility is a NLSE which is nonlocal in time rather than space, as for example,

$$i\psi_t + \frac{1}{2}\psi_{xx} - \psi^2\tilde{\psi} = 0, \tag{4.114}$$

where $\tilde{\psi} = \psi^*(x,-t)$. It was found that this equation admits a LP only when the coefficient of the time derivative is real [175, 185]. Nevertheless, in the following discussion, we present three exact solutions to (4.114) using the traditional separation-of-variables method.

(i) $t-$independent solution:

Let us write

$$\psi(x,t) = F(x), \tag{4.115}$$

and substitute into (4.114) to get

$$F''(x) - 2F^3(x) = 0, \tag{4.116}$$

with the solution

$$F(x) = \frac{c}{cx-1}, \tag{4.117}$$

where c is an arbitrary real constant.

(ii) $x-$independent solution:

We express the solution as

$$\psi(x,t) = Z(T), \tag{4.118}$$

where $T = it$. Substituting in (4.114) leads to

$$Z'(T) + Z^3(T) = 0, \tag{4.119}$$

with the solution

$$\psi(x,t) = \pm\frac{1}{\sqrt{2it-2c}}, \tag{4.120}$$

where c is an arbitrary real constant.

(iii) $t-$ and $x-$dependent solution:

Finally, we express the solution as

$$\psi(x,t) = Z(T)\, e^{ix}. \tag{4.121}$$

Substituting this in (4.114) leads to

$$Z'(T) + Z^3(T) + Z(T) = 0, \tag{4.122}$$

which yields to the following exact solution to (4.114)

$$\psi(x,t) = \pm \frac{c\, e^{ix}}{\sqrt{e^{it} - 2c^2}}, \tag{4.123}$$

where c is an arbitrary real constant.

Chapter 5

Conclusions and Outlook

In this thesis we investigated the static and the dynamics of 1D nonlocal soliton and soliton molecules in the framework of the nonlocal GPE.

We first considered the static and the scattering properties of a three-soliton molecule in 1D dipolar BEC with competing nonlinearities. We demonstrated that the interplay of repulsive local and attractive nonlocal nonlinearities leads to remarkable features. The binding mechanism in the molecule has been examined by means of a variational approach where a suitable trial function and a Gaussian nonlocal response function have been introduced. We showed that the stability and the dynamics of the three solitons bound state strongly depend on the degree of nonlocality, the relative phase, and the separation between adjacent solitons. In addition, we studied the interaction of a three-soliton molecule with a potential barrier. We explored in particular effects produced by variations of the soliton velocity, barrier height and its width. The mechanism of molecule reflection and transmission through the barrier has been also addressed. Our variational results have checked by a direct numerica simulation of the nonlocal GPE.

Furthermore, we numerically studied interwire effects on the formation of polar soliton molecules in a biwire system where dipole moments are aligned head-to-tail across the wires by solving the coupled 1D nonlocal GPE. We showed that the intertube interactions play a key role in the formation of a stable bound state of unconnected solitons. The stability and the interaction of such dimer molecules depends also on the interwire distance and also depends with the interaction dipolar constant. The breathing oscillations of the width

and the center-of-mass of the soliton have been deeply analyzed in terms of the interaction strength, rotonization effects and the interwire separation.

Moreover, we derived a new two-soliton solution of the 1D local NLSE using the LP and DT method with an algebraically-decaying seed solution. Within this seed, the DT method leads to the so-called singular molecule soliton which is a higher-order solution composed of two diverging peaks. The constructed solution allowed us to control practically all the characteristics of the molecule such as the binding energy, the force, and potential of interaction between the two solitons. We discussed in addition the scattering properties of such solitons. The time evolution of the soliton width has been addressed to reveal the survival of these new structures. Employing this LP in DT with the same algebraically-decaying solution, we obtained a new exact solution for the nonlocal NLSE presented an elastic interaction between one soliton and two breather solitons, on a flat and ramp backgrounds. The case with reverse-time nonlocal NLSE has been also highlighted.

Let us now outline some possible directions for future works. A compelling topics is to investigate the properties of dark three-soliton molecules with nonlocal response function. The study the interaction of nonlocal three-soliton molecules with potential wells rather than barriers is also of a particular interest. Interwire effects on the generation and the stability of dark solitons in biwire systems could be also addressed using the same technique used in Chapter 3. A systematic analysis on the modulation instability of the singular solitons is still to be performed to identify the stability criterion.

Bibliography

[1] E. P. Gross. *,Nuovo Cimento*, **20**(454), 1961.

[2] L. Pitaevskii. *,Sov. Phys. JETP*, **13**(451), 1961.

[3] J. Scott Russell. Report on waves". Fourteenth meeting of the British Association for the Advancement of Science. 1844.

[4] D. J, Korteweg, and G. de Vries. On the Change of Form of Long Waves advancing in a Rectangular Canal and on a New Type of Long Stationary Waves. *Phil. Mag*, **39**(422), 1895.

[5] J. Frenkel and T. Kontorova. On the theory of plastic deformation and twinning. *Phys. Z. Sowjetunion,*, **1**(137), 1939.

[6] E. Fermi, J. R. Pasta, and S. M. Ulam. Studies of Nonlinear Problems. . *Techn. Rep. , LA-1940, Los Alamos Sci. Lab.*, 1955.

[7] J. E. Allen. *Physica Scripta*, **57**(436), 1998.

[8] Zabusky and M. D N. J. Kruskal. *Phys. Rev. Lett.*, **15**(240), 1965.

[9] Gardner, S. Clifford, Greene, M. John, Kruskal, and Robert M. *Phys. Rev. Lett.*, **19**(19), 1967.

[10] M. Toda. *Journal of the Physical Society of Japan,*, **22**(431), 1967.

[11] J T. Tsuzuki. *Low Temp. Phys.*, **4**(441), 1971.

[12] N. Bogoliubov. *J. Phys*, **11**(23), 1947.

[13] V. E. and Zh. Eksp. Theor.Fiz A.B. Shabat. *Sov.Phys. JETP*, **64**(1627), 1973.

[14] V. E. Zakharov, A. B. Shabat, and Zh. Eksp. Theor.Fiz. *Sov. Phys. JETP*, **37**(823), 1973.

[15] A. Hasegawa and Y. Kodama. Solitons in Optical Communications (Oxford University Press, New York,. 1995.

[16] S. Burger et al. *Phys. Rev. Lett*, **83**(5198), 1999.

[17] L. Khaykovich et al. *Science*, **296**(1290), 2002.

[18] K.E. Strecker, G.B. Partridge, A. Truscott, and R.G. Hulet. *Nature*, **417**(150), 2002.

[19] Y. S. Kivshar and B. Luther-Davies. *Physics Reports*, **298**:81–197, 1998.

[20] S. N. Bose. *Z. phys.*, **26**(178), 1924.

[21] A. Einstein. *Sitzungsber. Preuss. Akad. Wiss., Bericht.*, **3**(18), 1925.

[22] S. Chu. *Rev. Mod. Phys.*, **70**(685), 1998.

[23] C. N. Cohen-Tannoudji. *Rev. Mod. Phys*, **70**(707), 1998.

[24] W. D. Phillips. *Rev. Mod. Phys*, **70**(707), 1998.

[25] M.H. Anderson, J.R. Ensher, M.R. Matthews, C.E. Wieman, and E.A. Cornell. *Science*, **269**(198), 1995.

[26] K.B. Davis, M.O. Mewes, M. R. Andrews, N.J. Van Druten, D.S. Durfee, D.M. Kurn, and W. Ketterle. *Phys. Rev. Lett*, **75**(3969), 1995.

[27] C. C. Bradley, C. A. Sackett, J. J. Tollett, and R. G. Hulet. *Phys. Rev. Lett*, **75**(1687), 1996.

[28] J. Denschlag et al. *Science*, **287**(97), 2000.

[29] B. P. Anderson et al. *Phys. Rev. Lett*, **86**(2926), 2001.

[30] U. Al Khawaja, H.T.C. Stoof, R.G. Hulet, K.E. Strecker, and G.B. Partridge. *Phys. Rev. Lett*, **89**(200404), 2002.

[31] T. Lahaye et al. *Rep. Prog. Phys*, **72**(126401), 2009.

[32] M. Lu et al. *Phys. Rev. Lett*, **107**(190401), 2011.

[33] K. Aikawa et al. *Phys. Rev. Lett*, 1**08**(210401), 2012.

[34] M. Lu, N. Q. Burdick, and B. L. Lev. *Phys. Rev. Lett*, **108**(215301), 2012.

[35] M. A. Baranov. *Physics Reports*, **464**(71), 2008.

[36] L.D. Carr, D. DeMille, R.V. Krems, and J. Ye. *New Journal of Physics*, **11**(055049), 2009.

[37] M.A. Baranov, M. Delmonte, G. Pupillo, and P. Zoller. *Chemical Reviews*, **112**(5012), 2012.

[38] K. Aikawa, D. Akamatsu, M. Hayashi, K. Oasa, J. Kobayashi, P. Naidon, T. Kishimoto, M. Ueda, , and S. Inouye. *Phys. Rev.Lett*, **105**(203001), 2010.

[39] K. K. Ni, S. Ospelkaus, M. H. G. de Miranda, B. Neyenhuis A. Péer, J. J. Zirbel, S. Kotochigova, P. S. Julienne, D. S. Jin, and J. Ye. *Chemical Reviews*, **112**(5012), 2012.

[40] J. Cuevas, B. A. Malomed, P. G. Kevrekidis, and D. J. Frantzeskakis. *Phys. Rev. A*, **79**(053608), 2009.

[41] K. Lakomy, R. Nath, and L. Santos. *Phys. Rev. A*, **85**(033618), 2012.

[42] K. Pawlowski and K. Rzazewski. *New J. Phys*, **17**(105006), 2015.

[43] B. B. Baizakov, S. M. Al-Marzoug, and H. Bahlouli. *Phys. Rev. A*, **92**(033605), 2015.

[44] M. J. Edmonds, T. Bland, D. H. J. O'Dell, and N. G. Parker. *Phys. Rev. A*, **93**(063617), 2016.

[45] T. Bland, M. J. Edmonds, N. P. Proukakis, A. M. Martin, D. H. J. O'Dell, and N. G. Parker. *Phys. Rev. A*, **92**(063601), 2015.

[46] F.Kh. Abdullaev, A. Gammal, B.A. Malomed, and L. Tomio. *Phys. Rev. A*, **87**(063621), 2013.

[47] S. Sinha and L. Santos. *Rev. Lett*, **99**(140406), 2007.

[48] .E. Young-s, P. Murunganandam, and S.K. Adhikari. *J. Phys. B: At. Mol. Opt. Phys*, **44**(101001), 2011.

[49] I. Tikhonenkov, B. A. Malomed, and A. Vardi. *Phys. Rev. A*, **78**(043614), 2008.

[50] G. Gligoric, A. Maluckov, M. Stepic, L. Hadievski, and B. A. Malomed. *Phys. Rev. A*, **81**(013633), 2010.

[51] Ai-Xia Zhang and Ju-Kui Xue. *Phys. Rev. A*, **82**(013606), 2010.

[52] S. K. Adhikari and P. Muruganandam. *J. Phys. B: At. Mol. Opt. Phys*, **45**(045301), 2012.

[53] Z. Fan, Y. Shi, Y. Liu, W. Pang, Y. Li, and B. A. Malomed. *Phys. Rev. E*, **95**(032226), 2017.

[54] S. K. Adhikari. *Phys. Rev. A*, **89**(043615), 2014.

[55] S. K. Adhikari. *Phys. Rev. A*, **89**(013630), 2014.

[56] P. Pedri and L. Santos. *Phys. Rev. Lett*, **95**(200404), 2005.

[57] I. Tikhonenkov, B. A. Malomed, and A. Vardi. *Phys. Rev. Lett*, **100**(090406), 2008.

[58] R. Eichler, D. Zajec, P. Koberle, J. Main, and G. Wunner. *Phys. Rev. A*, **86**(053611), 2012.

[59] P. Koberle, D. Zajec, G. Wunner, and B. A. Malomed. *Phys. Rev. A*, **85**(023630), 2012.

[60] M. Raghunandan. *Phys. Rev. A*, **92**(013637), 2015.

[61] R. Nath, P. Pedri, and L. Santos. *Phys. Rev. Lett*, **101**(210402), 2008.

[62] N. V. Tabiryan, A. V. Sukhov, and B. Ya. Zeldovich. *Mol. Cryst. Liq. Cryst*, **136**(1), 1986.

[63] M. Segev et al. *Phys. Rev. Lett.*, **68**(923), 1992.

[64] G. Duree et al. *Phys. Rev. Lett*, **71**(533), 1993.

[65] M. Shih et al. *Phys. Rev. Lett*, **31**(826), 1995.

[66] A. Ciattoni E. DelRe and A. J. Agranat. *Opt. Lett*, **26**(908), 2001.

[67] D. Neshev et al. *Opt. Lett*, **26**(1185), 2001.

[68] O. Bang P. D. Rasmussen and W. Krolikowski. *Phys. Rev. E*, **72**(066611), 2005.

[69] S. Skupin, M. Saffman, and W. Krolikowski. *Phys. Rev. Lett.*, **98**(263902), 2007.

[70] A. Hasegawa and Y. Kodama. Solitons in Optical Communincations, Oxford University Press, Oxford . *Phys. Rev. Lett.*, 1995.

[71] L. F. Mollenauer and J. P. Gordon. Solitons in Optical Fibers, Acadamic, Boston. 2006.

[72] G. P. Agrawal. Nonlinear Fiber Optics, 3rd ed. Academic, San Diego. 2001.

[73] J. R. Taylor. Optical Solitons theory and Experiment, Cambridge University Press, Cambridge, England. 1992.

[74] L.C. Crasovan et all. *Phys. Rev. E*, **67**(046610), 2003.

[75] R. Nath and P. L. Santos. *Phys. Rev. Lett*, **76**(013606), 2007.

[76] M. Stratmann, T. Pagel, and F. Mitschke. *Phys.Rev.Lett*, **95**(143902), 2005.

[77] U. Al Khawaja. *J. Phys. A: Math. Theor*, **42**(265206), 2009.

[78] U. Al Khawaja. *Phys. Rev. E*, **81**(056603), 2010.

[79] U. Al Khawaja and A. Boudjemâa. *Phys. Rev. E*, **86**(036606), 2012.

[80] V. N. Serkin, A. Hasegawa, and T. L. Belyaeva. *Phys. Rev. Lett*, **98**(074102), 2007.

[81] U. Al Khawaja. *J. Phys. A*, **39**(9679), 2006.

[82] V. I. Karpman and V. V. Solovev. *Physica D*, **3**(487), 1981.

[83] J. P. Gordon. *Opt. Lett*, **8**(596), 1983.

[84] D. Anderson and M. Lisak. *Opt. Lett*, **11**(174), 1986.

[85] B. A. Malomed. *Phys. Rev. A*, **44**(6954), 1991.

[86] A. Hause, H. Hartwig, B. Seifert, M. Bohm H. Stolz, and F. Mitschke. *Phys. Rev. A*, **75**(063836), 2007.

[87] A. Hause, H. Hartwig, M. Bohm, , and F.Mitschkeand ibid. *Phys. Rev. A*, **78**(063817), 2008.

[88] U. Al Khawaja and H. T. C. Stoof. *New J. Phys*, **13**(085003), 2011.

[89] B. A. Malomed. Soliton management in periodic systems. *Springer, New York*, 2006.

[90] V. I. Kruglov, A. C. Peacock, and J. D. Harvey. *Phys. Rev. Lett*, **90**(113902), 2003.

[91] Kevin E. Strecker, Guthrie B. Partridge, Andrew G. Truscott, and Randall G. Hulet. *Nature*, **417**:150–153, 2002.

[92] P. Rohrmann, A. Hause, and F. Mitschke. *Phys. Rev. A*, **87**(043834), 2013.

[93] A. Boudjemâa. *Int. J. Mod. Phys. B*, **31**(1750178), 2017.

[94] K. A. Brzdakiewicz M. Peccianti and G. Assanto. *Opt. Lett*, **27**(1460), 2002.

[95] A. Fratalocchi, M. Peccianti, C. Conti, and G. Assanto. *Mol. Cryst. Liq. Cryst*, **421**(297), 2004.

[96] A. Alberucci, M. Peccianti, G. Assanto, A. Dyadyusha, and M. Kaczmarek. *Phys. Rev. Lett*, **97**(153903), 2006.

[97] A. Fratalocchi, A. Piccardi, M. Peccianti, and G. Assanto. *Opt. Lett*, **32**(1447), 2007.

[98] A. Fratalocchi, A. Piccardi, M. Peccianti, and G. Assanto. *Phys. Rev. A*, **32**(063835), 2007.

[99] C. Garca Reimbert, T.R. Marchant, A. A. Minzoni, N.F. Smyth, and A.L. Worthy. *Physica D*, **273**(1088), 2008.

[100] G. Assanto, N.F. Smyth, and A.L. Worthy. *Phys. Rev. A*, **78**(013832), 2008.

[101] .D. Skuse and N.F. Smyth. *Phys. Rev. A*, **79**(063806), 2009.

[102] Z. Xu, Y.V. Kartashov, and L. Torner. *Opt. Lett.*, **30**(3171), 2005.

[103] B. K. Esbensen, M. Bache, O. Bang, and W. Krolikowski. *Phys. Rev. A*, **86**(033838), 2012.

[104] W. Chen, M. Shen, Q. Kong, J. Shi, Q. Wang, and W. Krolikowski. *Opt. Lett*, **39**(1764), 2014.

[105] B. A. Umarov B. Kh. Turmanov, B. B. Baizakov and F.Kh.Abdullaev. *Phys Lett. A*, **379**(1828), 2015.

[106] R. Nath, P. Pedri, and L. Santos. *Phys. Rev. Lett*, **102**(050401), 2009.

[107] G. Assanto, C. GarcaReimbert, A. Minzoni, N.F. Smyth, and A.L.Worthy. *Physica D*, **240**(1213), 2011.

[108] M. Salerno and B. B. Baizakov. *Phys. Rev. E*, **98**(062220), 2018.

[109] L. Pitaevskii and S. Stringari. Bose-Einstein Condensation, Oxford University Press . *Phys. Rev. A.*, 2003.

[110] C. J. Pethick and H. Smith. Bose-Einstein Condensation in dilute Gases. *Cambridge university press. Second edition*, 2008.

[111] A. Gorlitz et al. *Phys. Rev. Lett*, **87**(130402), 2001.

[112] . Schreck et al. *Phys. Rev. Lett.*, **87**(080403), 2001.

[113] H. Moritz, T. Stoferle, M. Kohl, and T. Esslinger. *Phys. Rev. Lett*, **91**(250402), 2003.

[114] A. L. Marchant, T. P. Billam, T. P. Wiles, M. M. H. Yu, S. A. Gardiner, and S. L. Cornish. *Nat. Commun*, **4**(1865), 2013.

[115] D. DeMille. *Phys. Rev. Lett*, **88**(067901), 2002.

[116] C. Gluck, J. Lange, O. Dulieu, R. Wester, and M. Weidenmuller. ***101***, 133004, 2008.

[117] K. K. Ni, S. Ospelkaus, M. H. G. de, A. Peer, B. Neyenhuis, J. J. Zirbel, S. Kotochigova, P. S. Julienne, D. S. Jin, and J. Ye. *Science*, **322**, 2008.

[118] K. K. Ni, S. Ospelkaus, D. Wang, G. Quemener, B. Neyenhuis, M. H. G. de Miranda, J. L. Bohn, J. Ye, , and D. S. Jin. ***464***, 1324, 2010.

[119] S. Ospelkaus, K. K. Ni, D. Wang, M. H. G. de Miranda, B. Neyenhuis, G. Quemener, P. S. Julienne, J. L. Bohn, D. S. Jin, and J. Ye. *Science*, **327**(853), 2010.

[120] W. Li, T. Pohl, J. M. Rost, S. T. Rittenhouse, H. R. Sadeghpour, J. Nipper, B. Butscher, J. B. Balewski, V. Bendkowsky, R. Low, , and T. Pfau. *Science*, **334**(1110), 2011.

[121] M. H. G. de Miranda, A. Chotia, B. Neyenhuis, D. Wang, G. Quemener, S. Ospelkaus, J. L. Bohn, J. Ye, , and D. S. Jin. *Nat. Phys*, **7**(502), 2011.

[122] M. Zeppenfeld, B. G. U. Englert, R. Glockner, A. Prehn, M. Mielenz, C. Sommer, L. D. van Buuren, M. Motsch, and G. Rempe. *Nature*, **491**(570), 2012.

[123] C. H. Wu, J. W. Park, P. Ahmadi, S. Will, , and M. W. Zwielein. *Phys. Rev. Lett*, **109**(085301), 2012.

[124] D. Tong, S. M. Farooqi, J. Stanojevic, S. Krishnan, Y. P. Zhang, R. Cote, E. E. Eyler, and P. L. Gould. *Phys. Rev. Lett*, **93**(063001), 2004.

[125] V. Bendkowsky, B. Butcher, J. Nipper, J. P. Shaffer, R. Low, and T. Pfau. *Nature*, **458**(1005), 2009.

[126] H. Weimer, M. Muller, I. Lesanovsky, P. Zoller, and H. P. Buchler. *Nat. Phys*, **6**(382), 2010.

[127] N. Henkel, R. Nath, and T. Pohl. *Phys. Rev. Lett*, **104**(195302), 2010.

[128] P. Schau, M. Cheneau, M. Endres, T. Fukuhara, S. Hild, A. Omran, T. Pohl, C. Gross, S. Kuhr, and I. Bloch. *Nature*, **491**(87), 2012.

[129] T. Peyronel, O. Firstenberg, Q. Y. Liang, S. Hofferberth, A. V. Gorshkov, T. Pohl, M. D. Lukin, and V. Vuletic. *Nature*, **488**(57), 2012.

[130] I. C. Khoo. Liquid Crystals: Physical Properties and Nonlinear Optical Phenomena,Wiley, New York. *,Wiley, New York*, 1995.

[131] G. Assanto. Nematicons: Spatial Optical Solitons in Nematic Liquid Crystals,Wiley, John Wiley. 2012.

[132] J. Cuevas, P. G. Kevrekidis, B. A., P. Dyke, and R. G. Hulet.

[133] B. B. Baizakov B. A. Umarov, N. A. B. Aklan and F. Kh. Abdullaev. *Journal of Physics: Conference Series*, **697**(012023), 2016.

[134] U. Al Khawaja. *J. Math. Phys*, **51**(053506), 2010.

[135] B. Kh. Turmanova, B. B. Baizakov, B. A. Umarov, and F. Kh. Abdullaev. *Phys. Lett. A*, **379**(1828), 2015.

[136] S. Sinha and L. Santos. *Phys. Rev. Lett*, **99**(0140406), 2007.

[137] O. Bang, W. Krolikowski, J. Wyller, and J. J. Rasmussen. *Phys. Rev. E*, **66**(046619), 2002.

[138] A. Boudjemâa and U. Al Khawaja. *Phys. Rev. A*, **88**(045801), 2013.

[139] D. W. Wang, M. D. Lukin, and E. Demler. *Rev. Lett.*, **97**(180413), 2006.

[140] A. Pikovski, M. Klawunn, G. V. Shlyapnikov, , and L. Santos. *Phys. Rev. Lett*, **105**(0215302), 2010.

[141] M. A. Baranov, A. Micheli, S. Ronen, and P. Zoller. *Phys. Rev. A*, **83**(043602), 2011.

[142] S. M. Shih and D. W. Wang. *Phys. Rev. A*, **79**(065603), 2009.

[143] A. C. Potter, E. Berg, D. W. Wang, B. I. Halperin, and E. Demler. *Phys. Rev. Lett*, **105**(220406), 2010.

[144] M. Rosenkranz and W. Bao. *Phys. Rev. A*, **84**(050701(R)), 2011.

[145] A. S. Jensen A. G. Volosniev, D. V. Fedorov and N. T. Zinner. *Phys. Rev. Lett*, **106**(250401), 2011.

[146] P. Zoller G. Pupillo M. Dalmonte. *Phys. Rev. Lett*, **107**(163202), 2011.

[147] P. Pedri R. Nath and L. Santos. *Phys. Rev. A*, **86**(013610), 2012.

[148] Y. A. Chen et All. *Nature Phys*, **07**(61), 2011.

[149] S. Hofferberth et al. *Nature Phys*, **02**(710), 2006.

[150] A. K. Fedorov, S.I. Matveenko, V.I. Yudson, and G.V. Shlyapnikov. *Sci. Rep*, **06**(27448), 2016.

[151] A. Boudjemâa. *J. Low. Temp. Phys*, **189**(76), 2017.

[152] Y. Cai, M. Rosenkranz, Z. Lei, and W. Bao. *Phys. Rev. A*, **82**(043623), 2010.

[153] A. Boudjemâa. *Phys. Rev. A*, **97**(033627), 2018.

[154] A. Boudjemâa. *Phys. Rev. A*, **381**(1745), 2017.

[155] E. A. Donley, N. R. Claussen, S. L. Cornish, J. L. Roberts, E. A. Cornell, and C. E. Wieman. *Nature*, **412**(295), 2001.

[156] A. Boudjemâa. *Commun. Nonlinear Sci. Numer. Simul*, **48**(376), 2017.

[157] A. Boudjemâa. *Commun. Nonlinear Sci. Numer. Simul*, **33**(85), 2016.

[158] De Nicholas Manton and P. Sutcliffe. *Topological Solitons,(Cambridge University Press)*, 2004.

[159] R. Conte. *Phys. Lett. A*, **140**(383), 1989.

[160] T. Brugarino and M. Sciacca. *J. Math. Phys*, **51**(053506), 2010.

[161] R. Hirota. *Phys. Rev. Lett*, **27**(1192), 1971.

[162] C. Q. Dai, X. G. Wang, and G. Q. Zhou. *Phy. Rev. A*, **89**(013834), 2014.

[163] P. D. Lax. *Commun. Pure Appl. Math*, **21**(467), 1968.

[164] A. Coely et al. Bäcklund and Darboux Transformations,(American Mathematical Society, Providence, RI) . 2001.

[165] V. B. Matveev and M. A. Salle. Darboux Transformations and Solitons (Springer, Berlin. 1991.

[166] R. M. Miura. *J. Math. Phys*, **9**(1202), 1968.

[167] R. M. Miura, C. S. Gardner, and M. D. Kruskal. *J. Math. Phys.*, **9**(1204), 1968.

[168] M. Ablowitz and P. A. Clarkson. Solitons, Nonlinear Evolution Equations and Inverse Scattering, Cambridge Univ. Press, Cambridge. 1991.

[169] S. Li and S. J. Liao. Applied Mathematics and Computation. **169**, 2005.

[170] D. D. Ganji, A. Asgari, and Z. Z. Ganji. Acta Applicandae Mathematicae. **104**(201), 2008.

[171] H. A. Abdusalam and Int. J. Nonlin. *Sci.Numer. Simul*, **6**(99), 2005.

[172] Z. Y. Yan. *Phys. Lett. A*, **292**(100), 2001.

[173] M. L. Wang. *Phys. Lett. A*, **213**(279), 1996.

[174] Y. B. Zhou, M. L. Wang, and Y. M. Wang. *Phys. Lett. A*, **308**(31), 2013.

[175] M. J. Ablowitz and Z. H. Musslimani. *Phys Rev Lett*, **110**(064105), 2013.

[176] A. K. Sarmaand, M. A. Miri, Z. H. Musslimani, and D.N. Christodoulides. *Phys Rev E*, **89**(052918), 2014.

[177] A. Khare and A. Saxena. *Journal of Mathematical Physics*, **56**(032104), 2015.

[178] P. S. Vinayagam, R. Radha, U. Al Khawaja, and L. Ling. *Nonlinear Sci. Numer. Simul*, **59**(387), 2018.

[179] U. Al Khawaja. *Physical Review E*, **81**(056603), 2010.

[180] B. Feng and B. A. Malomed. *Opt. Commun*, **229**(173), 2004.

[181] F. Mitschke A. Hause, H. Hartwig. *Phys. Rev. A*, **82**(053833), 2010.

[182] M. P. Fedoruk S. K. Turitsyn, B. G. Bale. *Phys. Rep*, **521**(135203), 2012.

[183] A. Boudjemâa and U. Al Khawaja. *Phys. Rev. A*, **88**(045801), 2013.

[184] A. Boudjemâa. *Commun. Nonlinear Sci. Numer. Simul*, **48**(376), 2017.

[185] M. J. Ablowitz and Z.H. Musslimani. *Phys Rev Lett*, **29**(915), 2016.